Using non-synonymous single nucleotide polymorphic variants of the human angiotensin II type 1 receptor to characterize biased signalling signatures of heterotrimeric G proteins and β-arrestin

Sahil Kumar
Laboratory of Dr. Stéphane A. Laporte

Division of Experimental Medicine
Department of Medicine
McGill University
Montréal, Québec, Canada

December 2016

A thesis submitted to McGill University in partial fulfillment of the requirements of the degree of Master of Science

Abstract

Hypertension and its risks can be partially ascribed to the endogenous hormone angiotensin II (Ang II), which is critical to regulate blood volume and vascular resistance through the angiotensin II type 1 receptor's (AT_1R) role in the Renin-Angiotensin-Aldosterone System. Naturally-occurring variations in the AT_1R coding sequence, also known as single nucleotide polymorphisms (SNPs), have been reported to cause pathophysiology, reduced binding of the endogenous hormone Ang II, or altered pharmacodynamics of prescribed angiotensin receptor blockers, where only few SNPs have been validated as possible mediators of disease variability or linked to pathophysiological outcomes.

Herein, we characterized three SNPs of the human angiotensin II type 1 receptor–A163T, T282M, and C289W–reported to differentially affect binding of anti-hypertensive drugs due to their close proximity to the AT_1R's orthosteric binding pocket. To assess how these receptors engage with their signalling effectors, we used a panel of bioluminescence resonance energy transfer (BRET)-based biosensors to determine the relative activity of the AT_1R with its cognate G proteins ($G\alpha_q$, $G\alpha_{12}$, $G\alpha_{i2}$, $G\alpha_{i3}$), its downstream effectors in the signalling cascade (PKC, Rho), and β-arrestin recruitment and trafficking upon Ang II stimulation.

Results show that the A163T-AT_1R had similar potency and efficacy in all pathways compared to the wild-type AT_1R. Conversely, T282M-AT_1R and C289W-AT_1R had diminished relative activity in all pathways assessed. In particular, the T282M-AT_1R promoted biased signalling, which translated to a significant decrease in $G\alpha_{12}$ coupling upon Ang II stimulation, whereas it retained robust activity to the other G proteins assessed. Upon Ang II stimulation, T282M-AT_1R and C289W-AT_1R recruited β-arrestin-2 to the plasma membrane; however, of the two, only C289W-AT_1R associated with β-arrestin-2 in early endosomes, similar to the A163T-

AT_1R and wild-type AT_1R. Although, T282M-AT_1R was still able to internalize into early endosomes, as shown by immunofluorescence confocal microscopy. This suggests that the T282M site is important for regulating the avidity of the β-arrestin/receptor complex to traffic to the endosome. Taken together, our results proposed a unique signalling signature of the T282M-AT_1R that shows bias opposing $G\alpha_{12}$ signalling and β-arrestin-2 enrichment in the endosomes, as these pathways were found to be significantly attenuated from all other responses assessed.

We show interplay between G proteins and β-arrestins that can now be modulated by naturally-occurring mutations in the receptor and that this mosaicism of behaviours can potentially impact cellular responses. Understanding the links between the signalling signatures and the physiological or pathophysiological responses may help identify and developing new biased ligands – and perhaps better targeted therapeutics.

Résumé

L'hypertension et ses risques peuvent être attribués en partie à l'hormone endogène angiotensine II (Ang II), qui est essentielle à la régulation de la tension artérielle et la résistance vasculaire. Ang II agit en se liant au récepteur de l'angiotensine II type 1 (AT_1R) affectant le système Rénine-Angiotensine-Aldostérone. Des variations polymorphique nucléotidique (PSNs) se trouvant dans la séquence génétic de l'AT_1R, ont été rapportées comme pouvant jouer un rôle dans la physiopathologie de l'hypertension, en réduisant la capacité d'occupation du récepteur par l'hormone endogènee l'angiotensine II, ou en modifiant les effects pharmacodynamiques des bloqueurs du récepteur angiotensine. À ce jour, il existe peu de liens entre ces polymorphismes et les pathologies associées à un défaut du récepteur AT_1 ont été établis.

Dans cette étude, nous avons caractérisé trois PSN du récepteur de l'angiotensine II type 1 humaine – A163T, T282M, et C289W. Ces trois mutations ont été rapportées comme pouvant affecter de manière différente la capacité des drogues antihypertensives à se lier au récepteur. De manière à évaluer comment les voies de signalisation de ces récepteurs sont affectés, nous avons utilize divers biosenseurs BRET pour établir l'activité relative des récepteur à se lier aux protéines G ($G\alpha_q$, $G\alpha_{12}$, $G\alpha_{i2}$, $G\alpha_{i3}$), et d'activer ses effecteurs de signalisation en celles-ci (par exemple: PKC, Rho, etc.), mais aussi à la capacité du récepteur à recruter et à transporter la β-arrestine dans les endosomes, suite à une stimulation des cellules a l'angiotensine II.

Nos résultats montrent que le A163T-AT_1R est capable d'activer toutes les voies de signalisations avec la même puissance et la même efficacité que le récepteur de type naturel. Réciproquement, les T282M-AT_1R et C289W-AT_1R voient leurs activités relatives diminuées dans toutes des voies de signalisation évaluées. En particulier, le T282M-AT_1R s'est démarqué en biaisant de manière significative la voie de signalisation à la protéine $G\alpha_{12}$, tout en conservant une

activité robuste aux autres protéines G. Suite à un traitement avec l'agoniste, les T282M-AT_1R et C289W-AT_1R recrutent la β-arrestine-2 à la membrane plasmique; cependant, des deux, seulement le C289W-AT_1R associe avec la β-arrestine-2 au niveau des endosomes précoces de manière similaire au récepteur de type naturel ou à A163T-AT_1R. Le T282M-AT_1R retient toutefois la capacité d'être internalisé dans les endosomes précoces, comme démontré en utilisant des techniques de microscopie confocale. Ceci laisse à penser que la position T282M est importante pour l'avidité du transport du complexe β-arrestine/récepteur aux endosomes. Ensemble, ces résultats proposent une signature signalétique unique de T282M-AT_1R, qui montre une signalisation biaisée où l'association à la protéine $G\alpha_{12}$ ainsi que l'enrichissement de la β-arrestine au niveau des endosomes sont grandement affectés.

Nous démontrons que l'interaction entre les protéines G et la β-arrestine peuvent être modulée par des mutations naturelles dans le récepteur AT_1R et cette mosaïque de nouveaux comportements pourrait avoir un impact potentiellement important sur les réponses cellulaire. Mieux comprendre les liens entre les diverses signatures de signalisation et leurs réponses physiologiques ou pathologique pourrait aider à identifier et à développer de nouveaux ligands biaisés pouvant mener à de nouveaux composés thérapeutiques mieux ciblés.

Table of Contents

Acknowledgements

I would first and foremost like to thank my supervisor Dr. Stéphane Laporte and the members of the Laporte lab, both current and former, for moulding my mind and developing my understanding of G protein coupled receptors so I could offer even a sliver of contribution to our field of research: Ljiljana Nikolajev, Stéphanie Clément, Jenna Giubilaro, Dr. Yoon Namkung, Dr. Lama Yamani, Frank Cao, Dana Sedki, Mideum Song, Dr. Étienne Khoury, Dr. Olivier Radresa, Dr. Min Fu, and Dr. Eugénie Goupil. I am grateful to the esteemed members of my committee Drs. Christian Rocheleau, Terence Hébert, and Louise Larose for their mentorship, encouragement, and above all, friendship during my time as a graduate student; I only hope more graduate students are fortunate enough to surround themselves with committed colleagues in academe. Going to work has never felt like a job because of the members of the Polypeptide Lab Group that have supported me throughout this process: Kimberley Gauthier, Fiona Law, Icten Meras, Jung Hwa Seo, Erin Coyne, Rohini Bose, Nathalie Bedard, Kai Sheng, Nida Haider, George Kefalas, Dr. Hui Li, Dr. Bing Li, Dr. Julie Dusseault, Victor Dumas, Gerry Baquiran, Dr. Simon Wing, and Mary Lapenna.

The writing of this work could not have been done without the assistance of Katherine Hales and Keegan Lathe-LeBlanc in the library for hours and hours on end. I have to thank my A-squad: Natasha Fenn, Margaret Markin, and Jessica Ferkul; I know I have and always will have their unwavering support and shoulders to lay my head. A shout out to my gurus that have helped me get to where I am today as a jack of (many) trades: Mitchell Miller, Eva Monson, and Beyoncé. Of course, I would like to thank the Division of Experimental Medicine – Dominique Besso, Marylin Linhares, and Dr. Anne-Marie Lauzon – for their fantastic work in making sure every trainee in the Division thrives.

I have to ultimately thank my parents, Ramla and Yajnish Kumar, and brother Dr. Munish Kumar for always understanding when I put work before home and still attending to me when I needed it the most. They have anchored me, fed me, and nurtured me throughout this degree, the ones before, and I'm sure they will be there for the ones to come.

Finally, I know I'm mentioning him again, but I owe a great debt of gratitude to my supervisor Dr. Stéphane Laporte for taking a chance on me, offering me a home in his lab, his sage advice, and providing me with endless resources to leave McGill with the confidence and knowledge to take on the world (or be back in a couple years for a Ph.D. – who knows). I came looking for a mentor and I found much more. Not every trainee can say they had a supervisor that checks in, offers advice and guidance, lightens the mood, and genuinely cares for his students and lab members. I know I am a better scholar for the experiences I have had in this lab and will remain with me beyond the walls of McGill University and the Glen.

And finally, this research was also made possible through the generosity of my Master's Studentship awarded from the Faculty of Medicine, as well as through operating grants awarded to Dr. Laporte from the Canadian Institutes of Health Research.

Author Contributions

It is recognized that the following work involves the contribution of many parties:

Dr. Stéphane Alain Laporte, Supervisor: provided substantial contribution in an advisory capacity for all aspects of this Master's project, from conception of the idea, to formulation of the research questions, to the final review of this thesis.

Sahil Kumar, M.Sc. candidate: designed and performed the experiments, data collection and analysis, statistics, and writing of this thesis.

Dr. Yoon Namkung, Research Associate: developed and tested the biosensors used in this thesis. Provided SK with guidance and troubleshooting for experimental protocols.

Ljiljana Nikolajev, M.Sc: trained SK in the protocols and aided in the experimental designs and editing the translation of the abstract.

Abbreviations

Ang II	: Angiotensin II
hAng III	: Human Angiotensin III
AC	: Adenylyl cyclase
ACE	: Angiotensin converting enzyme
AT_1R	: Angiotensin II type 1 Receptor
ATP	: Adenosine triphosphate
BRET	: Bioluminescence resonance energy transfer
BSA	: Bovine serum albumin
cAMP	: Cyclic adenosine monophosphate
C-terminus	: Carboxy terminus
CCR5	: C-C chemokine receptor type 5
CCV	: Clathrin-coated vesicles
$CaCl_2$	: Calcium chloride
CaSR	: Calcium sensing receptor
DAG	: Diacylglycerol
DMEM	: Dulbecco's Modified Eagle Medium
ebBRET	: Enhanced bystander BRET
ECL	: Extracellular loops (ECL1-3)
EDTA	: Ethylenediaminetetraacetic acid
EGF	: Epidermal growth factor
EGFR	: Epidermal growth factor receptor
ERK1/2	: Extracellular signal-regulated kinase 1 and 2

FACS : Fluorescence-activated cell sorting

FBS : Fetal Bovine Serum

FFA2 : Free Fatty Acid Receptor 2

G protein : Guanine nucleotide-binding protein

GAP : GTPase activating protein

GDP : Guanosine diphosphate

GFP : Green fluorescent protein

GHRHG : Growth Hormone Releasing Hormone Receptor

GRK : G protein-coupled receptor kinase (GRK1-7)

GTP : Guanosine triphosphate

GPCR : G protein-coupled receptor

HEK293 : Human embryonic kidney cells

ICL : Intracellular loops (ICL1-3)

IP_3 : Inositol-1,4,5-triphosphate

JNK : c-Jun N-terminal kinase

mRNA : Messenger ribonucleic acid

MAPK : Mitogen-activated protein kinase

MEM : Minimum Essential Medium

N-terminus : Amino terminus

NaOH : Sodium hydroxide

NAM : Negative allosteric modulator

PAM : Positive allosteric modulator

PBS : Phosphate buffered saline

PCR : Polymerase chain reaction

PDGF : Platelet-derived growth factor

PDGFR : Platelet-derived Growth Factor Receptor

PI3K : Phosphatidylinositol-3-kinase

PIP_2 : Phosphatidylinositol-4,5-bisphosphate

PKA : Protein Kinase A

PKC : Protein kinase C

PLCβ : Phospholipase C-β

PTHR : Parathyroid Hormone Receptor

rGFP : *Renilla reniformis* green fluorescent protein

rLuc : *Renilla reniformis* luciferase

RA : Relative Activity

RAAS : Renin-Angiotensin-Aldosterone System

RTK : Receptor tyrosine kinase

SNP : Single nucleotide polymorphism

TM : Transmembrane

VSMC : Vascular smooth muscle cells

WT : Wild-type

List of Figures and Tables

Chapter 1

Chapter 3

Chapter 1: Introduction and Review of Literature

CHAPTER I: Introduction and review of literature

1.1 G protein-coupled receptors (GPCRs)

1.1.1 Overview

Evolutionary influences have required organisms to be able to sense and adapt to their external environment for survival. The cellular membrane provides a barrier between the internal and external milieux and houses many integral proteins for adhesion, ion conductivity, and transducing cellular signals for second messenger production, gene transcription, and translation. Of these proteins, the plasma membrane-bound receptors provide the capacity for cells to respond to external stimuli. Whereas several classes of cell-membrane receptors exist, the family of G protein-coupled receptors (GPCRs) constitute the largest family of receptors and these receptors are found to be implicated in most physiological responses, including, but not limited to, hormonal homeostasis, neurotransmission, taste, vision, and smell (Foord et al., 2005). In actuality, nearly 50% of marketed therapeutic agents that target GPRCs or their downstream effectors are found in the 100 top-selling drugs and have produced several billion dollars in profit, making these receptors a focus of many drug discovery and research programs (Marinissen & Gutkind, 2001; Overington, Al-Lazikani, & Hopkins, 2006; Lagerström & Schiöth, 2008; Conn, Christopoulos, & Lindsley, 2009). These heptahelical receptors owe their moniker to the fact that a majority interact with one or more intracellular guanine nucleotide-binding protein (G proteins), specifically, the heterotrimeric G proteins: $\alpha\beta\gamma$ (continued in Chapter 1.2.2). From a change in conformation of the receptor, generated in most cases by a stimulus, these G proteins (specifically the Gα subunits) are able to exchange their bound guanosine diphosphate (GDP) for a guanosine triphosphate (GTP), resulting in their activation and the induction of intracellular events through various effectors.

These effectors generate second messengers to amplify the intracellular signalling cascade, which in turn promotes gene transcription and protein synthesis required for many cellular processes, including proliferation, differentiation, and survival (Marinissen & Gutkind, 2001). Beyond the dogma of "GPCR–G protein" interactions, research has shown there are biological responses not mediated by heterotrimeric G proteins, but by canonical β-arrestin signalling following receptor desensitization and endocytosis (Marinissen & Gutkind, 2001; Khoury, Clément, & Laporte, 2014).

1.1.2 Structure

The GPCR possesses seven α-helical hydrophobic transmembrane domains (TM), which are connected by three extracellular loops (ECL1-3) and three intracellular loops (ICL1-3) (Kobilka, 2007). The helices are oriented perpendicularly to the plasma membrane and are referred to as TM-I through TM-VII. These transmembrane domains form the orthosteric ligand binding site for many classes of G protein-coupled receptors. The amino (N-)terminus of the receptor is found in the extracellular milieu, whereas the carboxy (C-)terminus is exclusively in the cytosol and is implicated in cell signalling (Kobilka, 2007). The receptor's N-terminus and residues of the extracellular loops undergo post-translational modifications, such as glycosylation, which are vital for maturation, receptor expression at the plasma membrane, and the binding of some endogenous ligands to the receptor (Bannert et al., 2001; Maurice et al., 2011; Khoury, Clément, & Laporte, 2014). The C-terminal tail and intracellular loops provide sites for palmitoylation and phosphorylation, which are important for G protein and effector coupling (Maurice et al., 2011). A conserved disulfide bond between the cysteine on the ECL2 and the cysteine of TM-III near the

hydrophilic surface is found in over 91% of all human GPCRs (Klco, Nikiforovich, & Baranski, 2006).

1.1.3 Ligands

The superfamily of G protein-coupled receptors are known to bind a myriad of ligands and stimuli, such as the biogenic amines noradrenaline, dopamine, histamine, and acetylcholine; lipids such as prostaglandins, lysophosphatidic acid, and platelet-activating factor; amino acids and ions including glutamate, calcium, and γ-aminobutyric acid; peptides and proteins covering angiotensin, bradykinin, vasopressin, endorphins, follicle-stimulating hormone, and luteinizing hormone; and others, including cannabinoids, light, pheromones, odorants, and opiates (reviewed in Marinissen & Gutkind, 2001). Pharmacologically, compounds binding at a receptor[1] can be clustered to in four main categories based on their efficacies[2]: full agonists, partial agonists, neutral antagonists, or inverse agonists (Fig. 1.1; Kobilka, 2007; Rosenbaum, Rasmussen, & Kobilka, 2009). A ligand would be classified in each category according to its ability to stabilize the "on" state of the receptor. However, the efficacy of a given ligand will vary with the signalling pathway being examined and the level of receptor expression (Zheng et al., 2010). When considering an agonist that elicits a response through the activation of G proteins, a full agonist would produce the maximal response and fully activate the receptor, whereas a partial agonist would induce a submaximal response even when saturation of the receptor is achieved (Kobilka, 2007). The endogenous orthosteric ligands for a given target GPCR are commonly found to be full agonists in physiological conditions (Conn et al., 2009). A neutral antagonist can bind to the receptor and

[1] These ligands can bind either within an orthosteric site (i.e., the binding site for the endogenous ligand of the receptor) or an allosteric site (i.e., a topographically distinct site from the orthosteric site on the receptor).

[2] Kobilka (2007) defines the term efficacy as "the effect of a ligand on the functional properties of the receptor."

cause no discernible effect nor change in conformation, whereas an inverse agonist can bind to basally-active receptors and induce a conformational change that will lead to their inactivation and promote a converse activation. Inverse agonism can be observed physiologically at melanocortin subtype 1 and 4 receptors in the arcuate nucleus of the hypothalamus with either their ligands agouti signalling peptide or agouti-related peptide (Chai et al., 2003).

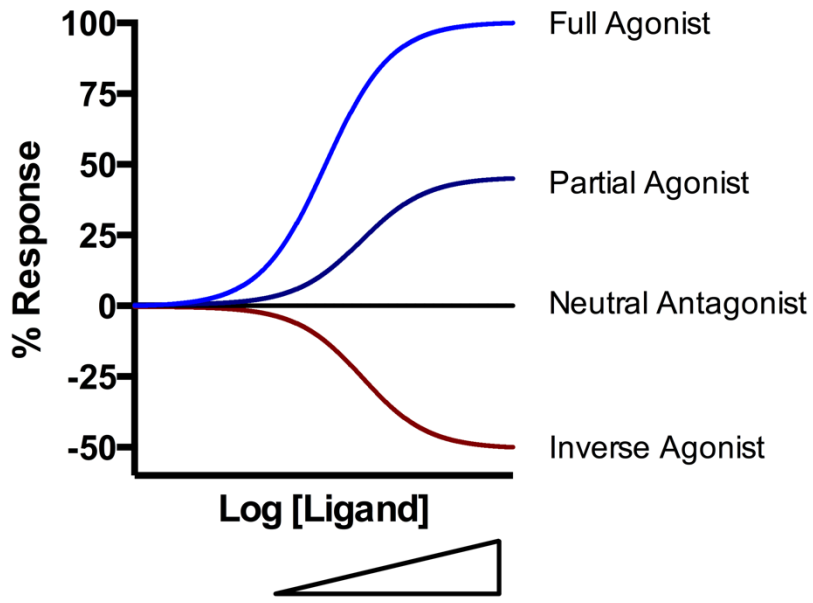

Figure 1.1: Classification of ligands based on their efficiency to bind and activate the receptor for a specific pathway at increasing concentrations. A full agonist is able to produce the maximal response and fully activate the receptor (light blue). A partial agonist would induce a submaximal response (0% < response > 100%) for that receptor, even at saturating concentrations (navy). A neutral antagonist causes no discernible effect (black), whereas an inverse agonist can bind to basally-active receptors and induce a converse activation (red). (Adapted from Rosenbaum et al., 2009).

The orthosteric binding site, also referred to as the "natural binding pocket", for a particular endogenous ligand has been shown to be highly conserved across subfamilies of GPCRs. Thereby, a ligand can mediate systemic physiological responses, regardless of the receptor subtype; however, this poses the challenge in achieving selectivity of the responses elicited across different receptor subtypes in tissues (Conn et al., 2009). Alternatively, allosteric modulators, such as ions, small molecules, antibodies, peptides, or protein complexes (e.g., receptor dimers and receptor-effector complexes) can act at a topographically distinct binding sites from the orthosteric ligand (Conn et al., 2009). These allosteric ligands offer the advantage of greater receptor subtype specificity due to the sequence divergence of allosteric sites through evolution, which allow the allosteric modulators to display activity only at a given subtype and not others (Conn et al., 2009). The range of allosteric response can be classified into four groups: positive allosteric modulators (PAMs), negative allosteric modulators (NAMs), allosteric agonists, or neutral allosteric ligands. PAMs increase the response of the receptor in the presence of the endogenous ligand, whereas NAMs inhibit or reduce this response (Conn et al., 2009). Neutral ligands have no effect on the receptor's responsiveness to the orthosteric ligand (Conn et al., 2009). Currently marketed allosteric modulators of GPCRs include cinacalet (Sensipar/Mimpara; Amgen), a PAM that increases the sensitivity of the calcium-sensing receptor (CaSR) to circulating calcium and is indicated for its use in hyperparathyroidism, and more recently, maraviroc (Celsentri/Selzentry; Pfizer), which is a NAM for the treatment of HIV-1 viral entry into cells by binding to the C-C chemokine receptor type 5 (CCR5) and attenuating the affinity of the receptor for the virus (Conn et al., 2009). Although most allosteric modulators exert their effects only in the presence of the endogenous orthosteric ligand, which maintains temporal and spatial effects of endogenous physiological signalling, modulators defined as allosteric agonists can regulate the receptor's

activity by engaging an active conformation upon their binding (Khoury, Clément, & Laporte, 2014). For example, Lee *et al.* (2008) discovered a series of small molecule phenylacetamides that were able to activate the Free Fatty Acid Receptor 2 (FFA2) unaccompanied by an orthosteric ligand to a similar efficacy to that of endogenous short-chain fatty acids.

1.1.4 Classes

As a way to categorize the 791 identified GPCRs in the human genome, the GRAFS (Glutamate, Rhodopsin, Adhesion, Frizzled/Taste2, Secretin) classification system was established based on sequence homology within TM-I to TM-VII (Fredriksson, Lagerström, Lundin, & Schiöth, 2003; Latek, Modzelewska, Trzaskowski, Palczewski, & Filipek, 2012). The rhodopsin-like receptors, or the Class A family of GPCRs, contains approximately 701 members, making it the largest group amongst the classes (Fredriksson et al., 2003). The secretin-like receptors, or the Class B family of GPCRs, are comprised of a total of 15 receptors, including the growth hormone releasing hormone receptor (GHRHR), parathyroid hormone receptor (PTHR), and calcitonin receptor. These receptors share conserved cysteine bridges found on the extracellular surface, which aid in the binding of large peptides, with the Class A receptors (Fredriksson et al., 2003). The glutamate-like receptors, or the Class C family of GPCRs, are characterized by the largest N-terminal domain, otherwise referred to as the "Venus flytrap-like" (VFT) domain, containing the orthosteric ligand binding cavity (Fredriksson et al., 2003). Composed of two lobes, the VFT domain induces conformational changes and regulates the level of receptor activation upon ligand binding (Tateyama, Abe, Nakata, Saito, & Kubo, 2004). The Class C family of receptors includes metabotropic glutamate receptors (mGluRs), γ-aminobutyric acid receptors ($GABA_BR$), calcium sensing receptors (CaSR), and the type 1 taste receptors (TAS1R; Conn et al., 2009). The Class A, Class B, and Class C receptors are depicted in Figure

1.2. The receptor families can be differentiated by their orthosteric ligand binding pocket: for Class A, the site is located in the 7TM domain, whereas Class B uses its large extracellular N-terminus, and Class C employs its bilobed extracellular Venus-flytrap-like domain (Bridges & Lindsley, 2008). The Frizzled/Taste2 receptors, or the Class F receptor family, includes the Frizzled and smoothin receptors, which are involved in Wnt and Hedgehog signalling during embryonic development, controlling cell fate, proliferation, and polarity (Fredriksson et al., 2003). Other receptor families excluded from the GRAFS classification are covered in the A–F clan system, such as class D (fungal mating pheromone receptors) and class E (cyclic AMP receptors; Fredriksson et al., 2003). In this thesis, we will focus on the angiotensin II type I receptor, which is classified as a rhodopsin-like β-group (or Class A) receptor (Fredriksson et al., 2003).

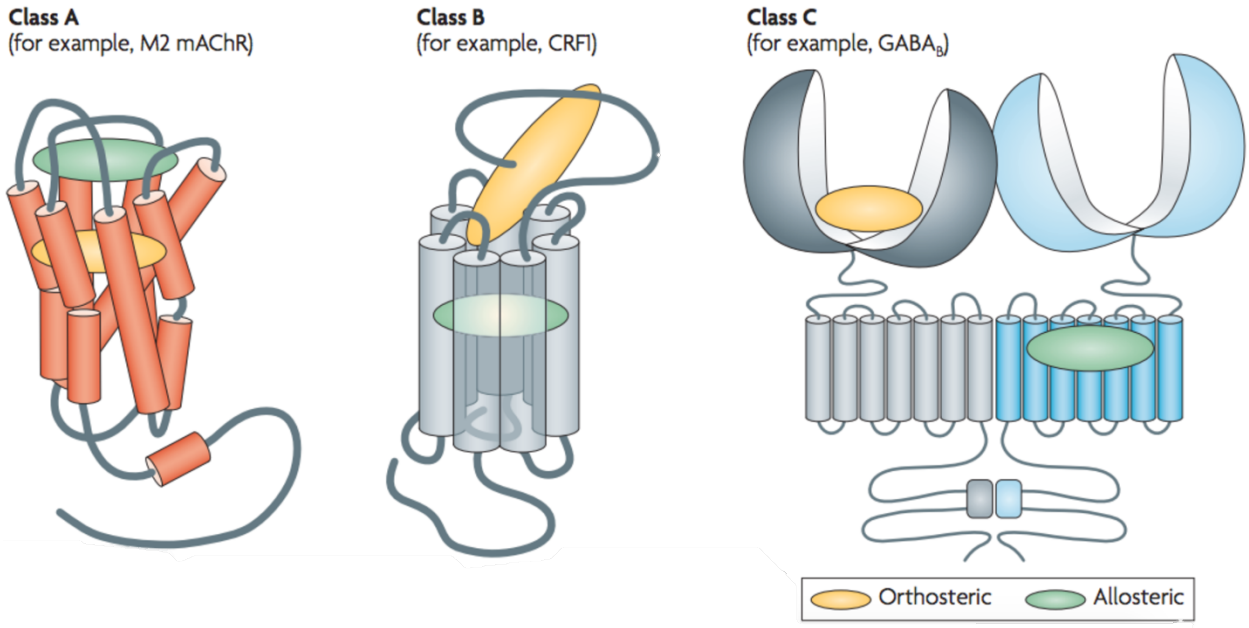

Figure 1.2: Schematic representation of the three major classes of GPCRs: A, B, and C. Orthostatic binding sites are shown in yellow and an allostersic binding site is depicted in green. Class A (left) and Class B (middle) GPCRs use their extracellular surface and opening of the transmembrane domain to form their orthosteric binding pocket. Class C GPCRs (right) employ their bilobed "Venus-flytrap-like" N-terminal domains to bind their orthosteric ligand and induce conformational changes through dimerization. (Adapted from Conn et al., 2009)

1.2 GPCR Mechanism of Action

1.2.1 GPCR activation

A number of models have been proposed to explain how GPCRs are activated, the simplest of them being the two-state (classical) model. This model presents the receptor in two states: the inactive state (R) and an active state (R*; summarized in Kobilka, 2007). The level of basal activity of the receptor is defined as the equilibrium between the R and R* states, whereas the ligand can shift this equilibrium to the R* state. However, the model is limited and can explain only simple experimental systems consisting of one receptor and one G protein. Is it now widely understood that the receptor may yield multiple conformational states. Upon ligand binding, a unique conformation will induce and/or stabilize an active state for different effector molecules or complexes (e.g., G proteins, kinases, arrestins). This multi-state model describes a ligand binding to the inactive receptor provides energy to stabilize "hybrid" activation states of R* (such as R**, R***, and so forth), which will be distinct in their conformation and action from other ligands in directing the GPCR's signalling through unique intracellular pathways; this phenomenon is termed "ligand-biased signalling", or more commonly, "functional selectivity" (continued in Chapter 1.2.7; Hunyady, Vauquelin, & Vanderheyden, 2003; Kobilka, 2007; Conn et al., 2009; Khoury, Clément, & Laporte, 2014).

Despite the myriad of ligands and diversity of ligand binding domains in GPCRs, there is considerable evidence that suggests a common mechanism of receptor activation. There is vast sequence homology in the cytoplasmic regions of TM-II and TM-III where the receptor interacts with G proteins (Kobilka, 2007). Although receptors are activated by different ligands, they retain the ability to couple to the same G protein, which requires the structural changes in the cytoplasmic domains of receptors to be very similar between receptors. For example, the prostaglandin F

receptor is activated by prostagladin F2α, whereas the angiotensin II type 1 receptor is activated by angiotensin II; yet, both of these receptors activate the same G protein ($G\alpha_q$). Further evidence supports the notion that GPCRs undergo similar conformational changes within transmembrane domains, involving the torsion and tilting of cytoplasmic regions upon agonist binding (Dunham & Farrens, 1999; Kobilka, 2007). In the absence of agonist, the receptor is kept in an inactive conformation by constraining intramolecular interactions, which can be disrupted with point mutations to produce constitutive activation of the receptor (Hunyady et al., 2003).

1.2.2 Heterotrimeric G protein signal transduction

The heterotrimeric guanine nucleotide-binding proteins are present in all eukaryotic cells, assisting in the control of metabolic, humoral, neural, and developmental functions (Simon, Strathmann, & Gautam, 1991). The ternary complex is formed by one alpha (α) subunit, one beta (β) subunit, and one gamma (γ) subunit. These proteins aid in signal transduction from cell surface receptors undergoing ligand-mediated conformational changes, which promote the exchange of guanosine diphosphate (GDP) to guanosine triphosphate (GTP) within the α subunit, resulting in the dissociation of the α-GTP from the stable βγ complex (Simon et al., 1991). The effect of the ligand-receptor complex is amplified via the activation of multiple G protein molecules, which can further amplify the signals to the generation of second messengers and the activation of downstream effectors, including ion channels, kinases, enzymes, and transcription factors (Figure 1.3; Simon et al., 1991; Marinissen & Gutkind, 2001). Termination of the signal occurs when the α-GTP is hydrolyzed to GDP by a GTPase activating protein (GAP), thereby increasing the affinity of the α subunit for the βγ heterodimer and returning the complex to its basal state (Simon et al.,

1991). To date, twenty-three α subtypes, six β subtypes, and fourteen γ subtypes have been described. The following paragraphs will describe these subunits and their effectors in more detail.

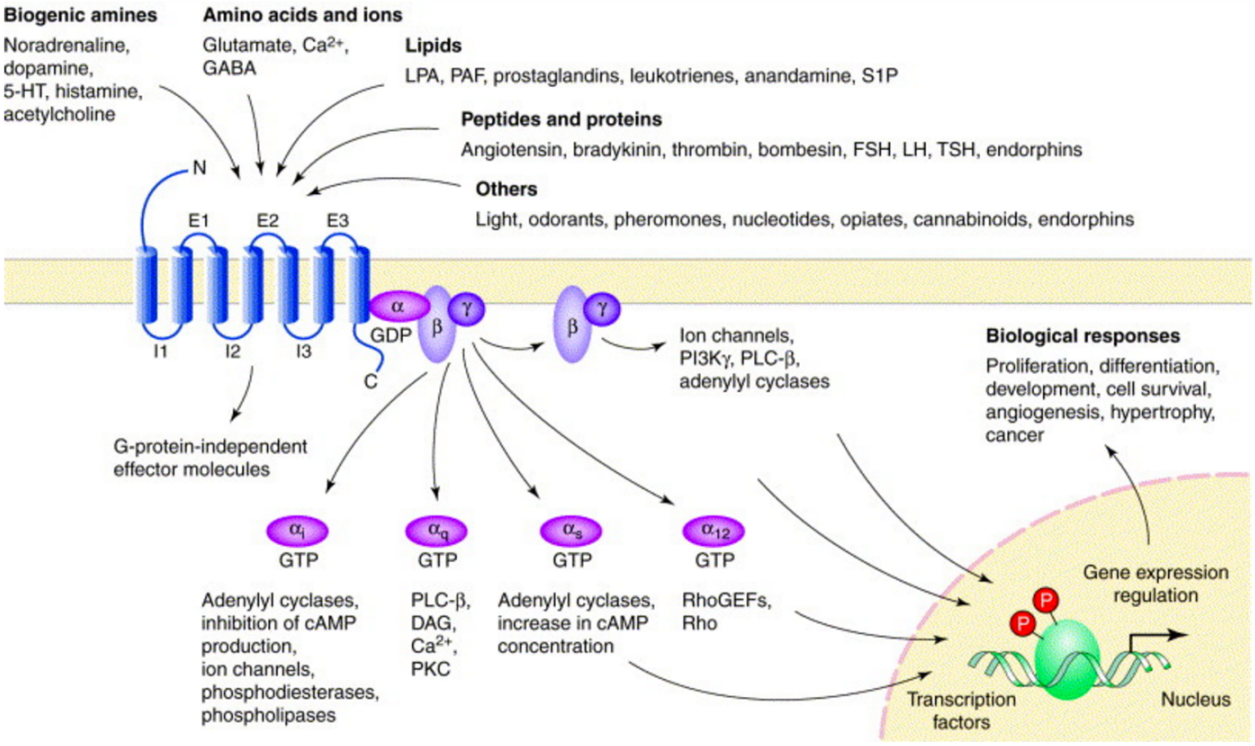

Figure 1.3: Activation of G protein coupled receptors (GPCRs) and their effectors. GPCRs are known to bind a myriad of ligands or stimuli, including biogenic amines, amino acids and ions, lipids, peptides and proteins, light, and odorants, among others. These agonists can activate G protein-mediated or G protein-independent effectors. GPCRs are known to couple to $G\alpha_i$, $G\alpha_{q/11}$, $G\alpha_{s/olf}$, $G\alpha_{12/13}$, and $G\beta\gamma$. These effectors activate second messengers to propagate the signal within the cell and elicit biological responses, including proliferation, cell survival, and differentiation. E1-E3, extracellular loops; I1-I3, intracellular loops; N, amino terminus; C, carboxy terminus (Adapted from Marinissen & Gutkind, 2001).

1.2.3 Gα subunits and their downstream effectors

The α-subunit can be divided into four groups: $G\alpha_s$, $G\alpha_{i/o}$, $G\alpha_{q/11}$, and $G\alpha_{12/13}$ (Simon et al., 1991). The NH_2-terminal region of the Gα subunit interacts with the βγ subunits for heterotrimer formation, whereas the COOH-terminal region is involved in interactions with the receptor (Simon et al., 1991). Antibodies and peptides (e.g., pertussis toxin) specific for the Gα C-terminus has shown to block this receptor/Gα protein interaction (Hamm, Deretic, Hofmann, Schleicher, & Kohl, 1987; Simon et al., 1991). With certain subtypes of Gα proteins ($G\alpha_o$, $G\alpha_{i1}$, $G\alpha_{i2}$, $G\alpha_{i3}$), a post-translational myristoylation modification at the NH_2-terminal region increases the affinity of the α subunit for the βγ subunit (Simon et al., 1991). The Gα subunit can independently activate a multitude of downstream effectors to create a complex regulatory network to control cellular functions, including gene expression, cell metabolism, migration, proliferation, and membrane potential (Bridges & Lindsley, 2008).

1.2.3.1 $G\alpha_{s/olf}$ signalling

The primary effector of the $G\alpha_{s/olf}$ proteins is adenylyl cyclase (AC), a plasma membrane-bound enzyme that catalyzes the conversion of adenosine triphosphate (ATP) to cyclic adenosine monophosphate (cAMP), discovered by Martin Rodbell in 1971 (Pierce, Premont, & Lefkowitz, 2002; Bridges & Lindsley, 2008). When $G\alpha_s$ or $G\alpha_{olf}$ are bound to GTP, they will activate AC to induce intracellular cAMP production as a second messenger (Bridges & Lindsley, 2008). Downstream of $G\alpha_s$, these increases in cAMP levels will activate the serine/threonine kinase Protein Kinase A (PKA). When cAMP binds to PKA's regulatory subunits, this will lead to its dissociation from PKA's catalytic subunits to activate them (Pierce et al., 2002). PKA can phosphorylate the receptor directly to uncouple it from its respective G proteins, thereby serving

as a classical regulatory feedback loop, but can further propagate the signal to downstream protein kinases, phosphatases, and transcription factors (Pierce et al., 2002). Studies have shown that the $G\alpha_s$ subunit is also capable of regulating sodium, chloride, and L-type calcium channels to induce changes of the cell's membrane potential (Simon et al., 1991; Bridges & Lindsley, 2008). Examples of GPCRs that couple to $G\alpha_s$ include the β2-adrenergic receptor, the dopamine receptor D_1, and the serotonin receptor (Pierce et al., 2002). Furthermore, the $G\alpha_{olf}$ is solely activated by olfactory GPCRs in response to odorant molecules, resulting in increased cAMP levels, which open cyclic-nucleotide-gated ions channels and cause the depolarization of sensory neurons and subsequent transduction of action potentials to the brain (Ebrahimi & Chess, 1998).

1.2.3.2 $G\alpha_{i/o}$ signalling

The family of $G\alpha_{i/o}$ include the subtypes $G\alpha_{i1}$, $G\alpha_{i2}$, $G\alpha_{i3}$, $G\alpha_{o1}$, and $G\alpha_{o2}$. The primary effector of the $G\alpha_{i/o}$ proteins is also AC, however, binding of the G protein to this enzyme functions in opposition to $G\alpha_{s/olf}$ (i.e., to reduce the intracellular cAMP concentration). Activated $G\alpha_{i/o}$ binds to the catalytic region of AC to prevent ATP catalysis to cAMP, thus, blocking the activation of PKA or its downstream effectors, but $G\alpha_{i/o}$ has the potential to activate Src and protein kinases, including the extracellular regulated kinase (ERK)/mitogen-activated protein kinase (MAPK) cascade (Pierce et al., 2002). $G\alpha_{i1}$ and $G\alpha_{i3}$ have been shown to be able to couple to G protein-coupled inwardly rectifying potassium (GIRK) channels (Simon et al., 1991; Pierce et al., 2002). $G\alpha_o$ can regulate neuronal and atrial K^+ channels, as well as calcium channels in the dorsal root ganglia (Simon et al., 1991). Examples of GPCRs that can couple to $G\alpha_{i/o}$ include the γ-aminobutyric acid receptor ($GABA_BR$), dopamine receptor D_2, and both subtypes of cannabinoid receptors (CB_1 and CB_2; Navarro et al., 2008).

1.2.3.3 $G\alpha_{q/11}$ signalling

The primary effector for $G\alpha_{q/11}$ proteins is phospholipase C-β (PLC-β), a plasma membrane-bound enzyme responsible for the catalysis of phosphatidylinositol-4,5-bisphosphate (PIP_2) to two second messengers: diacylglycerol (DAG) and inositol-1,4,5-triphosphate (IP_3; Bridges & Lindsley, 2008). Cytosolic IP_3 binds and activates the IP_3 receptor (IP_3R) on the endoplasmic reticulum or sarcoplasmic reticulum surface, resulting in the release of calcium (Ca^{2+}) into the cytosol (Luciani et al., 2009). Thus, IP_3 controls various Ca^{2+}-dependent cellular functions, including but not limited to cell proliferation, differentiation, muscular contraction, immune responses, brain functions, and light transduction (Luciani et al., 2009). On the other hand, the plasma membrane-bound DAG is a physiological activator of PKC, a serine/threonine kinase responsible for the activation of intracellular proteins, amongst them being the cascade of Raf (a MAPKKK), MEK (a MAPKK), MAPK, and ERK1/2 (Gutkind, 2000). The phosphorylation of MAPKs result in their translocation to the nucleus, where they can regulate the functional activity of various transcription factors for cell growth, migration, and apoptosis (Gutkind, 2000). Examples of GPCRs that can couple to $G\alpha_{q/11}$ include vasopressin receptor type 2, oxytocin receptor, and the angiotensin II type 1 receptor (AT_1R; de Gasparo, Catt, Inagami, Wright, & Unger, 2000; Stoop, Hegoburu, & van den Burg, 2015).

1.2.3.4 $G\alpha_{12/13}$ signalling

The $G\alpha_{12/13}$ subunits are primary linked to the activation of the four members of the Rho family of GTPases (RhoGEFs): p115-RhoGEF, PSD-95/Disc-large/ZO-1 homology (PDZ)-RhoGEF, leukemia-associated RhoGEF (LARG), and lymphoid blast crisis (Lbc)-RhoGEF (Dutt,

Nguyen, & Toksoz, 2004). GTP-bound $G\alpha_{12/13}$ mediates the translocation of RhoGEF from the cytosol to the plasma membrane, resulting in its ability to hydrolyze the GTP within the α subunit for energy to become active and induce the downstream activation of the small, monomeric GTPase RhoA (Siehler, 2009). RhoA is responsible for actin cytoskeletal remodeling – through Rho-associated protein kinase 1/2's (ROCK1/2[4]) inhibition of myosin light chain phosphatase – and the induction of serum response element-based gene transcription (Dutt et al., 2004; Siehler, 2009). As a result, the downstream effects of the $G\alpha_{12/13}$ pathway elicit changes in cell shape, contraction, retraction, migration, and mitogenesis (Dutt et al., 2004). Examples of GPCRs that can couple to $G\alpha_{12/13}$ include M_1 and M_3 muscarinic acetylcholine receptors, AT_1R, and B_2 bradykinin receptors (Siehler, 2009).

1.2.4 Gβγ subunits and their downstream effectors

The βγ heterodimer, often seen as a single entity and tightly bound through non-covalent hydrophobic interactions, has several functions: (1) to stabilize the α subunit at the N-terminus in a confirmation that allows it to interact with the receptor at the α subunit's C-terminus, (2) to modulate downstream effects of the activate α subunit, and (3) to indirectly regulate ion channel and phospholipase activity at the plasma membrane, among other functions (Simon et al., 1991; Khan et al., 2013). Whereas it was initially believed only to be a regulatory component and scaffold of the Gα subunit, it is now understood that the βγ subunits can interact with multiple effectors, including twelve adenylyl cyclase subtypes, PLC-β, Kir3 inwardly rectifying potassium channels, voltage-gated calcium channels, phosphatidylinositol-3-kinase (PI3K), calcium ATPase

[4] ROCK1/2 are ubiquitously-expressed serine/threonine kinases shown to translocate from the cytosol to the plasma membrane upon activation by RhoA (Siehler, 2009)

transporters, and mitogen-activated protein kinases, among others (Khan et al., 2013). The responses of the βγ subunits are diversified by their ability to cross-talk with different α subunits (Simon et al., 1991). There was a hypothesis that the activation of a $G\alpha_x\beta\gamma$ heterotrimeric complex and the subsequent dissociation of the GTP-bound (active) $G\alpha_x$ subunit from the βγ heterodimer frees these latter subunits to inactivate another free GTP-bound $G\alpha_y$, where x and y are distinctive Gα subtypes. However, this theory was invalidated through experimenting with the use of other Gα binding partners, as they did not completely explain the activation kinetics initially proposed by this hypothesis (Simon et al., 1991).

A summary of all G protein subtypes with downstream signalling effectors is presented in Table 1.1 (adapted from Kristiansen, 2004).

Table 1.1: Summary of G protein subtypes and their downstream effectors.

G-protein class	G-protein subunits	Effectors	Regulation of effector	References
Gs	Gαs	AC1-9	Stimulation	Pierce et al., 2002;
		c-Src	Stimulation	Cabrera-Vera et al.,2003
		RGS-PX1	Stimulation	
		Tubulin	Stimulation of GTPase activity	
	Golf	ACS	Stimulation	
Gi	Gαtr	PDE6	Stimulation	Mochizuki et al., 1999;
	Gαtc	PDE6	Stimulation	Pierce et al., 2002;
	Gαg	PDE	Stimulation	Cabrera-Vera et al.,2003
	Gαi1 – 3,	AC5, AC6	Inhibition	
	Gαo	c-Src	Stimulation	
		RAP1GAPII	Sequestration of RAP1GAP	
		Ca^{2+} channels	Inhibition (Gαo)	
		G-protein-activated inwardly rectifying K^+ channel (GIRK) channels	Stimulation (Gαi)	
		Tubulin	Stimulation of GTPase activity	
		G-protein-regulated inducer of neurite outgrowth (GRIN) 1 and GRIN2	Unknown	
Gq	Gαq, 11, 14, 15/16	PLCβ1 – 4	Stimulation	Pierce et al., 2002;
		Leukemia-associated-RhoGEF (LARG-RhoGEF)	Stimulation (indirect activation of Rho)	Cabrera-Vera et al.,2003 Willets et al., 2003
		GRK2, GRK3	Stimulation	
		Bruton's tyrosine kinase	Stimulation (indirect stimulation of p38 MAPK)	Jiang et al., 1998;
G12	Gα12, Gα13	P115-RhoGEF, PDZ RhoGEF, LARG-RhoGEF	Stimulation (indirect activation of Rho and stress fiber formation)	Pierce et al., 2002
		GTPase-activating protein of ras (GAP1m)	Stimulation (indirect activation of ras)	
		E-cadherin	Stimulation (stimulation of β-catenin release)	
	Gβγ	PI3Kγ, PI3Kβ	Stimulation	Pierce et al., 2002;
		$AC2^a$, $AC4^a$, AC7	Stimulation	Cabrera-Vera et al.,2003
		AC1	Inhibition	Willets et al., 2003
		PLCβ1 – 3	Stimulation	
		GRK2, GRK3	Recruitment to plasma membrane	
		GIRK1, GIRK2, and GIRK4	Stimulation	
		ATP-sensitive K^+ channels	Stimulation	
		Ca^{2+} channels	Inhibition	
		Small GTP binding proteins (Rho and Rac)	Recruitment to plasma membrane	
		Bruton's tyrosine kinase	Stimulation	
		Tsk tyrosine kinase	Stimulation	
		Protein kinase D	Stimulation	
		Calmodulin	Inhibition of calmodulin kinase	
		Tubulin	Increased GTPase activity	
		Dynamin I	Increased GTPase activity	
		Shc	Stimulation (indirect activation of MAPK)	
		Raf1 protein kinase	Sequestration of Gβγ	
		Ras guanine nucleotide releasing factor/ CDC25Mm	Stimulation (indirect activation of ras)	
		KSR-1	Sequestration of Gβγ	

[a] AC2 and AC4 are synergistically activated by α_s and βγ.

Each G protein is able to activate and/or couple to a multitude of effectors, depending on the subtype. Equivalent G protein subtypes can recruit a protein to the plasma membrane, activate multiple effectors directly or indirectly, or activate one protein while inactivating another. AC, adenylyl cyclase; PDE, phosphodiesterase; PLC, phospholipase C; PI3K, phosphatidylinositol 3-kinase; GRK, G protein-regulated kinase; RhoGEF, Rho guanine nucleotide exchange factor; KSR, kinase suppressor of Ras. (Table adapted from Kristiansen, 2004).

1.2.5 GPCR desensitization and internalization

In the absence of a stimulus, constitutive GPCR internalization occurs from the cell surface into early endosomal structures at a relatively slow rate – a rate similar to that of integral membrane proteins (von Zastrow & Kobilka, 1994; Goh & Sorkin, 2013). The seven transmembrane (7TM) receptor expression within a cell is in equilibrium between expression at the cell surface, sequestration within intracellular compartments, protein synthesis of nascent receptors, and degradation. However, receptor-mediated endocytosis, also referred to as clathrin-mediated endocytosis, perturbs this equilibrium for many 7TM receptors (von Zastrow & Kobilka, 1994; Goh & Sorkin, 2013). Within minutes of ligand binding, the rate of receptor-mediated endocytosis is dramatically increased as a culmination of two key groups of effector proteins: G protein receptor kinases (GRKs) and β-arrestins (Koenig & Edwardson, 1997; Drake, Shenoy, & Lefkowitz, 2006). Agonist-bound 7TM receptors become substrates for G protein kinase-mediated receptor phosphorylation on their cytoplasmic domains, resulting in the recruitment of β-arrestins to the phosphorylated receptor to act as a scaffold for the assembly of endocytic machinery, ensuing the clathrin-dependent internalization of the complex (Drake et al., 2006). Additionally, the association of β-arrestin with the phosphorylated sites on the cytoplasmic domain of the receptor uncouples the receptor's G protein signalling capabilities, making the receptor refractory to stimuli and leading to short-term or long-term desensitization[5] (Chuang, Iacovelli, Sallese, & De Blasi, 1996; Oakley, Laporte, Holt, Barak, & Caron, 1999). Phosphorylation of only agonist-occupied receptors is termed homologous desensitization, which mainly involves GRKs and β-arrestins, whereas heterologous desensitization – the phosphorylation and uncoupling of both

[5] Desensitization prevents the continuous or repeated stimulation of the receptor, allowing the cell to regulate responsiveness and employ feedback loops to terminate cellular signalling responses.

agonist-bound and unbound surface receptors – involves the second-messenger dependent kinases PKA and PKC, which phosphorylate at different sites than the GRKs (Chuang et al., 1996; Oakley et al., 1999). These receptor/β-arrestin complexes will traffic to sorting endosomes, which can follow two distinct pathways: recycling to the plasma membrane or proteolytic degradation of the receptor (Oakley et al., 1999).

β-arrestin, a cytosolic scaffold protein that bridges GPCRs and intracellular effectors, is a member of the arrestin family of proteins (arrestin1-4; Zheng et al., 2010). Arrestin1 and arrestin4 (visual arrestins) are uniquely found in retinal rods and cones for phototransduction, whereas arrestin2 (β-arrestin-1) and arrestin3 (β-arrestin-2) are expressed ubiquitously (Zheng et al., 2010). GPCRs can be classified by another dichotomy as either type A or type B receptors, depending on their β-arrestin-internalization profile (Oakley et al., 1999; reviewed by Maurice et al., 2011). Type A GPCRs interact weakly with β-arrestins in a transient fashion near the cell surface, as these receptors are rapidly dephosphorylated in early endosomes and recycled quickly back to the plasma membrane following internalization (Oakley et al., 1999). Type A GPCRs have a higher affinity for β-arrestin-2 than β-arrestin-1 and archetypal members of this group include β2 adrenergic receptors, μ-opioid receptors, and the dopamine D_1 receptors (Maurice et al., 2011). Conversely, type B GPCRs engage both β-arrestin-2 and β-arrestin-1 with high avidity, leading to a prolonged half-life of the complex in endosomes and preferential trafficking to late endosomes (Oakley et al., 1999). Type B GPCRs include the neurotensin 1 receptors, AT_1Rs, and vasopressin V2 receptors (Maurice et al., 2011).

1.2.5.1 Clathrin-mediated endocytosis

For the majority of GPCRs, β-arrestins provide a scaffold to target the desensitized receptor to clathrin-coated vesicles for internalization (Oakley et al., 1999). The coupling of β-arrestin to the GRK-phosphorylated receptor initiates the association of the endocytoic machinery, including clathrin and the heterotetrameric assembly polypeptide (AP) complex (Laporte et al., 1999; Kirchhausen, 2000; Zimmerman et al., 2012).

Clathrin is a triskelion protein that forms a cage-like structure of pentagons and hexagons with itself to envelope an invagination of the lipid bilayer (Kirchhausen, 2000). In his review, Kirchhausen described clathrin-coated vesicles (CCVs) to be ubiquitously "found in all nucleated cells, from yeasts to humans" (2000). Not only do CCVs sequester proteins from the plasma membrane into endosomes, but they also export lipids and proteins from the *trans*-Golgi network to endosomes (Kirchhausen, 2000). The cycle of CCV formation begins with the nucleation or initiation of a pit, followed by the propagation of the clathrin lattice, invagination of the bilayer, and cargo recruitment. The completed polyhedral lattice and bilayer are pinched off to form the vesicle with a diameter ranging from ≥600 Å to ≥2000 Å. Finally, the coated vesicle is transported away from the membrane and internalization terminates with the dissociation of the clathrin coat in the cytosol, leaving the fully formed early endosome (Laporte et al., 1999; Kirchhausen, 2000). In order to uncage the CCV, an endothermic reaction must take the lattice apart. Heat shock protein 70 (Hsp70) is a chaperone that triggers protein disassembly and unfolding by using energy from the hydrolysis of ATP (Kirchhausen, 2000). Disassembly of the CCV proceeds very rapidly once the vesicle buds from the plasma membrane and the proton pumps acidify the vesicle lumen (Kirchhausen, 2000).

AP-2 belongs to a highly conserved heterotetrameric assembly polypeptide family with three other members: AP-1, AP-3, and AP-4 (Laporte et al., 1999; Kirchhausen, 2000). The AP-2 complex (α chain, β2 chain, μ2 chain, and σ2 chain) has been shown to interact with the clathrin heavy chain and the β-arrestin/receptor complex using its α chain and β2 chain, respectively (Laporte et al., 1999; Kirchhausen, 2000). AP-2 promotes clathrin lattice assembly upon its binding and forms CCVs, whereas β-arrestin alone is not able to promote the assembly of clathrin into its lattice structure (Laporte et al., 1999). AP-2 has also been implicated with dynamin interaction, a "pinchase" GTPase protein involved in separating the vesicle from its membrane, via its α chain (Kirchhausen, 2000).

1.2.5.2 Non-clathrin-mediated endocytosis

Although clathrin-mediated endocytosis has been well-established, the pathway involving internalization through non-coated pits remains somewhat obscure. It has been proposed that certain ligands do not cluster with clathrin, but rather invaginate in non-clathrin-coated vesicles (Tran, Carpentier, Sawano, Gorden, & Orci, 1987). This non-clathrin-mediated endocytosis has been observed in the presence of cholera toxin, which can bind to $G\alpha_s$ to activate adenylyl cyclase and induce internalization (Tran *et al.*, 1987). This form of 7TM receptor internalization independent of β-arrestin or clathrin intervention is called caveolin-dependent internalization (Nabi & Le, 2003). Caveolin is an integral membrane protein that is associated with caveolae, which are cholesterol- and sphingolipid-rich invaginations of the plasma membrane that are distinct from clathrin-coated pits (Nabi & Le, 2003). Like CCVs, caveolae require the assistance of the GTPase dynamin for the budding from the plasma membrane (Nabi & Le, 2003). Many receptors internalize through both pathways, where the inhibition of one endocytic pathway results

in compensation by the other. In Roettger *et al.* (1995), the authors demonstrate that the cholecystokinin (CCK) receptor internalizes via both clathrin-dependent and independent pathways. Whereas clathrin-mediated internalization was more abundant following CCK stimulation and formed both endosomes and lysosomes, the clathrin-independent processes lead to smooth vesicular caveolae, which do not transport the receptor deeper within the cell. Furthermore, clathrin-mediated endocytosis could be blocked by potassium depletion without obstructing caveolar transport of the receptor. However, the physiological consequences of using different routes of internalization remains largely unclear.

1.2.6 β-arrestin signalling

Independent from GPCR–G protein signaling, the role of β-arrestin as an adaptor and scaffolding protein, although previously unsuspected, has been implicated in its own downstream signalling events (Marinissen & Gutkind, 2001; Khoury, Nikolajev, Simaan, Namkung, & Laporte, 2014). However, the *in vivo* evidence and physiological relevance of β-arrestin-mediated signalling remains unclear, although, studies in mice have demonstrated the importance of β-arrestin-mediated signalling in dopaminergic slow synaptic transmission (Beaulieu et al., 2005). Furthermore, β-arrestin has been shown to recruit and activate the Src family of non-receptor tyrosine kinases. In particular, Src is recruited to the β-arrestin/receptor complex to phosphorylate the β subunit of the AP-2 heterotetramer, permitting CCV endocytosis (Zimmerman, Simaan, Lee, Luttrell, & Laporte, 2009). Furthermore, this β-arrestin scaffold permits Src kinase to directly activate the Akt pathway, which regulates glycogenesis, embryonic development, inflammation, apoptosis, and cell proliferation, among other cellular processes (Beaulieu et al., 2005). Thus, β-arrestin-mediated signalling may be relevant to these physiological processes associated with Akt

and MAPK. Src kinases have been shown to be responsible for MAPK and ERK1/2 phosphorylation independent from G proteins, leading to gene transcription and gene expression (Zimmerman et al., 2009). As a positive feedback mechanism, MAPK activity at a regulatory site in the β-arrestin-2 hinge domain was determined to increase the avidity of the β-arrestin-2/receptor complex and promote slower recycling of the receptor to the plasma membrane (Khoury, Nikolajev, et al., 2014). Recently, Eichel, Jullié, & von Zastrow (2016) have shown that β-arrestin can drive MAPK activation directly from clathrin-coated structures without forming endosomes.

1.2.7 Application of biased agonism

As previously mentioned, the multi-state model is capable of directing distinct signalling pathways from the same activated receptor, also referred to as "biased agonism" (Kobilka, 2007). Several ligands have this capacity to engage unique signalling transduction pathways and have been further developed for their therapeutic advantages to selectively activate desired outcomes and limit unwanted side effects. The angiotensin II analogue SII ([Sar^1-Ile^4-Ile^8]-Ang II) has been previously shown to have β-arrestin-2 pathway selectivity over canonical G protein activation (Zimmerman et al., 2012). Recently, new biased peptide ligands were developed: TRV120023 (Sar-Arg-Val-Tyr-Lys-His-Pro-Ala-OH) and TRV120027 (Sar-Arg-Val-Tyr-Ile-His-Pro-$_D$-Ala-OH). These peptides have higher binding affinities than SII for the AT_1R and the ability to selectively engage the β-arrestin–mediated signalling pathway, which has shown to possess beneficial effects on cardiac contractility and performance in rats and dogs (Szakadáti et al., 2015). Thus, these TRV compounds and their favourable properties are currently under investigation for their clinical applications in the treatment of acute heart failure (Szakadáti et al., 2015).

1.3 Role of the angiotensin II type 1 receptor (AT_1R)

1.3.1 Historical background

In their review, de Gasparo *et al.* (2000) eloquently summarize the findings and physiological examination of blood pressure since 1733 when it was first measured by Stephen Hales who inserted a brass pipe into the carotid artery of a horse. This achievement was followed by the discovery of a factor able to increase blood pressure by Tigerstedt & Bergman in 1897. This factor was termed "renin" because of its extraction from the kidney. Bruan-Menendez, Fasciolo, Leloir, & Munoz (1940) isolated a vasoconstrictor "substance" from the venous blood from the ischemic kidney of a hypertensive dog different from renin, naming it "hypertensin". In 1940, Page & Helmer discovered a "renin activator", which later proved to be the precursor peptide angiotensinogen for the pressor substance they called "angiotonin". In 1958, the two research groups agreed on the hybrid term for the peptide: angiotensin.

1.3.2 Angiotensin II (Ang II) and the Angiotensin II type 1 Receptor (AT_1R)

Angiotensin II (Asp^1-Arg^2-Val^3-Tyr^4-Ile^5-His^6-Pro^7-Phe^8) is the endogenous octapeptide hormone responsible for numerous physiological actions, including its hypertensive effects via the angiotensin II type 1 receptor (de Gasparo et al., 2000). Ang II shares the same peptide sequence in humans, horses, and pigs (de Gasparo et al., 2000). Following the discovery of angiotensin, the cascade leading to the formation of angiotensin II was elucidated to include, in succession, angiotensinogen, angiotensin converting enzyme (ACE), angiotensin I, angiotensin II, and the metabolites: angiotensin III, angiotensin IV, and angiotensin 1-7 (de Gasparo et al., 2000). Ang II is produced from the enzymatic cleavage of its precursor angiotensin I (Asp^1-Arg^2-Val^3-Tyr^4-Ile^5-His^6-Pro^7-Phe^8-His^9-Leu^{10}; de Gasparo et al., 2000). The understanding of the mechanism of Ang

II binding and activation of the angiotensin II type 1 receptor has been advanced by investigation of Ang II analogues[6] in conjunction with mutated AT_1 receptors (Hunyady et al., 2003).

The human angiotensin II receptor is a member of the rhodopsin-like β-group (or Class A) receptors, containing 359 amino acids encoded by the gene *AGTR1*, which is located on chromosome 3q22 (de Gasparo et al., 2000; Fredriksson et al., 2003). The extracellular regions contain three *N*-glycosylation sites and four conserved cysteine residues that participate in disulfide bonding to maintain the structure of the folded protein (de Gasparo et al., 2000). The AT_1 receptor is expressed in the adrenal glands, kidneys, brain, pituitary gland, vascular smooth muscle, endometrium, placenta, and the sympathetic nervous system (de Gasparo et al., 2000); Lin & Goodfriend (1970) were first to use radioiodinated Ang II (^{125}I-Ang II) binding to identify receptors in the adrenal glands *in vitro*. The heterogeneity and existence of receptor subtypes were elucidated with the help of non-peptide antagonists losartan and PD123177 for the angiotensin II type 1 (AT_1) receptor and angiotensin II type II (AT_2) receptor, respectively (de Gasparo et al., 2000). In addition to the AT_1 and AT_2 receptors, two other subtypes of the receptor are known: the AT_3 and AT_4. The AT_3 receptor was identified in mouse neuroblastoma cells and able to bind Ang II with nanomolar affinity (Karnik et al., 2015). Despite the AT_3 mRNA was found to be abundant in the adrenal cortex and pituitary tissues, a gene to that matches cDNA of the receptor has not been found (Karnik et al., 2015). Likewise, the AT4 receptor was identified by a Ang IV (VYIHPF) binding site and found in the brain, heart, kidney, adrenals, and blood vessels, but has not shown to play a physiological role in the body (Karnik et al., 2015). However, the Ang IV binding site is now considered not to be a GPCR, but rather an insulin regulated aminopeptidase (Karnik et al.,

[6] Analogues of the Ang II peptide, created by substituting amino acids in the octapeptide sequence, were created in the hopes of finding an antagonist of the receptor (de Gasparo et al., 2000).

2015). Of the angiotensin receptors cloned, the non-mammalian receptors possess 60% sequence homology with the mammalian receptors, however, both are pharmacologically distinct in their ligand binding properties (de Gasparo et al., 2000).

Figure 1.4 shows the mammalian AT_1 receptor structure with molecular contact sites of Ang II in purple and G protein binding sites in green (Hunyady et al., 2003). The biological activity of Ang II is highly dependent on its Phe^8 aromatic residue for receptor binding and intrinsic activity (de Gasparo et al., 2000). In contrast, the N-terminal residues are important for receptor binding to the first and third extracellular loops, but not specifically for the biological activity of Ang II (de Gasparo et al., 2000). This can be demonstrated by the heptapeptide Ang III, formed by cleavage of the Asp^1 residue on Ang II, which has similar potency to the native octapeptide angiotensin II (de Gasparo et al., 2000).

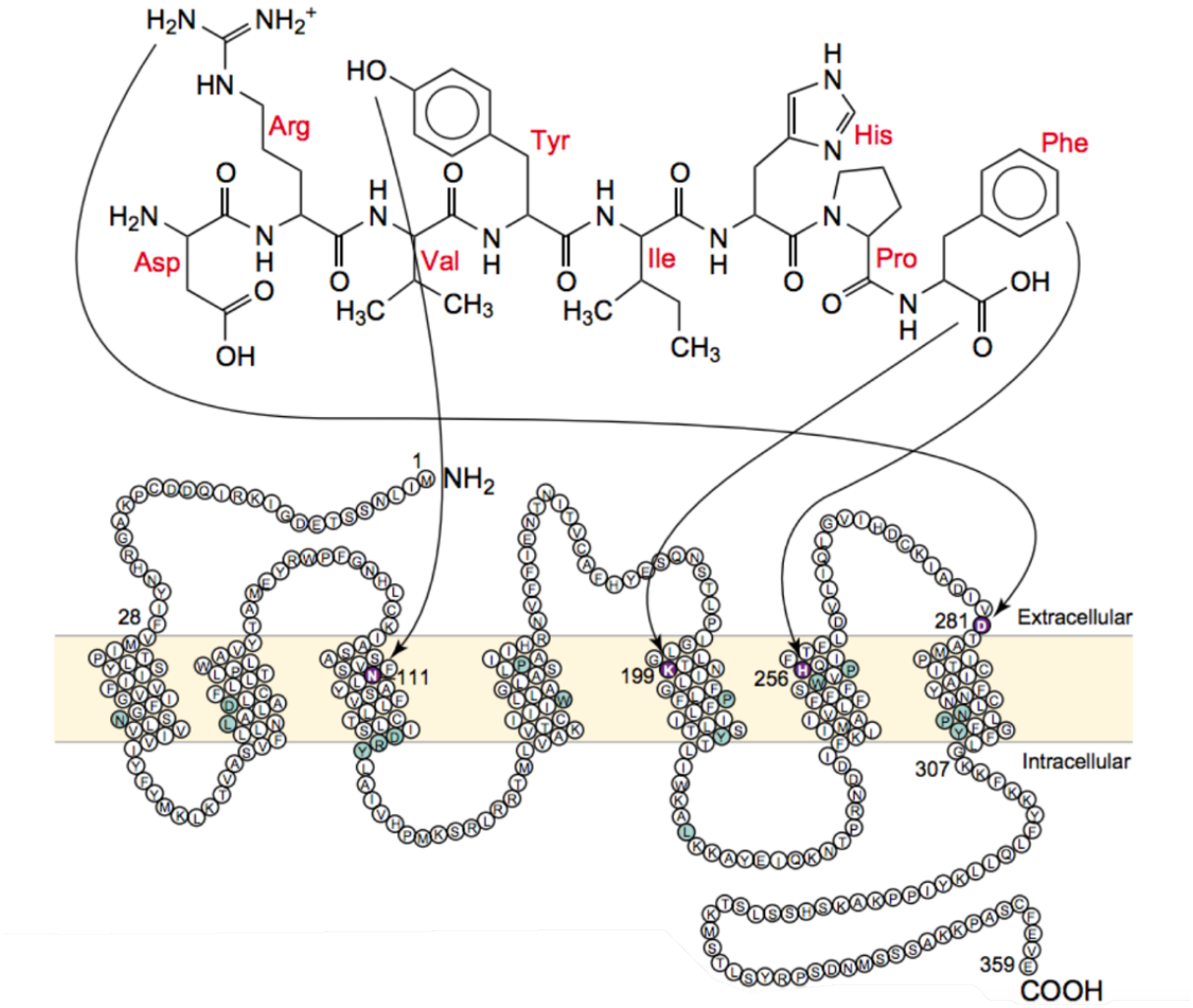

Figure 1.4: A two-dimensional representation of the mammalian AT_1 receptor structure and the molecular contact sites of angiotensin II (Ang II) octapeptide. The main amino acids in the receptor contributing to the Ang II binding are indicated in purple. The residues conserved among the superfamily of GPCRs for their interaction with heterotrimeric G proteins are depicted in green. The biological activity of Ang II is highly dependent on its Phe^8 aromatic residue for receptor binding and intrinsic activity. The extracellular and intracellular regions are indicated above and below the yellow shaded area, whereas the transmembrane region is depicted within the yellow shaded area. (Adapted from Hunyady et al., 2003).

1.3.3 Renin-Angiotensin-Aldosterone System

The Renin-Angiotensin-Aldosterone System (RAAS) is a hormone system that controls atrial blood pressure, vascular tone, electrolyte-water homeostasis, thirst, hormone secretion, and renal function through coordinated effects on the heart, kidneys, and blood vessels (de Gasparo et al., 2000; Hunyady et al., 2003; Remuzzi, Perico, Macia, & Ruggenenti, 2005). The RAAS functions as a negative feedback loop in response to a decrease in the mean arterial blood pressure, an increase in water and electrolyte resorption and retention, and/or an increase of the cardiac output (Palmer, 2004). Three sensory sites can regulate the actions of the RAAS: (1) low sodium sensed by the nephron, (2) low renal perfusion rates in the glomerulus, or (3) low blood pressure sensed in the carotid sinus. As a result of any perturbation in the homeostasis at any of these three sensory sites, the enzyme renin, also known as angiotensinogenase, is secreted from the juxtaglomerular cells of the kidney and acts on its circulating precursor angiotensinogen (Asp^{1}-Arg^{2}-Val^{3}-Tyr^{4}-Ile^{5}-His^{6}-Pro^{7}-Phe^{8}-His^{9}-Leu^{10}-Leu^{11}-Val^{12}-Tyr^{13}-Ser^{14}), which is produced by the liver (Palmer, 2004; Remuzzi et al., 2005). Angiotensinogen is cleaved by renin to angiotensin I (Asp^{1}-Arg^{2}-Val^{3}-Tyr^{4}-Ile^{5}-His^{6}-Pro^{7}-Phe^{8}-His^{9}-Leu^{10}), resulting in the removal of the final four amino acids (de Gasparo et al., 2000). Angiotensin I has little effect on blood pressure, but circulates to the lungs where the endothelial-bound angiotensin converting enzyme (ACE) further cleaves angiotensin I to the octapeptide angiotensin II (Asp^{1}-Arg^{2}-Val^{3}-Tyr^{4}-Ile^{5}-His^{6}-Pro^{7}-Phe^{8}; Remuzzi et al., 2005). Additionally, ACE can be found in the endothelial or kidney epithelial cells (de Gasparo et al., 2000), whereas ACE type-2 (ACE2) is only present in the glomerular epithelium and vascular smooth muscle cells, where it cleaves angiotensin I into the inactive angiotensin 1-9 (Remuzzi et al., 2005). Angiotensin II exerts its pressor effect predominantly on the post-glomerular arterioles to increase glomerular hydraulic pressure and the filtration fraction of the

kidney. Furthermore, angiotensin II acts indirectly to increase blood pressure by binding to AT_1 receptors on the adrenal glands to trigger the steroidogenesis of aldosterone (Remuzzi et al., 2005), and AT_1 receptors in the posterior pituitary gland to signal the release of the peptide hormone vasopressin, also known as antidiuretic hormone, resulting in the kidneys to increase fluid retention (de Gasparo et al., 2000). Aldosterone is the principal mineralocorticoid produced by the zona glomerulosa of the adrenal cortex and locally in the endothelial and vascular smooth muscle cells of the heart, blood vessels, and brain (Remuzzi et al., 2005). Aldosterone secretion from the adrenal cortex results in its binding to the aldosterone receptor in the cytosol of the collecting duct cells of the kidney, stimulating sodium reabsorption across sodium transport channels on the luminal membrane, trailed by the resorption of water (Palmer, 2004). As the electronegativity of the lumen increases, this results the secretion of potassium ions through potassium channels on the apical membrane into the lumen to maintain electrolyte homeostasis (Palmer, 2004). Figure 1.5 adapted from Palmer (2004) summarizes the Renin-Angiotensin-Aldosterone System.

If untreated, aberrant upregulation of the RAAS marks chronic renal disease due to sustained cell growth, inflammation, and fibrosis (Palmer, 2004), development of hypertensive vascular disease and congestive heart failure (de Gasparo et al., 2000; Palmer, 2004), and hypokalemia due to an increase in aldosterone production (Palmer, 2004). Thereby, the pharmacological inhibition of Ang II remains a popular mechanism for the prevention and treatment of RAAS pathophysiology, in addition to lifestyle changes. Two prevalent forms of pharmacological intervention target specific elements of this axis: the first being angiotensin converting enzyme inhibitors (ACEi), which prevent the formation of Ang II by inhibiting the angiotensin converting enzyme, and the second being competitive antagonists of the receptor, known as angiotensin II receptors blockers (ARBs). The first angiotensin converting enzyme

inhibitor captopril (Capoten; Bristol-Myers Squibb) became available for clinical use in the early 1980s and remains a popular first-line intervention for hypertension and congestive heart failure (Remuzzi et al., 2005). Losartan (Cozaar; Dupont, Merck and Co.) was the first clinically effective ARB to treat hypertension (Arsenault et al., 2010). As for ARBs, there is a growing understanding of the true complexity of biased receptor signalling that has illuminated possibilities for a more refined approach than simple activation or inhibition. Mutagenesis of G protein binding sites on the receptor or knockout studies of β-arrestin in mice helped elucidate the cardioprotective role of β-arrestin-2 when engaged to the AT_1 receptor by activating MAPK and Akt signalling (Beaulieu et al., 2005; DeWire & Violin, 2011; Zimmerman et al., 2012). Thus, ligands that stabilize a conformation that can selectively engage the β-arrestin pathway over G protein coupling have the potential to be superior over classic agonists or antagonists by two measures: (1) by reducing unwanted full "on-target" effects, or (2) by beneficially targeting the signaling pathway(s) required to mediate imperative physiological outcomes (DeWire & Violin, 2011).

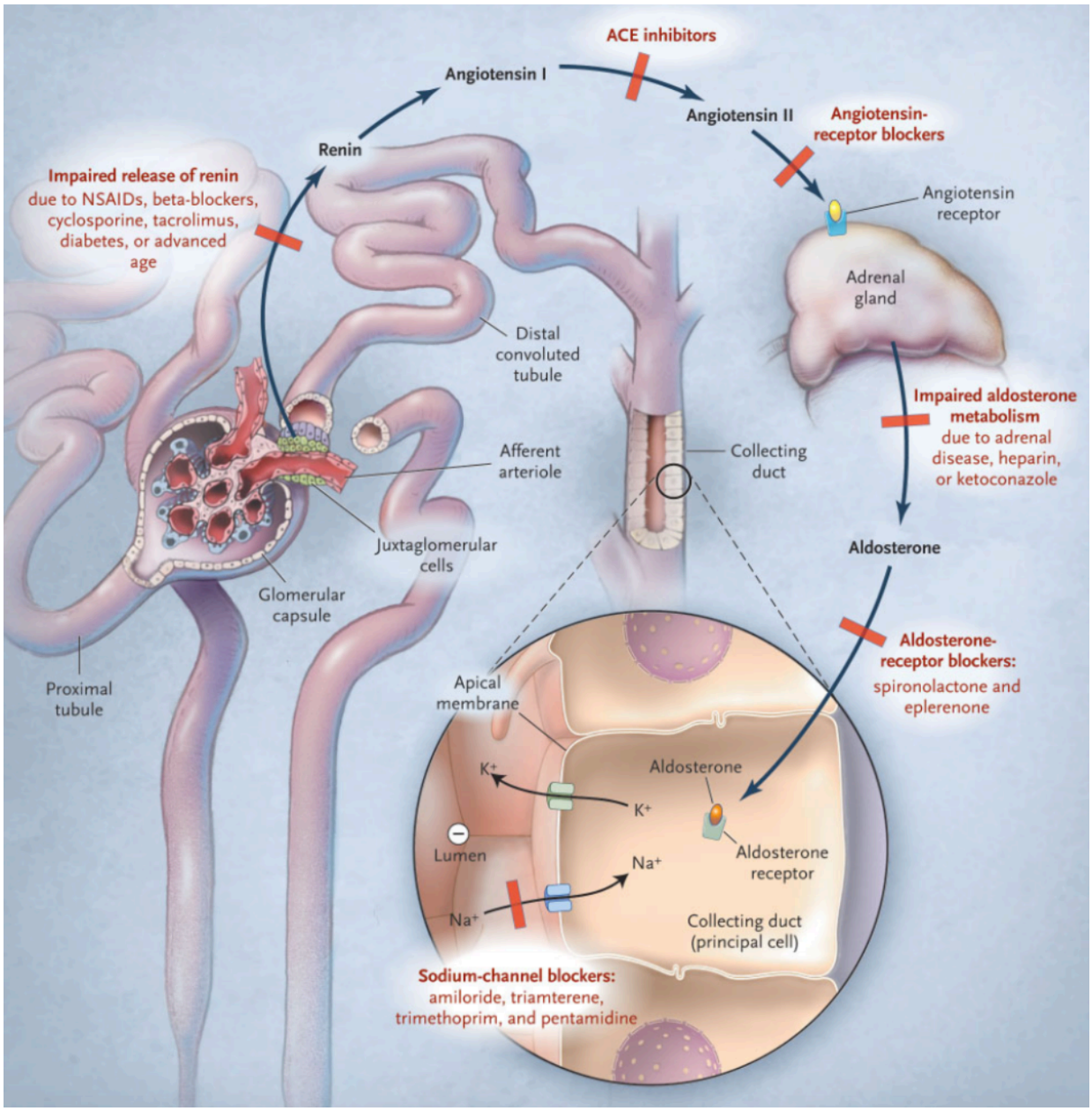

Figure 1.5: Overview of the Renin-Angiotensin-Aldosterone System (RAAS). The RAAS functions as a negative feedback loop in response to a decrease in the mean arterial blood pressure. Renin is secreted from juxtaglomerular cells of the kidney and acts on the circulating precursor angiotensinogen, which is produced by the liver. Angiotensinogen is cleaved to angiotensin I, which then circulates to the lungs where angiotensin converting enzyme (ACE) further cleaves angiotensin I to angiotensin II. Angiotensin II binds to AT_1 receptors in the adrenal cortex to

prompt steroidogenesis and the secretion of aldosterone. Aldosterone secretion into the blood results in its binding to the cytosolic aldosterone receptor found in the collecting duct cells of the kidney, resulting in sodium and water reabsorption. As the electronegativity of the lumen increases, this results the secretion of potassium ions into the lumen through potassium channels to maintain electrolyte homeostasis. Pharmacological interventions for modulation of this pathway or pathophysiological interferences of this axis are described in red, including ACE inhibitors. angiotensin II receptor blockers, and aldosterone receptor blockers (Adapted from Palmer, 2004).

1.3.4 AT_1R signalling

Angiotensin II activation of the AT_1R is triggered by the interaction between Tyr^4 of Ang II and the Asn^{111} residue in the third transmembrane domain of the receptor, and the interaction of Phe^8 of Ang II with His^{256} in the sixth transmembrane domain, the latter which coerces the AT_1R into its activated conformation (de Gasparo et al., 2000). AT_1 receptor activation results in the contraction of smooth muscle cells, adrenal steroidogenesis of aldosterone, secretion of neuropeptides, ion transport, and cell proliferation (de Gasparo et al., 2000).

Although the AT_1 receptor has been reported to interact with several G proteins, its canonical physiological functions are directed through $G\alpha_{q/11}$-mediated signaling (de Gasparo et al., 2000); the other significant agonist-mediated G protein interactions include the $G\alpha_{12/13}$, $G\alpha_{i2}$, and $G\alpha_{i3}$ proteins (de Gasparo et al., 2000). Studies in hepatocyte membranes showed that $G\alpha_{i3}$ is the major subtype of $G\alpha_i$ responsible for the inhibition of adenylyl cyclase activity by the AT_1R (Pobiner, Northup, Bauer, Fraser, & Garrison, 1991).

In vascular smooth muscle cells, AT_1R signalling stimulates DNA transcription and protein synthesis for the growth and remodeling of the human vascular system. This output is a consequence of the activation of the mitogen-activated protein kinase cascade and can be inhibited by the angiotensin II receptor blocker losartan or by the MAPK inhibitor PD-98059 (Morrell et al., 1999). Moreover, the AT_2 receptor has been shown to antagonize the effects of AT_1 receptor-mediated growth responses, in particular, within endothelial cells, cardiomyocytes, and ovarian granulosa cells (de Gasparo et al., 2000). The pathways that can mediate ERK1/2 phosphorylation by GPCRs include the PKC/PKA pathway and the β-arrestin signalling pathway, which involve G proteins and β-arrestins, respectively (Zheng, Loh, & Law, 2010). Ang II-mediated ERK1/2 activation is often subdivided temporally into two phases: an early G protein-dependent and β-

arrestin-dependent phase and a late/sustained β-arrestin-dependent phase (Zheng et al., 2010; Eichel, Jullié, & von Zastrow, 2016).

Beyond G protein or β-arrestin activation, AT_1R also activates ERK1/2 indirectly by Src kinases, Pyk2, and AT_1R-mediated transactivation of receptor tyrosine kinases (e.g., epidermal growth factor receptors and platelet-derived growth factor receptors; Zheng et al., 2010). Furthermore, if the receptor is phosphorylated on the tetrapeptide YIPP motif located within the C-terminal tail of the AT_1 receptor, this permits the rapid and transient activation of Janus Kinase 2/Signal Transducers and Activators of Transcription (Jak2/STAT); the latter can translocate to the nucleus and induces gene transcription (de Gasparo et al., 2000). Moreover, studies of AT_1R signalling have revealed its capability to directly activate L-type Ca^{2+} via its Gβγ subunits (Simon et al., 1991), its involvement in cytoskeletal remodelling via activation of Rho GTPases (Dutt et al., 2004), and its regulation of transcription factors for cellular survival, growth, or hypertrophy (Morrell et al., 1999).

1.4 AT_1 Receptor Gene Polymorphisms

1.4.1 Overview of Single Nucleotide Polymorphisms

The passing of genetic code requires the replication of DNA, and while the process of DNA replication is remarkably meticulous and precise, errors occasionally occur and produce changes in this DNA sequence. It is these errors that produce variation in the population and drive the evolution of species. As long as these changes are not deleterious to the individual or there are no discernible effects to the germ line, these mutations are propagated to the progeny from generation to generation. Although it is more common for substitutions, deletions, or changes in the DNA sequence to occur in the non-coding regions between the exons, there is also the possibility that

these small variations occur in the coding peptide sequence, but do not alter the phenotype or the function of the protein translated from this sequence. These small differences in the base pair sequence (e.g., C to T; G to A) are termed single nucleotide polymorphisms (SNPs), as they often include only a single base pair alteration during the replication or the repair of germ line DNA. This observed heterogeneity in the population from genomic variation also affects the susceptibility of the carriers to disease and altered efficacy of drugs currently on the market. The study of pharmacogenetics and hypothesis-based clinical testing would improve the safety of prescribing guidelines based on the refined understanding of drug absorption, distribution, metabolism, and excretion in these polymorphic populations.

The phenomenon permitting more than one codon to code for the same single amino acid is known as the Wobble Hypothesis, first described by Francis Crick in 1966. Using multiple codon sequences for coding an amino acid permits flexibility, especially in the case of errors and mutations in the DNA sequence. Thus, the change created by a mutation can be inert if it results in the same amino acid and the same gene product (Hansen, Haunsø, Brann, Sheikh, & Weiner, 2004). However, there are cases of non-synonymous single nucleotide polymorphisms, where the single base pair change within a codon results in a new amino acid (Hansen et al., 2004).

The National Center for Biotechnology Information SNP database lists over 600 putative single nucleotide polymorphisms for the human *AGTR1* gene – few of which have been validated as possible mediators of disease or linked to pathophysiological outcomes (Oro, Qian, & Thomas, 2007). Furthermore, the frequency of these polymorphism occurrences in the population has yet to be fully established and only a few of these polymorphisms have been functionally characterized (Oro et al., 2007). The first widely-researched gene polymorphism in the human *AGTR1* gene was

A1166C[7], which was found more frequently in hypertensive patients and acted synergistically with ACE polymorphisms to increase the risk of myocardial infarction (Bonnardeaux et al., 1994; de Gasparo et al., 2000; Oro et al., 2007). At least 19 SNP have been found to be located in the coding region of the AT_1R, of which, twelve are non-synonymous point mutations (Table 1.2; Figure 1.6).

Table 1.2: Single nucleotide polymorphisms reported in the human AT_1 receptor coding region.

SNP	Position	Amino Acid Change
C/T	191	Leu
T/C	285	Pro
T/G	300	Leu
G/A	306	Gly
A/G	317	Leu
A/G	323	Lys
A/G	354	Pro
T/C	6	Ser → Pro
T/G	41	Val → Gly
G/A	45	Gly → Arg
G/A	163	Ala → Thr
T/C	204	Phe → Ser
C/G	222	Leu → Val
G/T	244	Ala → Ser
C/T	282	Thr → Met
T/G	289	Cys → Trp
C/T	330	Leu → Phe
A/C	336	Thr → Pro
C/A	341	Pro → His

The single nucleotide polymorphisms (SNPs) are grouped depending on synonymous (black) or non-synonymous (purple) polymorphisms in the AT_1 receptor coding sequence. The position corresponds to the amino acid location in the receptor, starting with methionine as 1 at the N-terminus. (Data for table adapted from Hansen et al., 2004; Gribouval et al., 2005; Oro et al., 2007).

[7] Position 1166 is found in the 3'-untranslated region of the human *AGTR1* gene

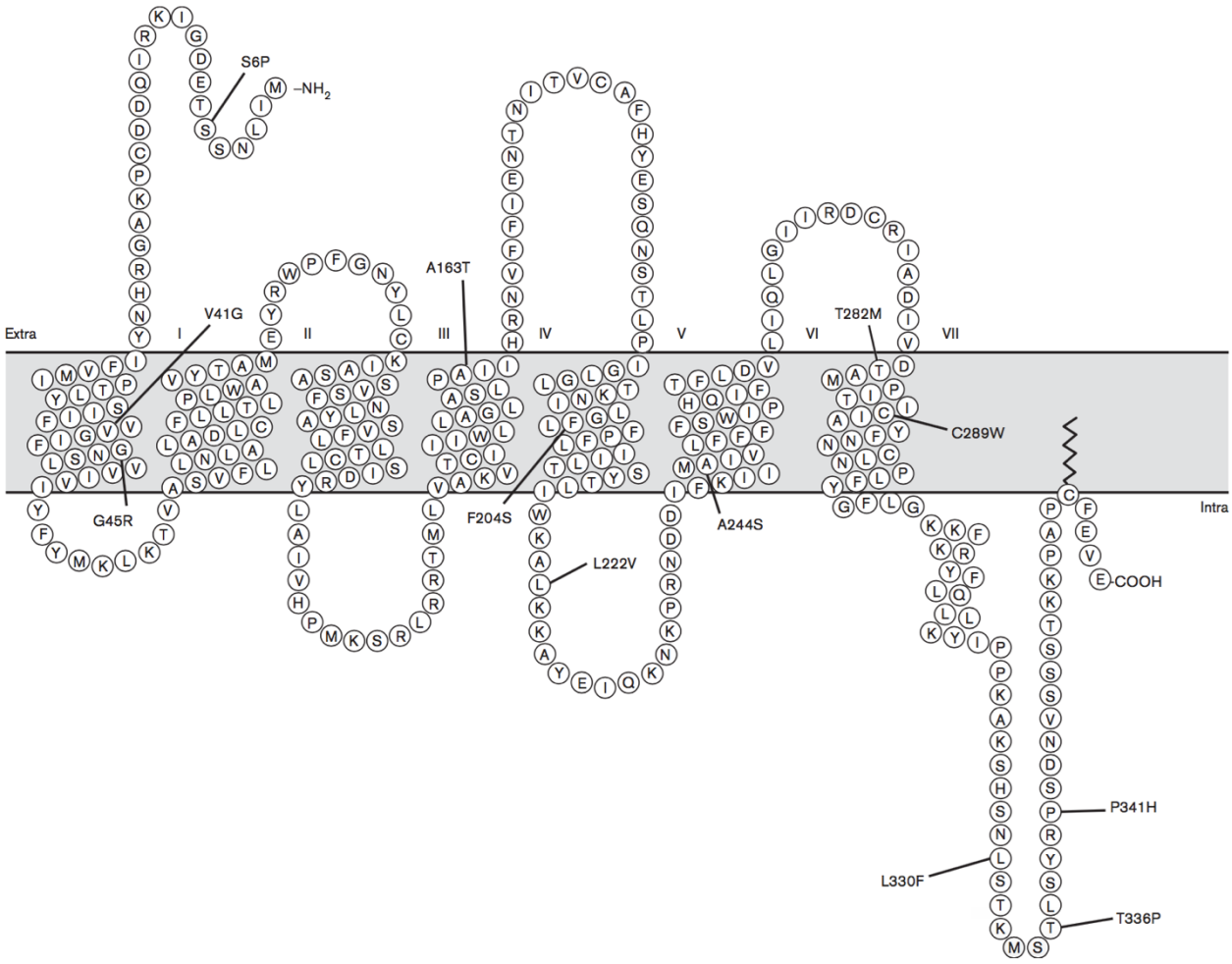

Figure 1.6: Reported non-synonymous single nucleotide polymorphisms in the AT_1 receptor. Twelve non-synonymous SNPs are schematically depicted by location in the amino acid sequence of the human AT_1 receptor. Each transmembrane domain (within grey region) is numbered by roman numerals from I to VII. The extracellular and intracellular regions are indicated. The black zigzag line is the palmitoylation site of the receptor. (Adapted from Arsenault et al., 2010)

Since the transmembrane regions of the receptor are involved in ligand binding and receptor activation, changes to the amino acid sequence in these regions (Val41Gly and Gly45Arg in TM-I; Ala163Thr in TM-IV; Phe204Ser in TM-V; Ala244Ser in TM-VI; Thr282Met and Cys289Trp in TM-VII) may affect the conformational change stabilized by the agonist-bound receptor and its resulting activation or effector coupling (Oro et al., 2007); thereby, the underlying signalling actions as a consequence of these SNPs remain to be clarified. This thesis will focus on elucidating the coupling of three polymorphic receptors to its cognate intracellular effectors: A163T, T282M, and C289W. These three SNPs were reported by Zhang *et al.* (2015) to differentially affect efficacies of specific ARBs in individuals carrying these SNPs due to their close proximity to the AT_1R orthosteric binding pocket.

1.4.2 [A163T]-AT_1 Receptor

The Ala163Thr polymorphism (rs12721226; www.ncbi.nlm.nih.gov/projects/SNP) was reported in three panels (published and unpublished) and found to be prevalent in 0.56% to 2.2% in their cohorts (Arsenault et al., 2010). It would be postulated that this change from a small-sized and hydrophobic alanine to a medium-sized and polar threonine would impair losartan[8] therapy in patients who bear the A163T mutation, as this position has been previously shown to be implicated in losartan binding (de Gasparo et al., 2000; Arsenault et al., 2010). Arsenault *et al.* (2010) demonstrated that the ferret AT_1R (f AT_1R), which possesses a threonine at position 163 and has been shown to have decreased binding for the sartan family of drugs, could greatly increase its ability to bind losartan when this threonine is changed to an alanine. Before 2010, there were no reports in the literature on the physiological and pharmacological significance of this AT_1R coding

[8] Losartan is a member of the family of sartans, which are competitive, non-peptide antagonists of the angiotensin II receptor, for the treatment of hypertension (Arsenault et al., 2010).

region mutation. Arsenault *et al.* (2010) reported that [A163T]-AT_1R displayed normal affinity for Ang II and its analogue SI, Ang II-mediated inositol phosphate production were almost identical between receptors, but there was a significant 7-fold decrease in the affinity of the A163T receptor to losartan treatment or its active metabolite EXP3174. Although this group reported that there was no difference in the signalling profiles and that the polymorphism should not result in any observable aberrant receptor physiology, this was a very limited approach to study the signalling signature of the polymorphic receptor.

1.4.3 [T282M]-AT_1 Receptor

The Thr282Met polymorphism results in a change from a highly conserved medium-sized and polar threonine at position 282 to a medium-sized and hydrophobic methionine. In 2005, Gribouval *et al.* reported cases of autosomal recessive renal tubular dysgenesis, where affected individuals die *in utero* or within 24 h postnatally. Furthermore, for the individuals that did survive, refractory hypotension was observed as a result of the loss in proximal tubule differentiation (Gribouval et al., 2005). Of the nine individuals in their study, one (Fetus VI) was a compound heterozygote with respect to a frameshift mutation at one locus of the *AGTR1* gene and a non-synonymous amino acid change (T282M) at the second locus. Although an *in vivo* homozygous model with this SNP has yet to be studied, defining the signalling signature associated with this receptor would provide indication of the underlying pathophysiology reported by Gribouval *et al.* (2005).

1.4.4 [C289W]-AT_1 Receptor

The Cys163Trp polymorphism (rs1064533; www.ncbi.nlm.nih.gov/projects/SNP) was first published in the seminal paper by Hansen *et al.* in 2004. This SNP results in the change from a medium-sized and polar cysteine to a large-sized and aromatic tryptophan. Along with this SNP, Hansen *et al.* pharmacologically characterized six other AT_1 receptor variants in COS-7 monkey kidney cells using a radioligand binding assay and three different functional assays (2004). This group reported that [C289W]-AT_1R displayed a 3-fold reduction in binding affinity, a 43% reduction in cell surface expression, and a 92% response of the angiotensin II-mediated ERK1/2 phosphorylation level in comparison to the wild-type AT_1 receptor. Furthermore, this mutant receptor displayed reduced potencies to two sartans: irbesartan and telmisartan. The reduced agonist and antagonist binding affinities may be attributed to the role of Cys289, which is located in close proximity to the Ang II binding site, but does not directly interact with the ARBs, however, it may indirectly alter ligand-receptor interactions (Karnik et al., 2015; Zhang et al., 2015).

Rationale and Objectives of the Study

The molecular mechanism by which a given GPCR can activate multiple G protein subtypes with the same ligand remains fundamentally unclear. Although, there is an improved understanding of how a ligand can bind to the receptor and direct downstream cellular responses by creating a specific, stabilized conformation of the receptor; this knowledge is largely dependent on the intermolecular and intramolecular interactions of the endogenous ligand with the receptor. For the AT_1 receptor, non-synonymous single nucleotide polymorphisms in the transmembrane regions could disrupt these inter- and intramolecular interactions required to stabilize the same active conformation. The findings about the A1166C polymorphism published in 1994 by Bonnardeaux *et al.* generated a tremendous amount of interest in investigating the possible link of SNPs with disease. However, few publications have directly studied the effect of *AGTR1* polymorphisms on the biological and pharmacological properties of the receptor protein. Other non-synonymous single nucleotide polymorphic variants (V41G, L222V, A244S, and P341H) have yet to be associated with aberrant receptor function, possibly because they are too similar to the wild-type human AT_1R (Arsenault et al., 2010). By affecting the receptor's ability to engage certain G proteins or β-arrestins, this can direct the signalling of the receptor through a specific therapeutic pathway, while mitigating the role of undesired responses – much like how many biased ligands are being developed for this purpose.

Thus, it is of interest to experimentally test whether the three polymorphic receptor variants (A163T, T282M, C289W) found in the transmembrane regions have altered G protein or β-arrestin biased signalling. Additionally, altered β-arrestin binding, recruitment, internalization, or trafficking might rationally show enhanced receptor activation as a consequence of diminished receptor desensitization and endocytosis.

We therefore hypothesized that non-synonymous single nucleotide polymorphisms of the human AT_1 receptor could alter the biological and pharmacological properties of the receptor protein to bias its coupling selectivity to G-proteins versus β-arrestin. This study would define a previously unidentified function for the underlying pathophysiology reported in literature of these single nucleotide changes in the population. Our objectives were:

1. To study the coupling efficiencies of the wild-type and polymorphic AT_1 receptors to their cognate G proteins ($G\alpha_q$, $G\alpha_{12}$, $G\alpha_{i2}$, and $G\alpha_{i3}$) and their downstream effectors using new bioluminescence resonance energy transfer (BRET)-based biosensors that were developed in the lab;
2. To study the ability of wild-type and polymorphic AT_1 receptors to recruit β-arrestin-2 to the plasma membrane and internalize into endosomes using again new BRET-based biosensors and confocal microscopy; and,
3. To define a signalling signature of each mutant receptor using the relative activity of each agonist-stimulated pathway and in relation to the wild-type AT_1 receptor.

Chapter 2:
Materials and Methods

CHAPTER II: Materials and Methods

2.1 Materials

Angiotensin II and poly-$_L$-ornithine were obtained from Sigma-Aldrich (St. Louis, MO). Iodine-125 salt were obtained from Perkin Elmer (Waltham, MA). Cell culture plates, dishes, and Costar 96-well flat bottom polypropylene plates were from Corning (Tewksbury, MA). Minimum Essential Medium (MEM), fetal bovine serum, and other cell culture reagents were purchased from Gibco, Life Technologies (Carlsbad, CA). Bovine serum albumin was purchased from EMD Chemicals Inc. (Gibbstown, NJ). Coelenterazine 400a was purchased from Nanolight Technology (Pinetop, AZ). Phusion DNA polymerase was obtained from Thermo Scientific (Rockford, IL). Restriction enzymes and T4 DNA ligase were obtained from New England Biolabs (Ipswich, MA). UBO-QIC [l-threonine,(3R)-*N*-acetyl-3-hydroxy-L-leucyl-(aR)-a-hydroxybenzenepropanoyl-2,3-idehydro-*N*-methylalanyl-L-alanyl-*N*-methyl-L-alanyl-(3R)-3-[[(2S,3R)-3-hydroxy-4-methyl-1-oxo-2-[(1-oxopropyl)amino]pentyl]oxy]-L-leucyl-*N*,*O*-dimethyl-,(7→1)-lactone(9CI)] was purchased from the Institute of Pharmaceutical Biology, University of Bonn (Bonn, Germany).

2.2 Methods

2.2.1 Plasmids and constructs

To create the AT_1R variants (A163T, T282M, C289W), two complementary oligonucleotides containing the single nucleotide change were synthesized and used to amplify the wild-type spliced human *AGTR1* gene. The PCR products were subcloned in-frame using the NEBuilder HiFi DNA Assembly Cloning Kit (New England Biolabs), as per manufacturer's protocol, into a pcDNA3 vector containing the FLAG sequence (DYKDDDDA) at the N-terminus and cut with EcoRI and

XbaI restriction enzymes. The assembled DNA product was transformed into NEB DH5α high efficiency competent *E.coli* cells (New England Biolabs) and cultured on luria broth agar plates containing ampicillin (100 μg/mL) to select for vector-containing colonies. The PCR was done using Phusion DNA polymerase and all the constructs were verified by DNA sequencing prior to use. The 5' primers were as follows, with the mutated nucleotides underlined; A163T:GCCAGTTTGCCAACTATAATCCATCGA; T282M:AATTGCAGATATTGTGGAC ATGGCCATGCC; C289W:GCCATGCCTATCACCATTTGGATAGCT. The sequences were validated by sequencing at the McGill University and Génome Québec Innovation Centre using EcoRI forward and XbaI reverse primers prior to use.

2.2.2 Cell culture and Transfection

HEK293 cells were cultured in MEM supplemented with 10% FBS, 5 mM L-glutamine, and 100 μg/mL gentamycin. Cells were grown at 37 °C in 5% CO_2 and 90% humidity. Cells were seeded at a density of ~7.5×10^5 cells per 100 mm dish one day before transfection. Transient transfection was carried out using the conventional calcium phosphate co-precipitation method (as described in Fessart, Simaan, & Laporte, 2005). The total amount of DNA transfected in each plate was adjusted to 11 μg with pcDNA. After 18 h post-transfection, the culture medium was replaced and cells were divided for subsequent experiments. All experiments were performed 48 h after transfection.

2.2.3 Bioluminescence resonance energy transfer (BRET) measurements

Transfected cells were detached by incubating in PBS containing 5 mM EDTA for 3 minutes at 37 ºC and 5% CO_2. Cells were re-seeded onto poly-$_L$-ornithine-coated, white, 96-well plates at a

density of ~2.5×10^5 cells per well. The next day, cells were washed once and serum starved with Tyrode's buffer (140 mM NaCl, 2.7 mM KCl, 1 mM $CaCl_2$, 12 mM $NaHCO_3$, 5.6 mM $_D$-glucose, 0.5 mM $MgCl_2$, 0.37 mM NaH_2PO_4, 25 mM HEPES, pH 7.4) for 1 hour either at room temperature or 37 ºC and 5% CO_2. Cells were stimulated with increasing concentrations of the ligand in Tyrode's buffer, with the maximum dose being 10 μM. The cell-permeable substrate, coelenterazine 400a (final concentration of 5 μM in Tyrode's buffer) was added 3-6 minutes prior to BRET measurements. The plate was read with a Synergy2 multi-mode microplate reader (BioTek®) with a filter set (center wavelength/band width) of 410/80nm (donor; RLucII) and 515/30 nm (acceptor; rGFP or GFP_{10}). The BRET signal was determined by calculating the ratio of the light intensity emitted by the GFP over the light intensity emitted by the RLucII.

2.2.4 ^{125}I-Angiotensin II binding assay

^{125}I-Ang II was prepared using the Iodogen method, and specific activity was determined from self-displacement and saturation experiments, as previously cited (Zimmerman et al., 2012). Relative angiotensin II binding and affinity was evaluated with a radioligand binding assay at 4 °C using ^{125}I-Ang II as the tracer ligand. HEK293 cells expressing either 3 μg of WT AT_1R or polymorphic AT_1R were seeded one day after transfection at a density of ~1.2×10^5 cells per well in poly-$_L$-ornithine-coated 24-well plates. The following day, cells were washed once with cold PBS and then incubated in the absence or presence of increasing concentrations of Ang II in binding buffer (0.2% BSA (weight/volume), 25 mM Tris-HCl, pH 7.4, 100 mM NaCl, 5 mM $MgCl_2$) on ice to prevent receptor internalization, with the highest concentration being 10 μM. Cells were incubated with 0.1 mL of ^{125}I-Ang II (~150,000 cpm) in binding buffer at 4 °C overnight. Nonspecific binding was determined in the presence of 10 μM unlabelled Ang II. The

following day, cells were washed three times with ice-cold PBS, and solubilized in 0.5 mL of 0.2 M NaOH. Radioactivity was counted using a PerkinElmer Wizard 1470 automatic γ-counter.

2.2.5 FACS assay

Cells were transiently transfected with 3 μg of either WT AT_1R or polymorphic AT_1R. Transfected cells were detached by incubating the plates in PBS containing 5mM EDTA for 3 minutes at room temperature. Plates were washed with PBS 1x and cells were counted and resuspended in PBS/0.2% BSA (weight/volume) for a final concentration of 5.0×10^5 cells per 400 μL. Cells were transferred to microcentrifuge tubes and incubated with an anti-FLAG mouse monoclonal antibody (Perkin Elmer) at a concentration of 1:250 μL in PBS/0.2% BSA (weight/volume) at room temperature for 1 hour. Cells were pelleted and washed twice with cold PBS 1x. Cells were incubated with goat anti-mouse IgG (H+L) secondary antibody, Alexa Fluor® 488 conjugate (Thermo Fisher Scientific) at a concentration of 1:500 μL in PBS/0.2% BSA (weight/volume) at room temperature for 45 minutes. A secondary antibody only control was used for each condition to determine background fluorescence. Again, cells were pelleted and washed twice with cold PBS 1x. Finally, cells were suspended in 200 μL of PBS 1x and transferred to 5 mL, 75×12 mm, polystyrol FACS tubes (Sarstedt). Data was acquired using a BD FACSCantoII flow cytometer and BD FACSDiva software with a blue laser (488-nm, 20-mW solid state). Samples results were analyzed using FlowJo software (FlowJo, LLC) to determine mean fluorescence in samples.

2.2.6 Confocal microscopy

For live cell imaging, HEK293 cells were seeded in 35 mm glass bottom dishes (MaTek corp., Ashland, MA) and transfected with either FLAG-AT_1R wild-type or variants (A163T, T282M, or

C289W) and YFP-tagged human β-arrestin-2. Live cells were followed at 5, 15, and 30 min post-stimulation on a Zeiss LSM-510 Meta laser scanning microscope with a LCI Plan-Neofluor 63x/1.3 Imm Korr DIC M27 lens, whereas fixed cells were visualized with a Plan-Neofluor 40x/1.3 Oil DIC lens. Images (1024×1024 pixels) were then collected using emission BP 530-600 nm filter for Alexa488 or YFP. For immunofluorescence, HEK293 cells were seeded in 6-well plates with microscope cover slides at a density of 1.0×10^5 cells per well and transfected with either FLAG-AT_1R wild-type or variants (A163T, T282M, or C289W) and mCherry-tagged β-arrestin-2. Forty-eight hours post-transfection, cells were serum starved for 30 min followed by stimulation with angiotensin II (1 μM) or vehicle. For immunofluorescence, cells were fixed in 4% formaldehyde (in PBS) and permeabilized in 0.05% Triton-X prior to antibody staining. For detecting mCherry, a HeNe I laser was used with 543 nm excitation and LP 560 nm emission filter sets.

2.2.7 Data analysis and Statistics

Statistical analysis was performed using GraphPad Prism 6 software (GraphPad Software Inc.; La Jolla, CA) using either Student's *t*-tests, two-way ANOVAs, or Tukey's post-hoc multiple comparisons tests, when appropriate. Curves presented throughout this study represent the best fits and were generated using GraphPad Prism software. P values ≤ 0.05 were considered significant.

Chapter 3: Results

CHAPTER III: Results

3.1 Assessing SNP variants for cell surface expression and binding of Ang II

Since these single point mutations occur within the transmembrane domain and orthosteric binding pocket of the AT_1 receptor, we wanted to confirm the normal expression of the receptors at the plasma membrane and normal ligand binding of Ang II. Transiently transfected HEK293 cells expressing the FLAG-tagged receptor (WT, A163T, T282M, or C289W) were tagged either with an Alexa488 fluorophore, or control conditions where cells were unlabelled with antibody or with a secondary antibody alone to determine levels of background signal and autofluorescence, respectively. The results of three independent experiments with 10 000 events were normalized to the mean FITC fluorescence of the wild-type AT_1R (Figure 3.1a). A one-way ANOVA found no significance between the mean fluorescence and the angiotensin receptors ($F(3,7) = 4.139$, $p = 0.06$). Next, we compared the extent of Ang II specific binding to the receptors expressed at the plasma membrane. Transiently transfected HEK293 cells expressing the FLAG-tagged receptor (WT, A163T, T282M, or C289W) were incubated overnight at 4 ºC (to prevent receptor internalization) with radiolabelled ^{125}I-Ang II and either vehicle (total binding) or a saturating concentration (1×10^{-6}) of unlabelled Ang II (non-specific binding) to displace ^{125}I-Ang II from its binding site(s). The results of three independent experiments measuring the specific binding (total binding – non-specific binding) were normalized to that of wild-type AT_1R (Figure 3.1b). We found the specific binding of Ang II was significantly reduced for the T282M- and C289W-AT_1 receptors (both $p < 0.001$), whereas there was no significant change in Ang II binding for A163T-AT_1R. Next, we determined if there was any change in the IC_{50} of Ang II for the receptors by a competition binding experiment. Transiently transfected HEK293 cells expressing the FLAG-tagged receptor (WT, A163T, T282M, or C289W) were incubated with radiolabelled ^{125}I-Ang II

and the displacement of radioligand was measured as a function of increasing concentrations of unlabelled Ang II from 1×10^{-11} to 1×10^{-5} or vehicle. Ang II displaced ^{125}I-Ang II binding to the AT_1 receptors in a dose-dependent manner with no significant change in potency (Figure 3.1c ; $LogIC_{50}$ = WT: –8.727±0.05, A163T: –8.512±0.23, T282M: –7.321±1.00, C289W: –8.337±0.38).

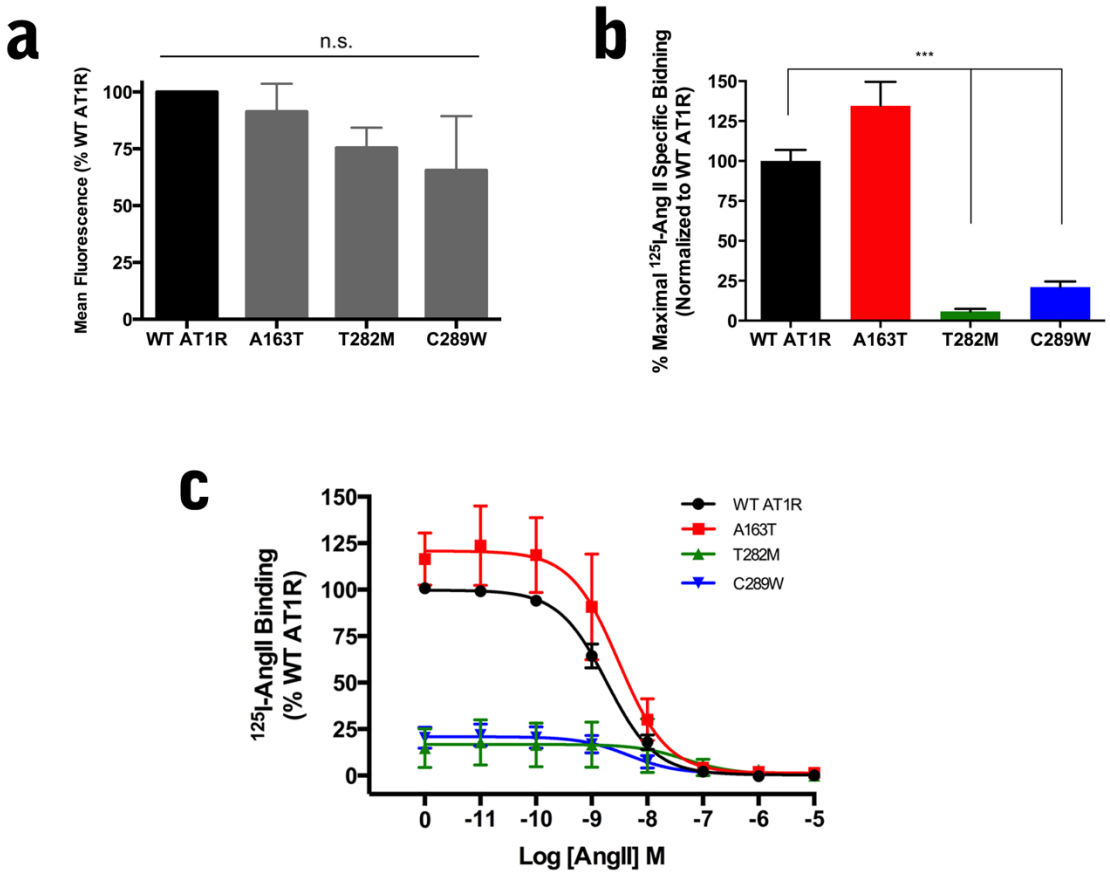

Figure 3.1: Assessing cell surface expression and binding of Ang II for polymorphic variants. (**a**) HEK293 cells were transfected with 3µg of receptor. Fluorescence-activated cell sorting measured the mean fluorescence and was normalized to the maximum florescence of the wild-type AT_1R-expressing cells. (**b**) Specific ^{125}I-Ang II binding at the plasma membrane was determined by the total binding (no unlabelled Ang II) subtracted from the non-specific binding (1 µM unlabelled Ang II). The specific binding was normalized to the wild-type AT_1R. (**c**) Competition displacement curve of wild-type and polymorphic variants. Ang II displaced ^{125}I-Ang II binding to the AT_1 receptors in a dose-dependent manner. All figures are presented with the mean ± s.e.m. from three independent experiments. Note: n.s. – non-significant, *** $p < 0.001$.

3.2 Polymorphic AT_1 receptors couple efficiently through the $G\alpha_q$ pathway

We wanted to first test the coupling of the receptor to the AT_1R's well-characterized G protein $G\alpha_q$. This was done by the help of a polycistronic BRET-based biosensor, which tags the $G\alpha_q$ subunit with an RLucII moiety and the $G\gamma_1$ subunit with GFP_{10} moiety (Namkung, Radresa et al., 2016). The activation of this pathway can be assessed through quantitatively measuring of association and distance between the $G\alpha_q$ subunit and $G\gamma_1$ subunit (Namkung, Radresa et al., 2016). At the basal state, the heteotrimeric $G\alpha\beta\gamma$ proteins are found in one complex when $G\alpha_q$ is bound to GDP. The binding of Ang II and the subsequent activation of the receptor allows $G\alpha_q$ to exchange its GDP for GTP, resulting in its dissociation from the $\beta\gamma$ heterodimer. The energy provided to RLucII via its substrate coelenterazine 400a can be measured at 410±80 nm. The wavelength of the energy emitted by RLucII falls within the absorption spectrum of the acceptor protein GFP_{10}, allowing for an efficient transfer of energy from the donor protein to the acceptor protein when in close proximity (Figure 3.2a; Namkung, Radresa et al., 2016). The energy absorbed by the acceptor protein and reemitted can be measured at 515±30 nm. HEK293 cells were co-transfected with the AT_1 receptor (WT, A163T, T282, or C289W) and the vector containing the components of the biosensor. The following day, cells were seeded in 96-well plates. After 18 hours, the cells were serum starved in Tyrode's buffer. Each condition was stimulated with an increasing concentration of Ang II from 1×10^{-11} to 1×10^{-5} or vehicle (Tyrode's buffer) in triplicate for 2 minutes. This sensor was shown to reach the maximal response at 120 s during its validation (Namkung, Radresa et al., 2016). The BRET signal from each well was calculated as a ratio of the emission from the donor protein RLucII at 410±80 nm divided by the emission of the acceptor protein GFP_{10} at 515±30 nm (termed BRET ratio). The dose-response curves in Figure 3.2b-d are expressed as baseline-corrected BRET ratio (ΔBRET). The data were

analyzed using three-parameter non-linear regression curve fitting and the $\log EC_{50}$ and E_{MAX} from an average of 5 independent experiments were extracted and averaged (Table 3.1). The data show the $\log EC_{50}$ values between the wild-type and A163T-AT_1 receptors were not significantly different ($t(8) = 0.34$, $p = 0.74$). However, when comparing the WT to either the T282M-AT_1 or C289W-AT_1 receptors, we found a significant rightward shift in the $\log EC_{50}$ values (T282M: $t(8) = 9.4$, $p = 1.34E\text{-}5$; C289W: $t(8) = 3.19$, $p = 0.013$). When comparing the E_{MAX} values from the dose-response curves at 1×10^{-5} M Ang II, we found no change in efficacy from the wild-type AT_1R ($F(3,16) = 0.1384$, $p = 0.9356$; Figure 3.2e).

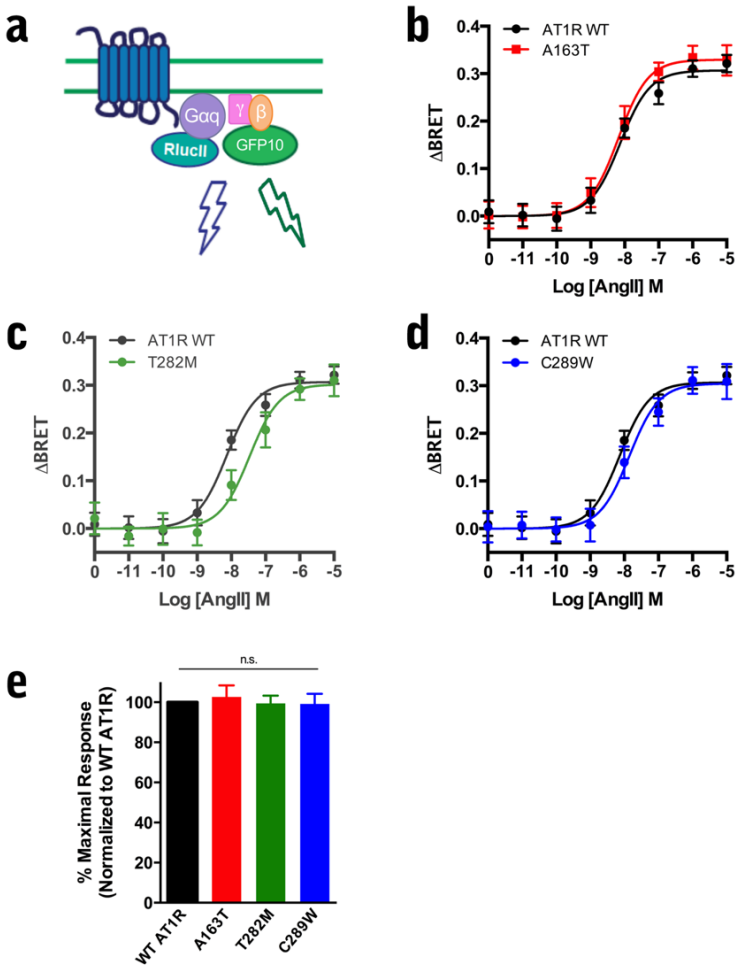

Figure 3.2: $G\alpha_q$ coupling to the AT_1 receptors. (**a**) Schematic of BRET pair with RlucII tagged to $G\alpha_q$ subunit and GFP_{10} tagged to the Gγ subunit, both at the plasma membrane. A basal BRET ratio can be recorded when both subunits are in close proximity. (**b**) Concentration-response curve of the A163T-AT_1R and wild-type AT_1R in ΔBRET from 1×10^{-11} M to 1×10^{-5} M Ang II. (**c**) Concentration-response curve of the T282M-AT_1R and wild-type AT_1R in ΔBRET from 1×10^{-11} M to 1×10^{-5} M Ang II. (**d**) Concentration-response curve of the C289W-AT_1R and wild-type AT_1R in ΔBRET from 1×10^{-11} M to 1×10^{-5} M Ang II. (**e**) Quantification of the maximum response at 1×10^{-5} M normalized to the wild-type AT_1R. All figures are presented with the mean ± s.e.m. from five independent experiments. Note: n.s. – non-significant.

3.3 Assessing the downstream activation of $G\alpha_q$ with its effector Protein Kinase C

Activation of PLC-β by $G\alpha_q$ results in the cleavage of PIP_2 to DAG and IP_3, recruiting PKC to the DAG anchored at the plasma membrane and initiating the subsequent activation of the MAPK cascade (Gutkind, 2000; Bridges & Lindsley, 2008). To further investigate the downstream effect, if any, of the loss in potency observed at the G protein level, we used a BRET-based sensor to evaluate the activation of the downstream effector protein PKC. Phosphorylation of a substrate biosensor by the family of PKC serine/threonine kinases results in a conformational change of its regulatory and catalytic domains, which can be measured by tagging the N-terminus with RLucII and the C-terminus with GFP_{10} (Figure 3.3a; Namkung et al., unpublished data). HEK293 cells were co-transfected with the AT_1 receptor (WT, A163T, T282, or C289W) and the biosensor. Each condition was stimulated with an increasing concentration of Ang II from 1×10^{-11} to 1×10^{-5} or vehicle (Tyrode's buffer) in triplicate for 2 minutes (Figure 3.3). The $logEC_{50}$ and E_{MAX} from an average of 3 independent experiments were extracted and averaged (Table 3.1). The data show the $logEC_{50}$ values between the wild-type and A163T-AT_1 receptors were not significantly different ($t(4) = 0.899$, $p = 0.419$). Comparing the $logEC_{50}$s of the WT to the T282M-AT_1 receptor, there is a significant decrease in potency of the receptor ($t(4) = 5.047$, $p = 0.007$; Figure 3.3c), which was also seen when comparing the EC_{50} values of the wild-type AT_1 to the C289W-AT1R ($t(4) = 7.5$, $p = 0.002$; Figure 3.3d). Pretreatment of a selective $G\alpha_{q/11}$ blocker FR900359 (UBO-QIC; 100 nM; Bernard, Thach, Kamato, Osman, & Little, 2014) for 30 min prior to agonist stimulation of the cells resulted in a complete termination of PKC signalling (Supplemental Figure 1), indicating PKC activation is only a component of the $G\alpha_{q/11}$ pathway. Finally, we observed no change in the E_{MAX} values from the dose-response curves at 1×10^{-5} M Ang II ($F(3,8) = 3.623$, $p = 0.0646$; Figure 3.3e).

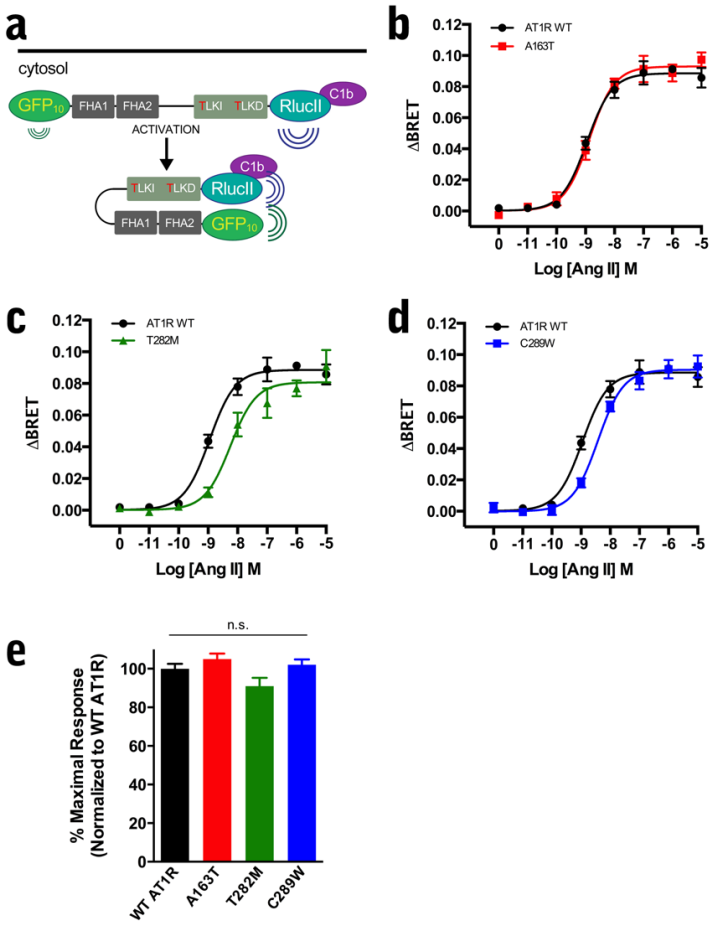

Figure 3.3: Protein Kinase C activation downstream of the $G\alpha_q$ response. (**a**) Schematic of the BRET biosensor of the protein kinase C substrate. When this substrate is phosphorylated on its tyrosine moieties by any subtype of PKC, it causes the rearrangement of the sensor and brings the RLucII and GFP_{10} into closer proximity. (**b**) Concentration-response curve of the A163T-AT_1R and wild-type AT_1R in ΔBRET from 1×10^{-11} M to 1×10^{-5} M Ang II. (**c**) Concentration-response curve of the T282M-AT_1R and wild-type AT_1R in ΔBRET from 1×10^{-11} M to 1×10^{-5} M Ang II. (**d**) Concentration-response curve of the C289W-AT_1R and wild-type AT_1R in ΔBRET from 1×10^{-11} M to 1×10^{-5} M Ang II. (**e**) Quantification of the maximum response at 1×10^{-5} M normalized to the wild-type AT_1R. All figures are presented with the mean ± s.e.m. from three independent experiments. Note: n.s. – non-significant.

3.4 T282M-AT_1R has a markedly diminished potency to activate the $G\alpha_{12}$ protein

The next G protein we assessed was $G\alpha_{12}$, whose intracellular actions results in changes in cell shape, contraction, retraction, migration, and mitogenesis (Dutt et al., 2004). Again, this novel BRET-based biosensor tags the $G\alpha_{12}$ subunit with RlucII and the $G\gamma$ subunit with GFP_{10}. HEK293 cells were co-transfected with the AT_1 receptor (WT, A163T, T282, or C289W) and the vectors containing the components of the biosensor. Each condition was stimulated with an increasing concentration of Ang II from 1×10^{-11} to 1×10^{-5} or vehicle (Tyrode's buffer) in triplicate for 10 minutes (i.e., the time point of the maximum BRET response; Namkung et al., unpublished data). The $logEC_{50}$ and E_{MAX} from an average of 5 independent experiments were extracted and averaged (Table 3.1). The data show the potency of $G\alpha_{12}$ activation between the wild-type and A163T-AT_1 receptors remains unchanged ($t(8) = 1.01$, $p = 0.34$). Comparing the EC_{50}s of the wild-type to the T282M-AT_1 receptor, there is a significant decrease in potency of the receptor to activate the $G\alpha_{12}\beta\gamma$ heterotrimer ($t(8) = 10.92$, $p = 4.38E\text{-}6$; Figure 3.4c). Furthermore, we found a significant rightward shift in the $logEC_{50}$ value of the C289W-AT_1R ($t(8) = 5.1$, $p = 0.0009$; Figure 3.4d). When comparing the E_{MAX} values from the dose-response curves at 1×10^{-5} M Ang II, we found no change in efficacy ($F(3,16) = 2.804$, $p = 0.0732$; Figure 3.4e).

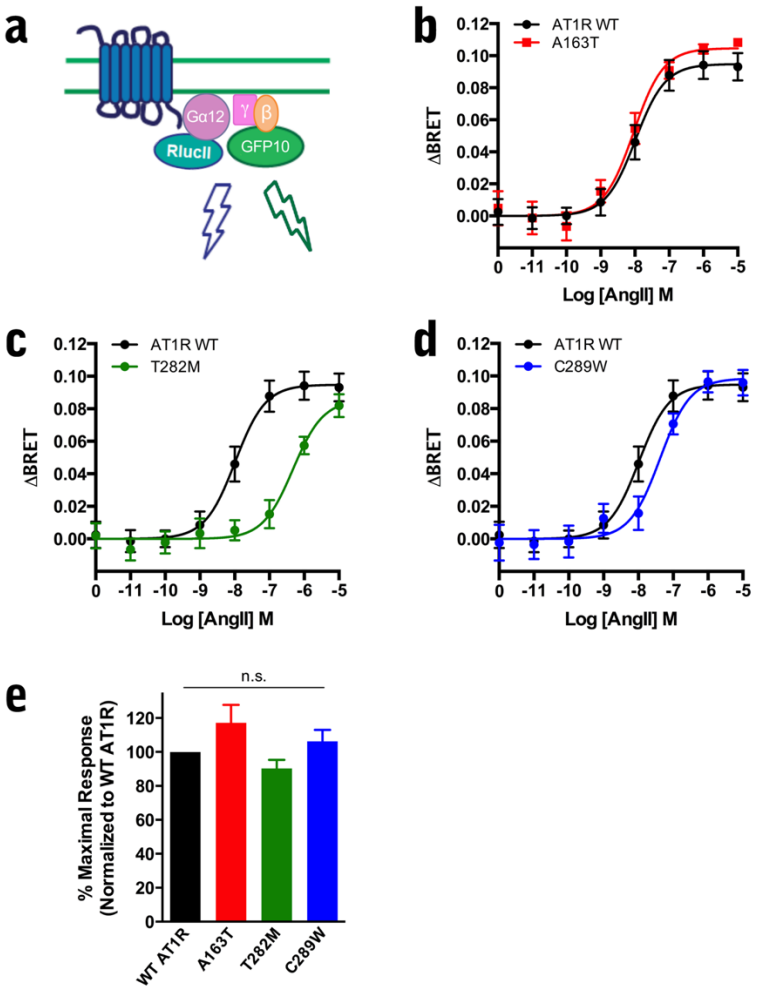

Figure 3.4: $G\alpha_{12}$ coupling to the polymorphic receptors. (**a**) Schematic of BRET pair with RlucII tagged to $G\alpha_{12}$ protein and GFP_{10} tagged to the Gγ subunit, both at the plasma membrane. (**b**) Concentration-response curve of the A163T-AT_1R and wild-type AT_1R in ΔBRET from 1×10^{-11} M to 1×10^{-5} M Ang II. (**c**) Concentration-response curve of the T282M-AT_1R and wild-type AT_1R in ΔBRET from 1×10^{-11} M to 1×10^{-5} M Ang II. (**d**) Concentration-response curve of the C289W-AT_1R and wild-type AT_1R in ΔBRET from 1×10^{-11} M to 1×10^{-5} M Ang II. (**e**) Quantification of the maximum response at 1×10^{-5} M normalized to the wild-type AT_1R. All figures are presented with the mean ± s.e.m. from five independent experiments recorded at 10 min post stimulation. Note: n.s. – non-significant.

3.5 The T282M-AT_1R and C289W-AT_1R show a tendency to activate the small GTPase Rho A downstream of the $G\alpha_{12}$ pathway with similar shifts in potency, but altered efficacy

Since our results suggested that the $G\alpha_{12}$ activation was quite significantly altered for T282M-AT_1R and C289W-AT_1R, we wanted to evaluate the downstream activation of the small GTPase Rho A through the $G\alpha_{12/13}$ cascade (Siehler, 2009). This is achieved by assessing the recruitment of its effector protein kinase N (PKN) to activated Rho A at the plasma membrane (Vogt, Grosse, Schultz, & Offermanns, 2003). The sensor employs an enhanced bystander (ebBRET) approach where an RLucII-tagged PKN translocates closer to its substrate Rho A at the plasma membrane, where *Renilla* GFP (rGFP) is anchored through a CAAX domain (rGFP-CAAX; Namkung, Le Gouill et al., 2016). HEK293 cells stimulated with increasing concentrations of Ang II from 1×10^{-11} to 1×10^{-5} or vehicle (Tyrode's buffer) in triplicate for 2 minutes (Figure 3.5). Since the activation of Rho A is component of both $G\alpha_{q/11}$ and $G\alpha_{12/13}$ signalling cascades, a selective $G\alpha_{q/11}$ blocker FR900359 (UBO-QIC; 100 nM; Bernard et al., 2014) was added as a pretreatment for 30 min prior to agonist stimulation of the cells (Figures 3.5b, d, f). Statistics were only performed on results obtained in the presence of UBO-QIC to reflect the $G\alpha_{12/13}$ proclivity (Table 3.1). The data show the $\log EC_{50}$ values between the wild-type and A163T-AT_1 receptors were not significantly different ($t(4) = 1.19$, $p = 0.30$; Figure 3.5b), but a significant decrease in potency of the T282M-AT_1 ($t(4) = 8.79$, $p = 0.0009$; Figure 3.5d) and C289W-AT_1 ($t(4) = 7.85$, $p = 0.0014$; Figure 3.5f) receptors. The efficacy of the response in the presence of UBO-QIC for each receptor relative to the wild-type AT_1R is depicted in Figure 3.5g. The E_{MAX} was significantly reduced for T282M-AT_1R ($t(4) = 6.94$, $p = 0.002$) and C289W-AT_1R ($t(4) = 4.79$, $p = 0.009$) at 1×10^{-5} M Ang II.

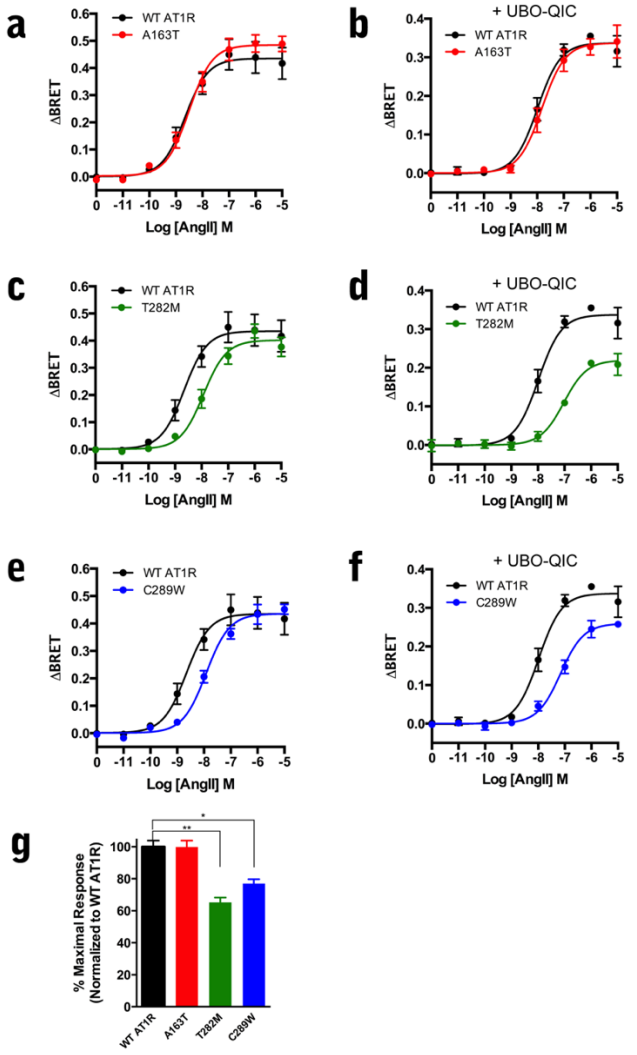

Figure 3.5: Rho A activation downstream of $G\alpha_{12}$. (**a, c, e**) Concentration-response curves of A163T-, T282M-, and C289W AT_1Rs of the Rho A sensor in ΔBRET. (**b**) Concentration-response curve of the A163T-AT_1R and wild-type AT_1R in the presence of UBO-QIC in ΔBRET. (**d**) Concentration-response curve of the T282M-AT_1R and wild-type AT_1R in the presence of UBO-QIC in ΔBRET. (**f**) Concentration-response curve of the C289W-AT_1R and wild-type AT_1R in the presence of UBO-QIC. (**g**) Quantification of the maximum response at 1×10^{-5} M of UBO-QIC-treated conditions normalized to the wild-type AT_1R. All figures are presented with the mean ± s.e.m. from three independent experiments. * $p < 0.05$, ** $p < 0.01$.

3.6 Characterizing the SNP variants for the $G\alpha_{i2}$ and $G\alpha_{i3}$ pathways

The AT_1R has been reported to signal through the $G\alpha_i$ pathway (Navarro et al., 2008), so we assessed the activation of both $G\alpha_{i2}$ and $G\alpha_{i3}$ ($G\alpha_{i1}$ does not couple well to the AT_1R; data not shown). Here, the BRET-based biosensors tag each $G\alpha_i$ subunit with RLucII and the $G\gamma$ subunit with GFP_{10}. Cells was stimulated with an increasing concentration of Ang II from 1×10^{-11} to 1×10^{-5} or vehicle (Tyrode's buffer) in triplicate for 2 minutes. The $logEC_{50}$ and E_{MAX} from an average of 3-5 independent experiments were extracted and averaged (Table 3.1).

For the $G\alpha_{i2}$ dose-response curves, the data show the $logEC_{50}$ values between the wild-type and A163T-AT_1 receptors were not significantly different ($t(8) = 1.01$, $p = 0.34$; Figure 3.6b). However, a significant decrease in potency was observed for both the T282M-AT_1 ($t(8) = 6.47$, $p = 1.94E\text{-}4$; Figure 3.6c) and C289W-AT_1 ($t(8) = 5.83$, $p = 3.93E\text{-}4$; Figure 3.5e) receptors. When comparing the E_{MAX} values from the dose-response curves, we found no change in the maximal response of all the receptors ($F(3,16) = 2.074$, $p = 0.144$; Figure 3.6e).

For the $G\alpha_{i3}$ dose-response curves, the data show the $logEC_{50}$ values between neither the wild-type and A163T-AT_1 nor the wild-type and T282M-AT_1 receptors were significantly different (A163T: $t(4) = 0.685$, $p = 0.53$, Figure 3.7b; T282M: $t(4) = 2.00$, $p = 0.12$, Figure 3.7c). However, the $logEC_{50}$ of the C289W-AT_1R was found to be significantly different from the wild-type receptor ($t(4) = 3.15$, $p = 0.034$, Figure 3.7d). When comparing the E_{MAX} values from the dose-response curves at 1×10^{-5} M Ang II, the T282M-AT_1 and C289W-AT_1 receptors were significantly decreased (Figure 3.7e; T282M: $t(4)=6.816$, $p = 0.0024$; C289W: $t(4)=8.074$, $p = 0.0013$).

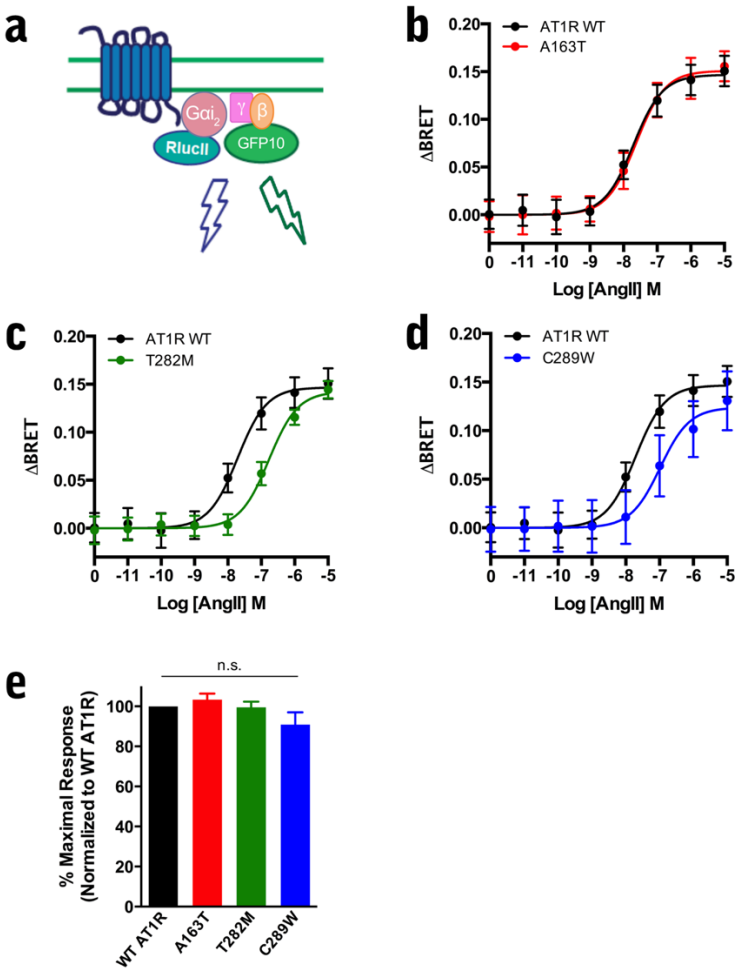

Figure 3.6: $G\alpha_{i2}$ coupling to the receptors. (**a**) Schematic of BRET pair with RlucII tagged to $G\alpha_{i2}$ protein and GFP_{10} tagged to the Gγ subunit, both at the plasma membrane. (**b**) Concentration-response curve of the A163T-AT_1R and wild-type AT_1R in ΔBRET from 1×10^{-11} M to 1×10^{-5} M Ang II. (**c**) Concentration-response curve of the T282M-AT_1R and wild-type AT_1R in ΔBRET from 1×10^{-11} M to 1×10^{-5} M Ang II. (**d**) Concentration-response curve of the C289W-AT_1R and wild-type AT_1R in ΔBRET from 1×10^{-11} M to 1×10^{-5} M Ang II. (**e**) Quantification of the maximum response at 1×10^{-5} M normalized to the wild-type AT_1R. All figures are presented with the mean ± s.e.m. from five independent experiments. Note: n.s. – non-significant.

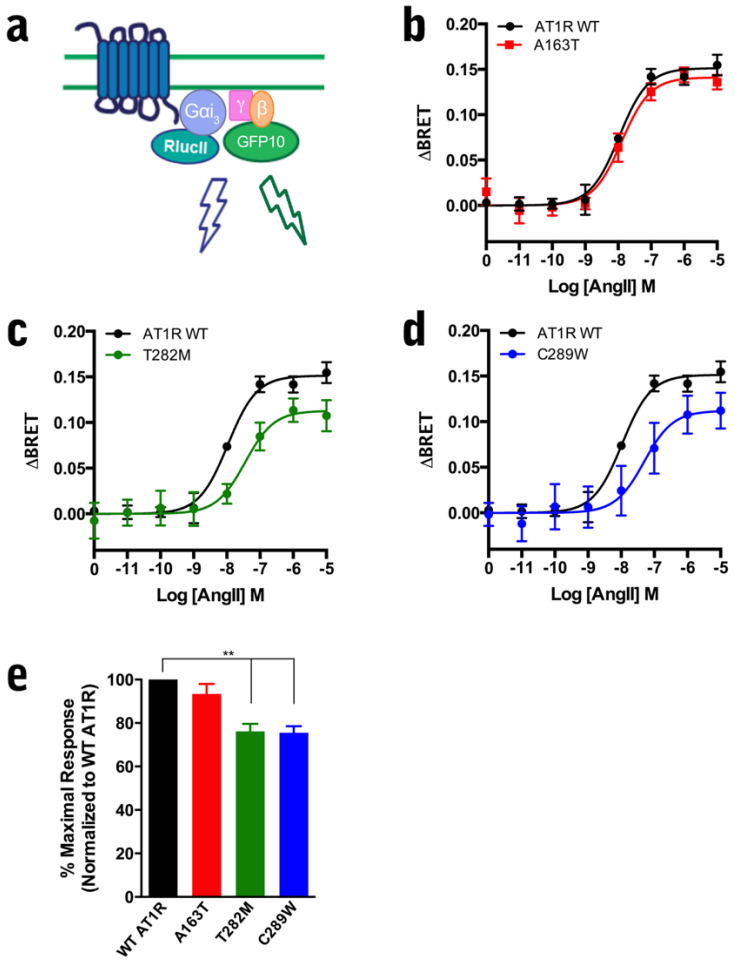

Figure 3.7: $G\alpha_{i3}$ coupling to the receptors. (**a**) Schematic of BRET pair with RlucII tagged to $G\alpha_{i3}$ protein and GFP_{10} tagged to the Gγ subunit, both at the plasma membrane. (**b**) Concentration-response curve of the A163T-AT_1R and wild-type AT_1R in ΔBRET from 1×10^{-11} M to 1×10^{-5} M Ang II. (**c**) Concentration-response curve of the T282M-AT_1R and wild-type AT_1R in ΔBRET from 1×10^{-11} M to 1×10^{-5} M Ang II. (**d**) Concentration-response curve of the C289W-AT_1R and wild-type AT_1R in ΔBRET from 1×10^{-11} M to 1×10^{-5} M Ang II. (**e**) Quantification of the maximum response at 1×10^{-5} M normalized to the wild-type AT_1R. All figures are presented with the mean ± s.e.m. from three independent experiments. ** $p < 0.01$.

3.7 Recruitment of β-arrestin-2 to the plasma membrane following receptor activation

Following ligand-induced activation, receptors can undergo homologous or heterologous desensitization by GRKs to recruit β-arrestins to the plasma membrane from the cytosol (Chuang et al., 1996; Drake et al., 2006). β-arrestin functions to uncouple the receptor from its G proteins and acts as a scaffold for adaptor proteins involved in endocytosis (Laporte et al., 1999; Fessart et al., 2005; Khoury, Nikolajev, et al., 2014). Measuring the translocation of β-arrestin-2 from the cytosol to the plasma membrane would provide insight into the dynamics of receptor internalization and G protein-independent signalling. Hence, we used a ebBRET-based biosensor with β-arrestin-2 tagged with RLucII and the acceptor rGFP localized to the plasma membrane with a CAAX prenylation motif (Figure 3.8a; Namkung, Le Gouill et al., 2016). Each condition was stimulated with an increasing concentration of Ang II from 1×10^{-11} to 1×10^{-5} or vehicle (Tyrode's buffer) in triplicate for 2 minutes. The $\log EC_{50}$ and E_{MAX} from an average of 4 independent experiments were extracted and averaged (Table 3.1). The results for the A163T-AT_1 receptor reflect that of the wild-type AT_1R dose-response curve (Figure 3.8b). The T282M-AT_1R had a significant reduction in its potency and efficacy to recruit β-arrestin (Figure 3.8c). Meanwhile, the C289W-AT_1R's shift in potency was not statistically significant ($t(6) = 2.41$, $p = 0.052$), but the efficacy was significantly reduced in comparison to the wild-type AT_1R ($t(6) = 3.329$, $p = 0.0158$; Figure 3.8e). It is important to note that although the difference between T282M-AT_1 and wild-type receptor is not significant at -5 logM Ang II, we find significance at Ang II concentrations of -8.00 logM, -7.00 logM, and -6.00 logM with a p value of less than 0.05.

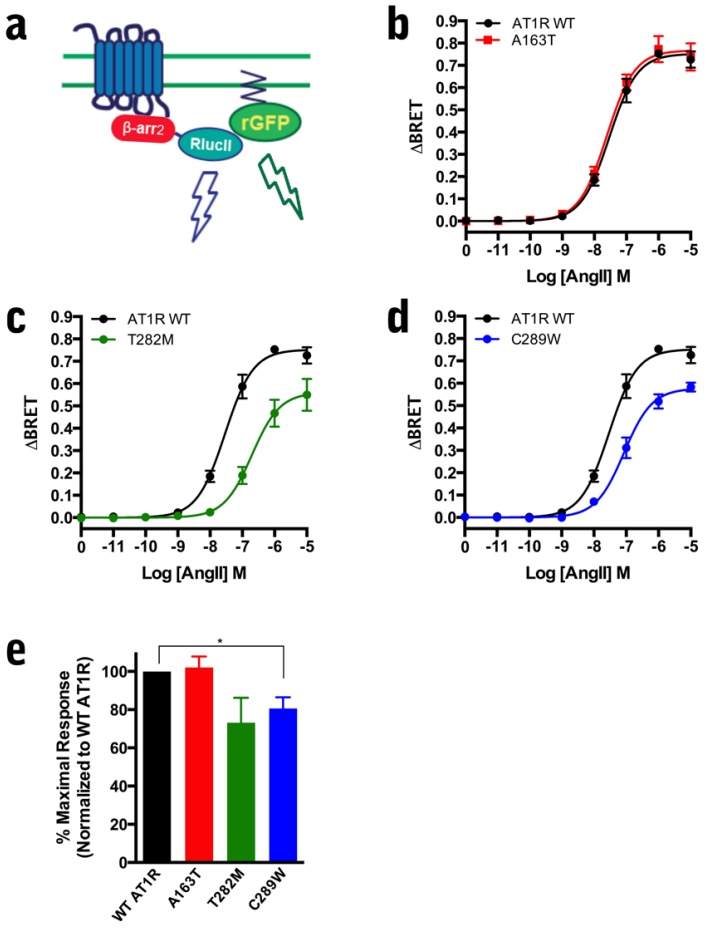

Figure 3.8: β-arrestin-2 recruitment to the activated receptor at the plasma membrane. (**a**) Schematic of the ebBRET pair with RlucII tagged to β-arrestin-2 in the cytosol and *Renilla* GFP (rGFP) anchored at the plasma membrane. Activation of the receptor promotes the recruitment of β-arrestin to the plasma membrane. (**b**) Concentration-response curve of the A163T-AT_1R and wild-type AT_1R in ΔBRET from 1×10^{-11} M to 1×10^{-5} M Ang II. (**c**) Concentration-response curve of the T282M-AT_1R and wild-type AT_1R in ΔBRET from 1×10^{-11} M to 1×10^{-5} M Ang II. (**d**) Concentration-response curve of the C289W-AT_1R and wild-type AT_1R in ΔBRET from 1×10^{-11} M to 1×10^{-5} M Ang II. (**e**) Quantification of the maximum response at 1×10^{-5} M normalized to the wild-type AT_1R. All figures are presented with the mean ± s.e.m. from four independent experiments. * $p < 0.05$.

3.8 T282M-AT_1R and β-arrestin-2 weakly complex in early endosomes

Following clathrin-mediated endocytosis, the receptor/β-arrestin-2 complex remains confined to the cytoplasm in early endosomes from where they can follow two distinct pathways: recycling back to the plasma membrane or proteolytic and/or lysosomal degradation of the receptor (Oakley et al., 1999). To assess this complex enrichment in endosomes, we used a novel ebBRET-based biosensor with β-arrestin-2 tagged with RLucII and rGFP localized to early endosomes with a FYVE zinc finger domain (Namkung, Le Gouill et al., 2016). Each condition was stimulated with an increasing concentration of Ang II from 1×10^{-11} to $1v10^{-5}$ or vehicle (Tyrode's buffer) in triplicate for 30 minutes at 37 ºC to promote internalization. The results for the A163T-AT_1 receptor reflect that of the wild-type AT_1R dose-response curve (Figure 3.9b). The T282M-AT_1R had an attenuated response of β-arrestin-2 with the early endosomal marker, whereas only 34.44 ± 1.55 % of the maximal response is reached at 1×10^{-5} M Ang II (Figures 3.9c and e). Although we observed a recruitment of β-arrestin-2 to the plasma membrane upon receptor activation (Figure 3.8c), it was surprising that T282M-AT_1R would not complex with β-arrestin-2 in the endosome. However, for C289W-AT_1R, which has a similar efficacy as T282M in β-arrestin-recruitment to the receptor (Figure 3.8d, e), the receptor was not significantly affected in its maximal response β-arrestin-2 accumulation at the endosome (Figure 3.9d, e).

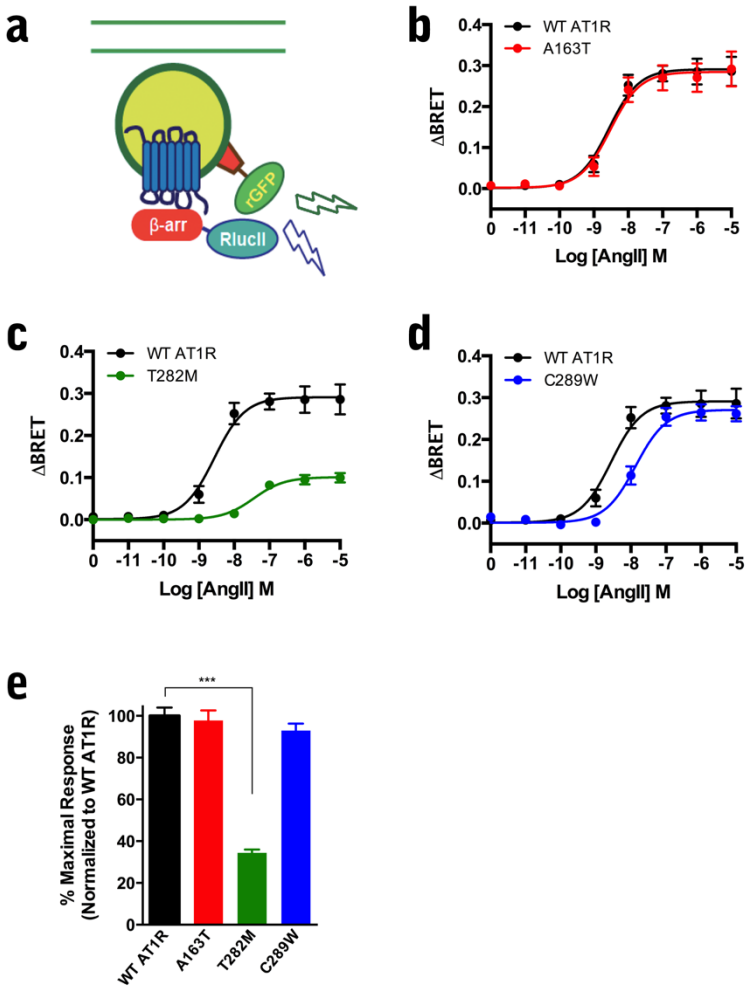

Figure 3.9: β-arrestin-2 enrichment at the endosome. (**a**) Schematic of ebBRET pair with RlucII tagged to β-arrestin-2 and rGFP anchored in the early endosomal membrane using an FYVE zinc finger domain. (**b**) Concentration-response curve of the A163T-AT_1R and wild-type AT_1R in ΔBRET from 1×10^{-11} M to 1×10^{-5} M Ang II. (**c**) Concentration-response curve of the T282M-AT_1R and wild-type AT_1R in ΔBRET from 1×10^{-11} M to 1×10^{-5} M Ang II. (**d**) Concentration-response curve of the C289W-AT_1R and wild-type AT_1R in ΔBRET from 1×10^{-11} M to 1×10^{-5} M Ang II. (**e**) Quantification of the maximum response at 1×10^{-5} M normalized to the wild-type AT_1R. All figures are presented with the mean ± s.e.m. from three independent experiments. *** $p < 0.001$.

3.9 T282M-AT_1R still internalizes into endosomes, but not in a complex with β-arrestin-2

When we observed that T282M-AT_1R recruits β-arrestin-2 to the plasma membrane (Figure 3.8), but does not remained complexed with β-arrestin-2 in endosomes (Figure 3.9), we wanted to validate if these results were due to the avidity between T282M-AT_1R and β-arrestin-2 once the complex was internalized – as shown for other receptors (e.g. class A GPCR; Oakley et al., 1999) – or simply whether the receptor failed to internalize from the plasma membrane. Thus, we used immunofluorescence to determine the receptor and β-arrestin-2 cellular localization before and after stimulation. HEK293 cells were seeded on glass coverslips and the following day were transfected with FLAG-AT_1R (WT, A163T, T282M, or C289W) and β-arrestin-2-mCherry. Cells were stimulated with Ang II for 30 minutes at 37 ºC to promote internalization or unstimulated with vehicle. Representative images were chosen for Figures 3.10 to 3.13 with scale bars of 10 μm. In the unstimulated conditions for the following figures, the receptor is localized to both the plasma membrane and some are seen inside the cell, whereas β-arrestin-2 is mostly dispersed within the cytosol. Following receptor stimulation with Ang II for 30 min, the wild-type AT_1R internalized from the plasma membrane into hollow endosomes, where it co-localized with the β-arrestin-2-mCherry signal in the cytosol (Figure 3.10, bottom row). We see this same pattern of distribution for the Ang II-stimulated A163T-AT_1R, where the receptor and β-arrestin-2 can be found together at hollow, endosomal structures after 30 minutes (Figure 3.11, bottom row). For the T282M-AT_1R, the unstimulated condition has a typical distribution of the FLAG-tagged receptor at the plasma membrane and β-arrestin-2-mCherry dispersed in the cytosol (Figure 3.12, top row). However, after Ang II stimulation for 30 minutes, the receptor is found in the cytosol in endosomal structures (Figure 3.12, bottom row), but these signals poorly co-localizes with the widely-dispersed β-arrestin-2 in the cytosol (i.e., green circles, not yellow, in the merged image).

Thus, the T282M-AT_1 receptor does still internalize from the plasma membrane, but does not complex with β-arrestin-2 in endosomes. Furthermore, the C289W-AT_1R displayed similar behaviour to the wild-type and A163T-AT_1 receptors, where it was found to co-localize in the cytosol with β-arrestin-2 following Ang II stimulation for 30 minutes (Figure 3.13, bottom row).

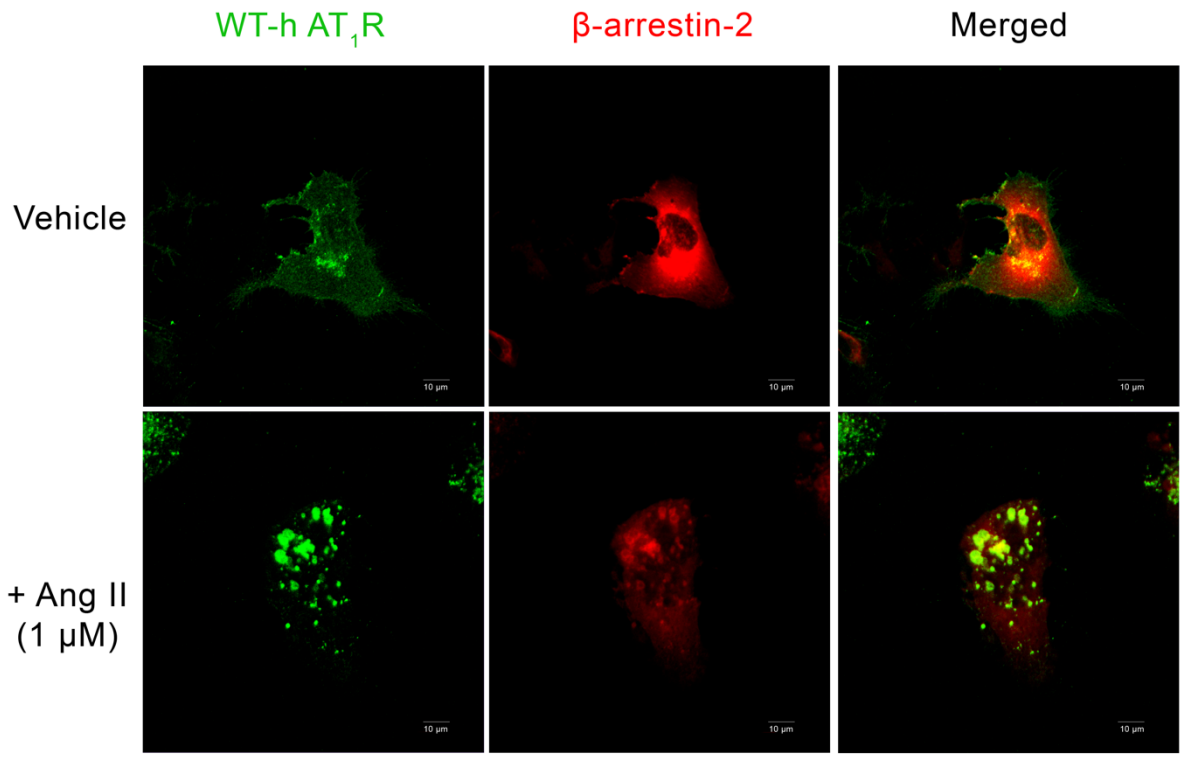

Figure 3.10: Immunofluorescence microscopy images of HEK293 cells expressing FLAG-tagged wild-type AT_1R and human β-arrestin-2-mCherry in the presence of basal (control, top row) or stimulated for 30 minutes at 37 ºC and 5% CO_2 with 1 μM Ang II (bottom row). For co-localization visualization, green (receptor) and red (β-arrestin-2) images were merged. Representative images are shown. Scale bars: 10 μm.

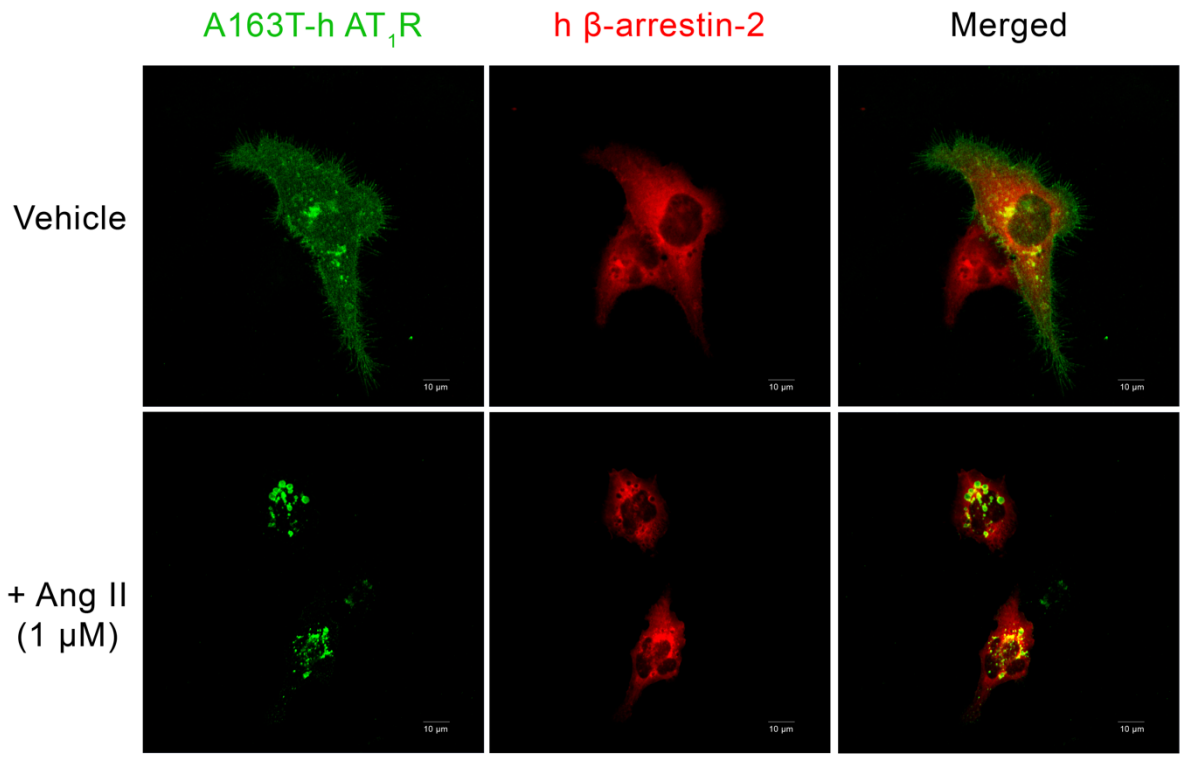

Figure 3.11: Immunofluorescence microscopy images of HEK293 cells expressing FLAG-tagged A163T-AT_1R and human β-arrestin-2-mCherry in the presence of basal (control, top row) or stimulated for 30 minutes at 37 ºC and 5% CO_2 with 1 μM Ang II (bottom row). For co-localization visualization, green (receptor) and red (β-arrestin-2) images were merged. Representative images are shown. Scale bars: 10 μm.

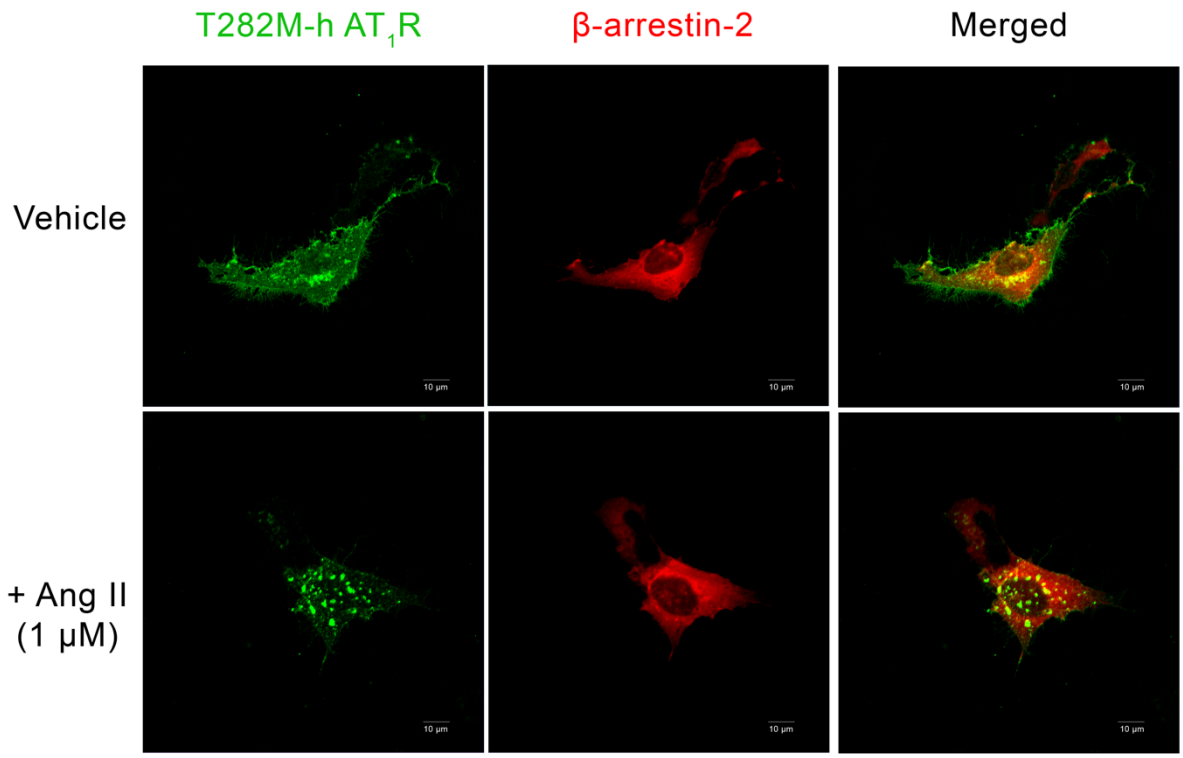

Figure 3.12: Immunofluorescence microscopy images of HEK293 cells expressing FLAG-tagged T282M-AT_1R and human β-arrestin-2-mCherry in the presence of basal (control, top row) or stimulated for 30 minutes at 37 ºC and 5% CO_2 with 1 μM Ang II (bottom row). For co-localization visualization, green (receptor) and red (β-arrestin-2) images were merged. Representative images are shown. Scale bars: 10 μm.

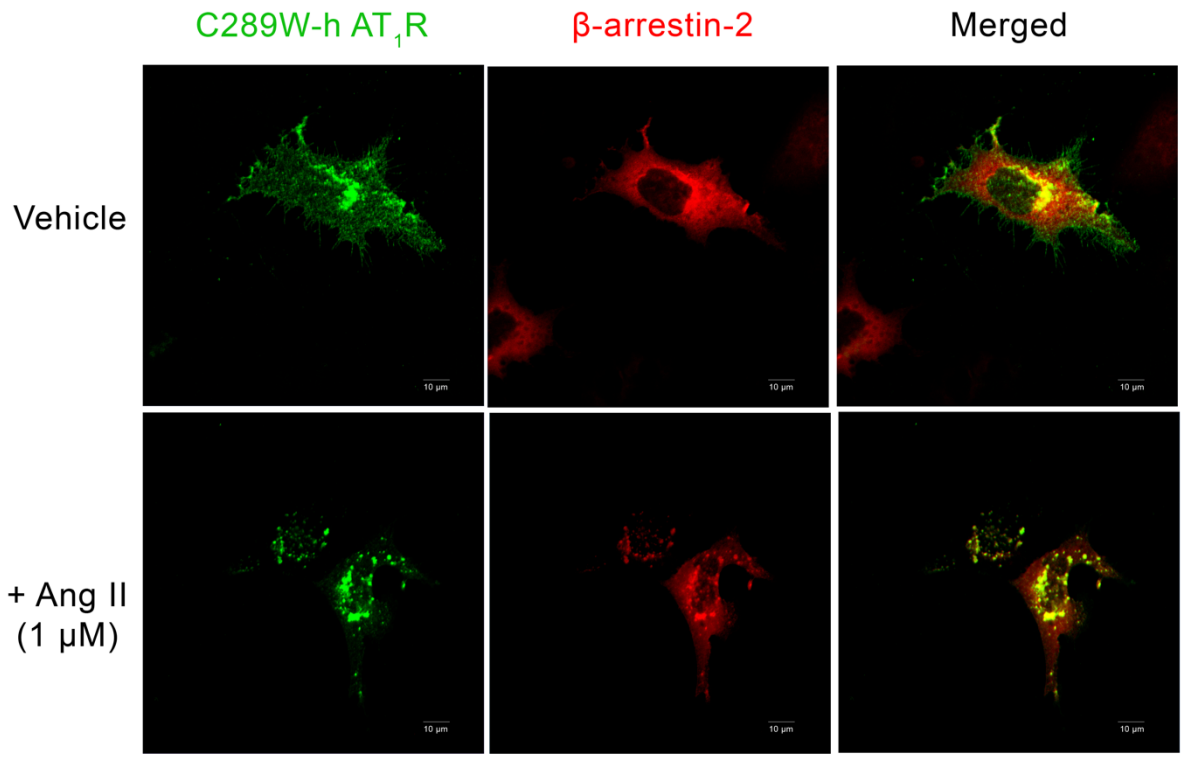

Figure 3.13: Immunofluorescence microscopy images of HEK293 cells expressing FLAG-tagged C289W-AT_1R and human β-arrestin-2-mCherry in the presence of basal (control, top row) or stimulated for 30 minutes at 37 ºC and 5% CO_2 with 1 μM Ang II (bottom row). For co-localization visualization, green (receptor) and red (β-arrestin-2) images were merged. Representative images are shown. Scale bars: 10 μm.

3.10 β-arrestin-2 is recruited to T282M-AT_1R at the plasma membrane initially, but does not remain complexed within the endosome

Although we do not see co-localization of the T282M-AT_1 receptor with β-arrestin-2 using immunofluorescence (30 min; Figure 3.12, bottom row), but we do see a well-defined response of β-arrestin-2 recruitment to the plasma membrane by BRET (2 min; Figure 3.8c), we performed a time-course experiment with β-arrestin-2-YFP in live cells using confocal microscopy to follow the internalization process following agonist stimulation. HEK293 cells were transfected with FLAG-AT_1R (WT, A163T, T282M, or C289W) and β-arrestin-2-YFP. An image was taken prior to agonist stimulation for each condition (0 min). Cells were stimulated with Ang II (1 μM) or vehicle at 37 ºC and images were captured at 5 min, 15 min, and 30 min intervals post-agonist treatment. Representative images of agonist-stimulated conditions were chosen for Figure 3.14 with scale bars of 10 μm. For the wild-type AT_1R, the β-arrestin-2 formed puncta at the plasma membrane 5 min post-stimulation with 1 μM of Ang II and formed small endosomes at 15 min, which became large, hollow endosomes by 30 min post-stimulation (white arrow, Figure 3.14a) consistent with the clathrin-mediated internalization of receptors and their targeting to EEs as previously reported (Fessart et al., 2005; Khoury, Nikolajev et al., 2014). The A163T-AT_1R follows the same pattern of β-arrestin-2 recruitment as the wild-type receptor, where large, hollow endosomes are formed after 30 min of stimulation (white arrow, Figure 3.14b). Interestingly, the T282M-AT_1R is able to recruit β-arrestin-2 to the plasma membrane after 5 min agonist stimulation, as seen by the punctate pattern of distribution in Figure 3.14c (white arrow, inset), however, these structures begin to disappear even at 15 minutes post-stimulation. For the C289W-AT_1R, we observed a punctate distribution of β-arrestin-2 at 5 minutes, followed by sustained hollow endosomal structures up to 30 min post-stimulation, similar to what we observed with wild-

type AT_1R (white arrow, Figure 3.14d), which also corroborates the results obtained in the BRET-based assay in Figure 3.9d.

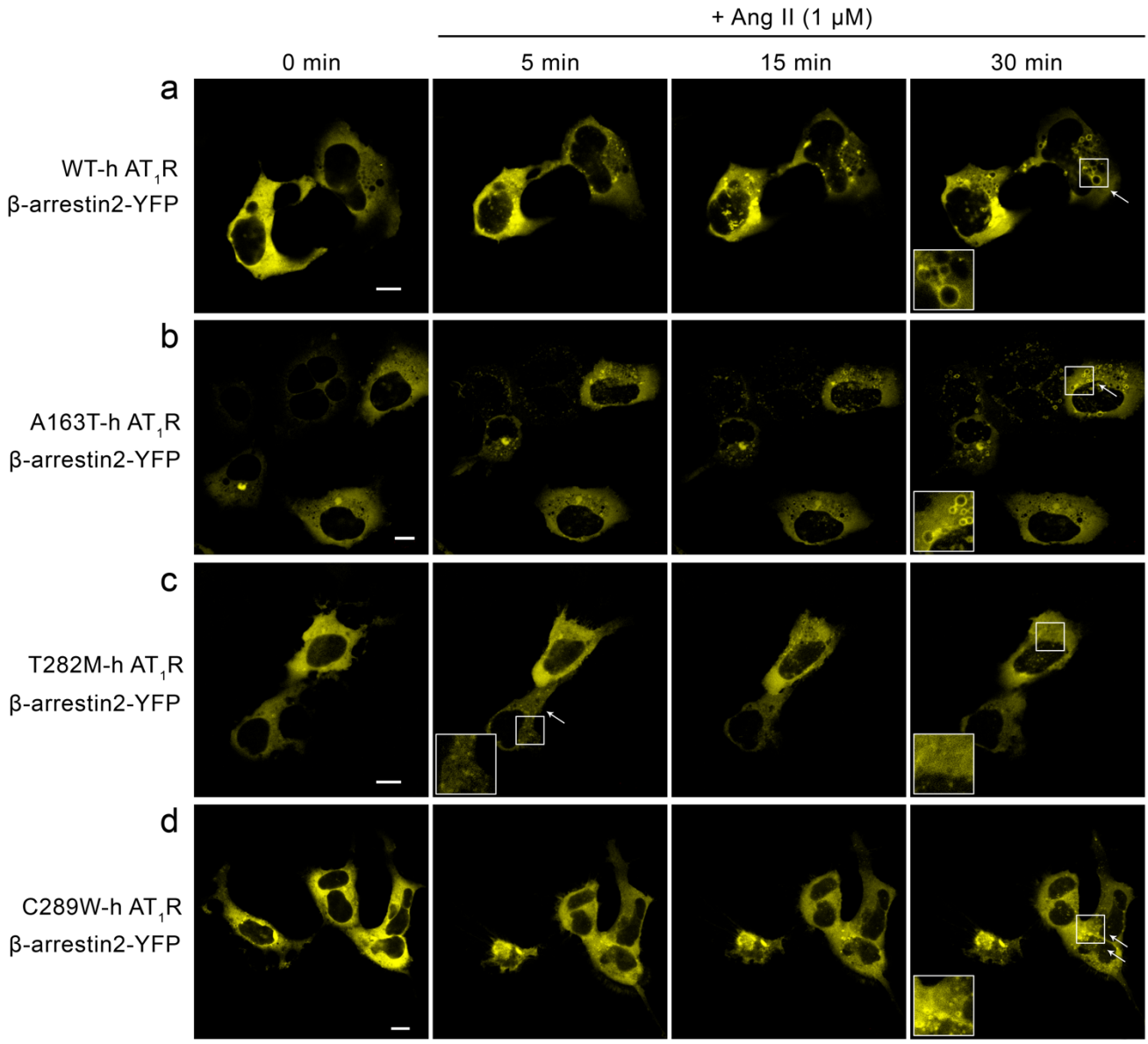

Figure 3.14: Live-cell confocal images of HEK293 cells expressing receptors and human β-arrestin-2-YFP. Prior to stimulation, images were taken at basal state (0 min). Cells were stimulated with 1 μM Ang II and pictures were taken at 5 min, 15 min, and 30 min intervals post-stimulation. (**a**) Wild-type AT_1R. (**b**) A163T-AT_1R. (**c**) T282M-AT_1R. (**d**) C289W-AT_1R. White arrows indicate endosomes for wild-type, A163T, and C289W at 30 min, whereas it indicates puncta for T282M at 5 min. Boxes depict expanded cytosolic sections of the images at 30 min post-stimulation. Representative images are shown. Scale bars: 10 μm.

3.11 Clustering the relative activity of receptor-coupled pathways using a heat map

It is difficult to compare each receptor's absolute activity directly from every assay because the observed response could be either G protein specific and/or influenced by other cellular signalling events. Concomitantly, the corresponding EC_{50} and E_{MAX} determined from each assay may vary from pathway to pathway due to intrinsic properties of the biosensors (observational bias) or sensitivity of the system (system bias; Kenakin & Christopoulos, 2013). Therefore, to quantify only biased agonism for the data collected across the panel of BRET-based biosensors and correct for these other two biases, we used a method to define a single parameter called relative activity (RA) to assess differences and be able to apply statistical analyses. Furthermore, biased signalling is typically calculated using a standard ligand as a reference, but in this work we were interested to calculate bias of polymorphic receptors relative to the wild-type receptor in the presence of the natural peptide Ang II, thus, we could not use the conventional calculation of the transduction coefficients τ/K_A (Kenakin & Christopoulos, 2013). Griffin, Figueroa, Liller, and Ehlert (2007) previously used the EC_{50} and E_{MAX} values as parameters to estimate relative activity (RA) of the receptor for G protein pathways, where the E_{MAX} is expressed as a fraction of 1.00, divided by the EC_{50} concentration represented in nM. We used a log transformed iteration of the relative activity calculation to adjust for skew and restore normality, where the formula is presented in Figure 3.15 and values are presented in Table 3.1. The heat map permits the visual clustering of the data, where a log of 0 (red) is closest to an EC_{50} of 1 nM and E_{MAX} of 100%, and a negative log represents a value between $0 < x < 1$, where the smallest relative activity represents a large EC_{50} and/or a small E_{MAX} (blue). The columns represent the receptors, whereas the rows are the assays assessed using the biosensors of interest. For $G\alpha_{12}$, the A163T-AT_1R retains a higher

coupling activity than the wild-type receptor, whereas the T282M-AT_1R's relative activity is significantly reduced (logRA = –2.632).

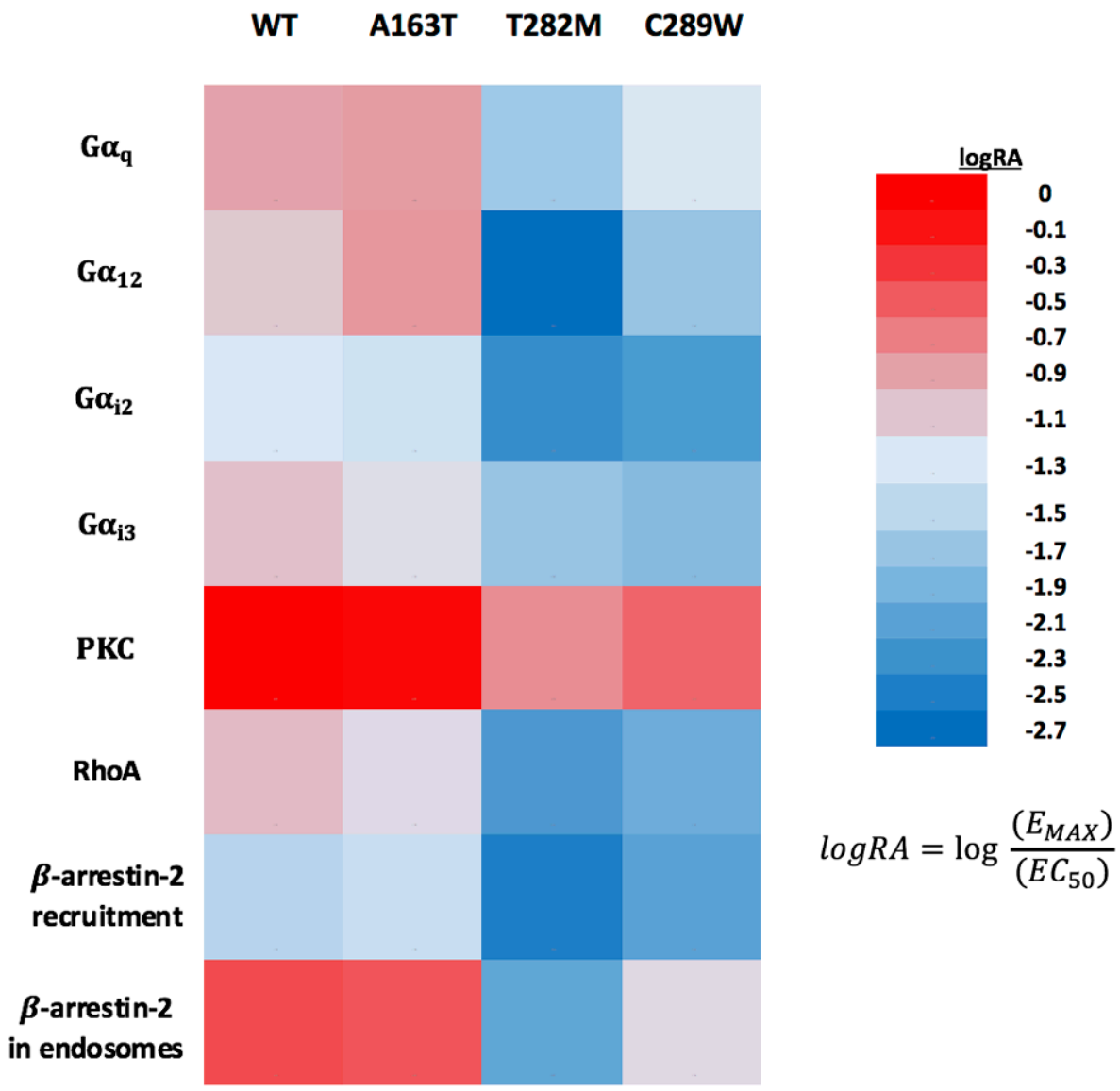

Figure 3.15: Heat map representing the log Relative Activity (logRA) of each receptor (column) in the BRET biosensors pathways assessed (rows). The equation used to calculate logRA substitutes the E_{MAX} and EC_{50} values found in Table 3.1. The coloured legend of logRA values is indicated to the right of the figure.

3.12 Using the Δlog Relative Activity to calculate bias of polymorphic variants

Although we are using the wild-type AT_1R is our reference, it does exclude the fact that its own signalling is biased. Hence, using the logRA values alone would not correct for the inherent observational bias of the system. We calculated the ΔlogRA for all pathways assessed with the polymorphic variants with respect to the wild-type AT1R (Kenakin & Christopoulos, 2013). The ΔlogRA calculated from each independent experiment was plotted with the mean ± S.E.M in Figure 3.16. The mean ΔlogRAs for T282M-AT_1R and C289W-AT_1R were found to be statistically significant from the wild-type AT_1R (Tukey's multiple comparison post-hoc test, $p <$ 0.05 or smaller), whereas the A163T-AT_1R maintains the same relative activity as the wild-type receptor in every assay assessed. Looking within the T282M-AT_1R's grouping of ΔlogRAs, the $G\alpha_{12}$ activation assay and β-arrestin-2 enrichment in early endosomes assay have significantly displaced ΔlogRAs from the other responses (Tukey's multiple comparison post-hoc test, $p < 0.01$ or smaller). Although, the C289W-AT_1R, which also has an attenuated relative activity from the wild-type receptor, did not have the same signalling bias between its pathways. The only comparisons found to be significant for C289W were $G\alpha_q$ vs $G\alpha_{i2}$ and $G\alpha_q$ vs RhoA; however, the $G\alpha_{i2}$ and RhoA responses were not statistically different from all the other pathways assessed, unlike the results from the T282M variant's Tukey's multiple comparison post-hoc test.

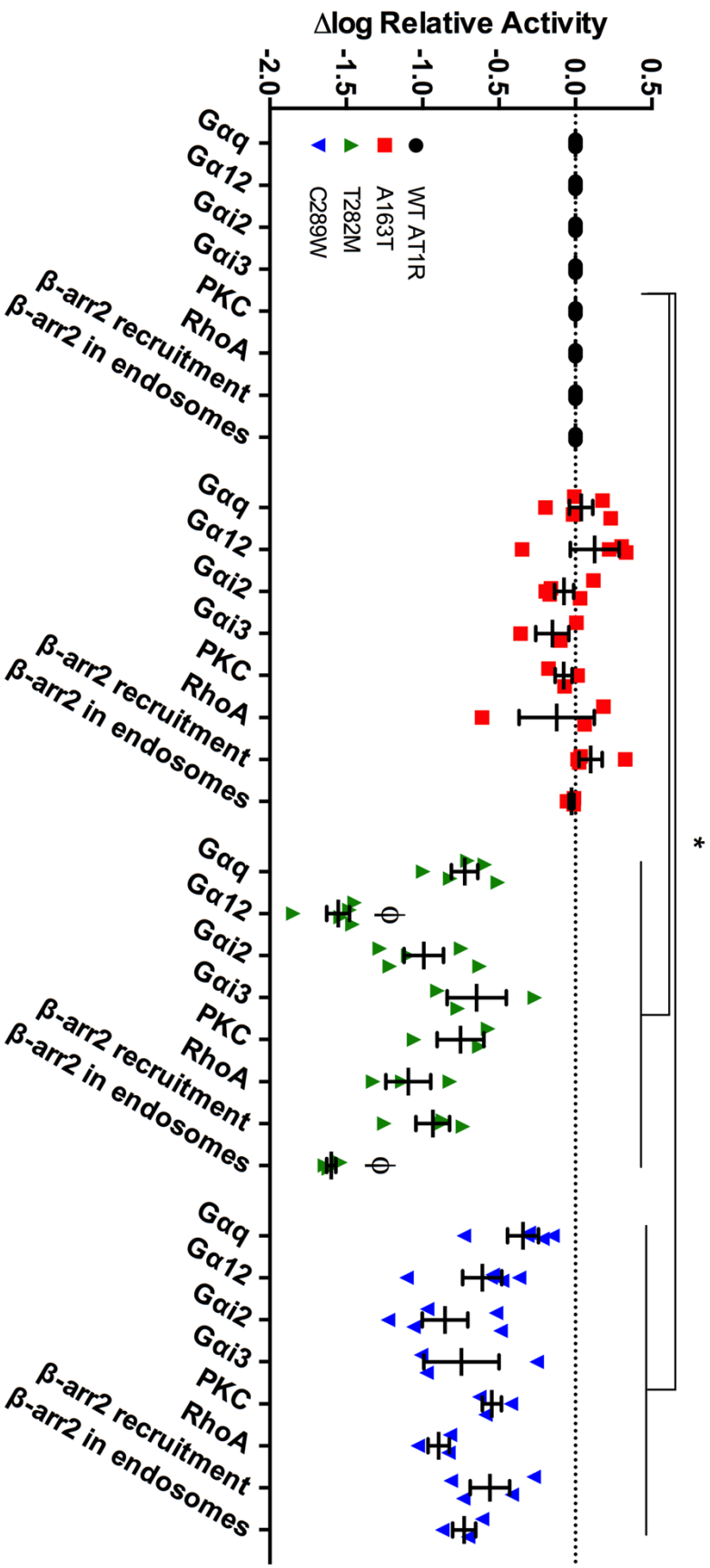
Δlog Relative Activity
-2.0
-1.5
-1.0
-0.5
0.0
0.5
WT AT1R
A163T
T282M
C289W
Gαq
Gα12
Gαi2
Gαi3
PKC
RhoA
β-arr2 recruitment
β-arr2 in endosomes
*

Figure 3.16: Δlog Relative Activity calculations of polymorphic receptors relative to the wild-type AT_1R. The mean ± s.e.m ΔlogRA are plotted for 3-5 independent experiments. Tukey's post-hoc multiple comparisons tests were used to compare wild-type and polymorphic receptors across the panel of assays, as well as within the receptor groups between assays. * $p < 0.05$ for comparisons with wild-type AT_1R, ϕ $p < 0.01$ for within receptor group comparisons.

Table 3.1: Activity of receptor with panel of BRET-based biosensors in HEK293 cells. Data are extracted from GraphPad Prism 6 curve fittings and values represent means ± s.e.m. logRAs are calculated with the formula presented in Figure 3.15. Significant *p* values are shown in red.

BRET Assay	Receptor	EC_{50} (logM)		E_{MAX} (%)		Relative Activity (RA)	logRA
		Mean ± SEM	***P* value**	**Mean ± SEM**	***P* value**		
$G\alpha_q$	WT	-8.10 ± 0.05	—	100	—	0.127	-0.898
	A163T	-8.13 ± 0.07	0.74	102.61 ± 5.75	0.66	0.139	-0.857
	T282M	-7.38 ± 0.06	1.34E-5	99.41 ± 3.85	0.88	0.024	-1.621
	C289W	-7.76 ± 0.09	0.013	99.12 ± 5.04	0.88	0.058	-1.239
$G\alpha_{12}$	WT	-7.92 ± 0.07	—	100	—	0.083	-1.082
	A163T	-8.10 ± 0.16	0.342	116.45 ± 10.87	0.17	0.148	-0.831
	T282M	-6.41 ± 0.12	4.38E-6	90.31 ± 5.06	0.09	0.002	-2.632
	C289W	-7.28 ± 0.10	9.31E-4	106.32 ± 6.65	0.37	0.020	-1.689
$G\alpha_{i2}$	WT	-7.72 ± 0.03	—	100	—	0.052	-1.284
	A163T	-7.63 ± 0.08	0.34	103.37 ± 2.99	0.29	0.044	-1.358
	T282M	-6.73 ± 0.15	1.94E-4	99.51 ± 2.85	0.87	0.005	-2.276
	C289W	-6.91 ± 0.13	3.93E-4	90.89 ± 6.13	0.18	0.007	-2.134
$G\alpha_{i3}$	WT	-7.96 ± 0.07	—	100	—	0.091	-1.041
	A163T	-7.84 ± 0.16	0.53	93.39 ± 4.58	0.22	0.064	-1.191
	T282M	-7.43 ± 0.25	0.12	76.15 ± 2.85	0.002	0.021	-1.687
	C289W	-7.34 ± 0.19	0.03	75.55 ± 3.03	0.001	0.016	-1.786
PKC	WT	-8.95 ± 0.06	—	100	—	0.892	-0.050
	A163T	-8.87 ± 0.07	0.42	105.0 ± 2.86	0.26	0.775	-0.111
	T282M	-8.26 ± 0.12	0.007	91.18 ± 4.27	0.14	0.165	-0.781
	C289W	-8.41 ± 0.04	0.002	102.1 ± 2.74	0.60	0.260	-0.585
RhoA	WT	-7.98 ± 0.09	—	100	—	0.097	-1.014
	A163T	-7.81 ± 0.06	0.30	99.88 ± 3.99	0.98	0.066	-1.183
	T282M	-7.02 ± 0.06	0.0009	65.27 ± 3.01	0.002	0.007	-2.160
	C289W	-7.15 ± 0.06	0.0014	77.01 ± 2.66	0.009	0.011	-1.953
β-arrestin-2 recruitment	WT	-7.51 ± 0.13	—	100	—	0.033	-1.487
	A163T	-7.61 ± 0.08	0.57	102.11 ± 5.78	0.73	0.041	-1.384
	T282M	-6.69 ± 0.14	0.005	80.15 ± 11.55	0.14	0.004	-2.443
	C289W	-7.05 ± 0.14	0.05	80.66 ± 5.81	0.02	0.009	-2.043
β-arrestin-2 in endosomes	WT	-8.56 ± 0.14	—	100	—	0.366	-0.436
	A163T	-8.52 ± 0.17	0.86	97.74 ± 4.89	0.74	0.325	-0.488
	T282M	-7.45 ± 0.13	0.004	34.44 ± 1.55	0.0001	0.010	-2.018
	C289W	-7.87 ± 0.10	0.016	93.01 ± 3.32	0.25	0.069	-1.162

Chapter 4: Discussion

CHAPTER IV: Discussion

The work herein describes the use of a panel of novel bioluminescence resonance energy transfer (BRET)-based biosensors[9] to assess the signalling of wild-type and polymorphic variants of the angiotensin II type 1 receptor. We assessed the wild-type AT_1R and three polymorphic variants for their ability to engage their cognate G proteins ($G\alpha_q$, $G\alpha_{12}$, $G\alpha_{i2}$, $G\alpha_{i3}$), their downstream effectors in the signalling cascade (Protein Kinase C, Rho A), and β-arrestin-2 recruitment and trafficking. By defining the signalling and trafficking of different AT_1R receptors bearing SNPs, not only were we able to characterize the role of polymorphisms on processes of receptor activation and trafficking from various vantage points, but also determine signalling signatures for these receptors. While we show some polymorphic variants have signalling paradigms similar to the wild-type AT_1R, we have uncovered a biased signalling profile of the T282M-AT_1R polymorphic variant, which yields a decline in both $G\alpha_{12}$ coupling and formation of β-arrestin-2/receptor complexes in endosomes when compared to the wild-type AT_1R. These data convey that the T282M polymorphic variant of the AT_1R has the ability to differentially engage certain G proteins or β-arrestin to direct the signalling of the receptor through a specific and unique pathway. This study was the first to report a non-synonymous single nucleotide polymorphism in the coding region of the AT_1R could direct Ang II-mediated signalling of the receptor in a biased manner.

[9] These novel BRET-based biosensors have been developed in our lab and initially published in Namkung, Radresa *et al.* (2016) and Namkung, Le Gouill *et al.* (2016). Other sensors presented in this work are currently in preparation for publication.

4.1 Effect of SNPs on AT_1R expression and Ang II binding

We reported that the level of expression of the polymorphic receptors remained consistent to the wild-type AT_1 receptor at the plasma membrane in HEK293 cells (Figure 3.1a), thus, refuting the possibility that a SNP at positions 163, 282, or 289 in the AT_1R causes misfolding or prevents the maturation of the receptor. These results were not surprising since the SNPs did not occur at important glycosylation or other post-translational modification sites of the protein that would prompt changes in receptor expression at the plasma membrane (Bannert et al., 2001; Maurice et al., 2011). The level of cell surface expression was visualized using confocal microscopy and the polymorphic variants were found to express to a similar extent as the wild-type receptor without large accumulation within the cells (Figures 3.10 to 3.13). This evidence can be further corroborated with the BRET data, where we can obtain a maximal response comparable to the wild-type AT_1R in multiple assays (Figure 3.2e); in order to attain consistent E_{MAX} values in these BRET assays, there cannot be a substantial decrease nor increase in receptor expression (Kenakin & Christopoulos, 2003). Thus, we can conclude the polymorphic receptors' expression was equal to the wild-type AT_1R.

Although the receptor expression remained unchanged, the specific binding of [^{125}I]-Ang II was significantly reduced for T282M-AT_1R and C289W-AT_1R (Figure 3.1b). Furthermore, this became problematic when generating the radioligand dose-displacement curve due to the reduced binding of the radioactive tracer (Figure 3.1c). An explanation for this could be that in order to assess the specific binding of the ligand at the receptor, a negligible amount of radioactive tracer must be used in order to not influence the binding of the competitive ligand and to occupy only a fraction of the expressed receptors (Hulme & Trevethick, 2010). Thus, 0.2 nM of the tracer ^{125}I-Ang II was used to remain below the K_d of Ang II for the AT_1R, which has been reported to be

around 1-5 nM (Zimmerman et al., 2012). If the receptor did lose affinity for the radioligand tracer due to the SNP near the orthosteric binding pocket, this would affect the proportion of receptors occupied by the radioligand tracer at equilibrium and would be reflected as a loss of radioactive counts (Hulme & Trevethick, 2010). This suggests that T282M-AT_1R and C289W-AT_1R have reduced affinity for Ang II, whereas A163T-AT_1R could have a greater affinity due to its slightly increased specific binding. The affinity of each polymorphic variant for Ang II could, thus, be validated with a saturation binding experiment, where increased concentrations of the radioligand (i.e., higher than 0.2 nM) are used (Hulme & Trevethick, 2010). In that respect, Arsenault *et al.* performed a saturation binding experiment with A163T-AT_1R and the wild-type AT_1R using [^{125}I]-SI ([Sar^1, Ile^8]-Ang II), which they concluded both receptors had normal affinity for Ang II and its analogue SI (2010). Furthermore, from their saturation binding experiments, this group reported the B_{max} of A163T-AT_1R to be 1.5 ± 0.9 pmol/mg of protein and the B_{max} of the wild-type AT_1R to be 1.4 ± 0.7 pmol/mg in COS-7 cells (Arsenault et al., 2010). Moreover, performing the saturation binding could corroborate the level of expression of all receptors that we assessed through fluorescence-activated cell sorting.

Although the affinity of each receptor was not determined directly with saturation binding curves, which require large amounts of the radioactive tracer, there were alternate experiments which alluded to the true affinity of each receptor for Ang II. For instance, from the BRET concentration-response curves, we could speculate the affinity of T282M-AT_1R and C289W-AT_1R were decreased by the same magnitude as the consistent rightward shift observed in the EC_{50} values of the curves (Table 3.1). This consistent decrease in affinity was also reflected in the Δlog Relative Activity (Figure 3.16), where the ΔlogRAs of both T282M-AT_1R and C289W-AT_1R varied from the wild-type AT_1R by 0.5 log to 1.0 log in the majority of pathways assessed, whereas

no change of log Relative Activity was evident for the A163T-AT_1R, which had consistent, superimposed concentration-response curves with the wild-type AT_1R in all pathways we assessed and no reported change in Ang II affinity by Arsenault *et al.* (2010). Although the affinity of the two polymorphic receptors were attenuated, this did not prevent receptors from reaching the maximal response of the wild-type AT_1R (Table 3.1). Although saturation binding experiments should be performed in the future, for all intents and purposes, we can demonstrate through BRET experiments that the decrease in affinity of Ang II for T282M-AT_1R and C289W-AT_1R does not impair the capacity of Ang II to bind the receptors nor initiate intracellular signalling events.

4.2 Biochemical implications of amino acid modifications in the AT_1R's orthosteric binding pocket

Since the amino acids at position 282 and 289 fall within the seventh transmembrane region of AT_1R, we could speculate the loss of affinity of Ang II was a result of altered intermolecular interactions within the orthosteric binding pocket. As we hypothesized in the rationale for this study, a disruption of the intermolecular interactions of the endogenous ligand with the receptor and the intramolecular interactions within the orthosteric binding site could direct downstream cellular responses by creating a specific, stabilized conformation. As previously reported, a single point mutation at position 111 of the AT_1R can stabilize the receptor in a constitutively active confirmation when an asparagine is substituted for a glycine (N111G; Le et al., 2003). For T282M and C289W (Figure 4.1), we consider that changes from the polar amino acids threonine and cysteine to the large, non-polar amino acids methionine and tryptophan, respectively, could sterically hinder adjacent interactions – such as the negatively-charged aspartic acid at position 281 of the AT_1R, which interacts with the positively-charged Arg^2 of Ang II (purple in Figure 1.4;

Hunyady et al., 2003) – and/or disrupt the intermolecular interactions with the nearby amino acids[10] Phe^{293}/Asn^{294}, which are two G protein binding sites on the AT_1R (green in Figure 1.4; de Gasparo et al., 2000; Hunyady et al., 2003). In 2015, Zhang *et al.* published a crystal structure of the AT_1R with olmesartan, demonstrating the three SNP locations in the orthosteric binding pocket and the orientation of their side chains, from which we could infer possible interactions with the bulky side chains of the amino acid substitutions. Hence, it is possible this the loss of affinity of Ang II and altered G protein activity observed is a result of introducing large, non-polar amino acids within the seventh transmembrane domain. Although our study only addresses the implications on the signalling of these SNPs, it would be worthwhile to further explore the trafficking and biochemical implications of these amino acid modifications.

[10] Phe is a non-polar, hydrophobic amino acid, whereas Asn is a polar, uncharged amino acid.

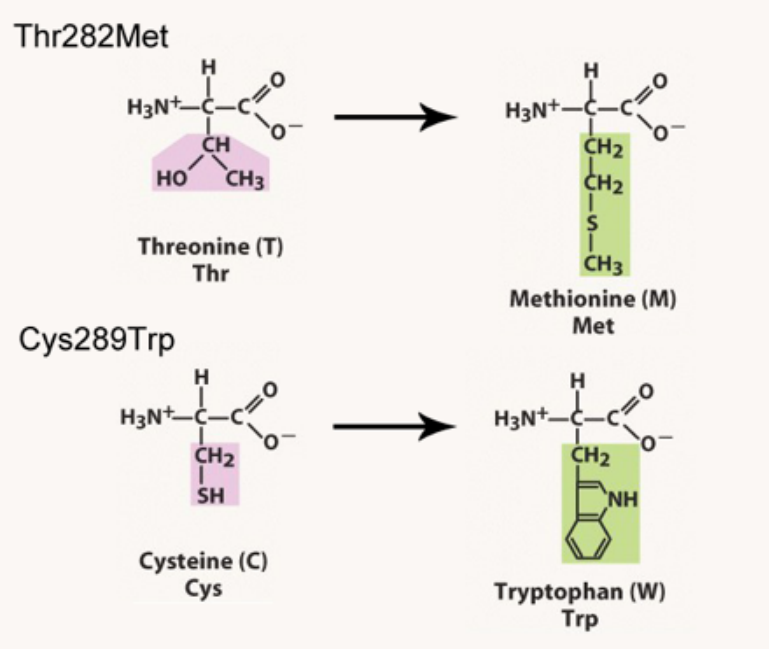

Figure 4.1: Structural changes in amino acid substitution as a result of single nucleotide polymorphisms in transmembrane VII. The Thr282Met polymorphism results in a change from a highly conserved medium-sized and polar threonine as position 282 to a medium-sized and hydrophobic methionine, whereas the Cys289Trp polymorphism results in a medium-sized and polar cysteine to a large-sized and aromatic tryptophan.

4.3 Effect of AT_1R SNPs on the activation of G proteins and their downstream effectors

We wanted to evaluate if the receptor variants had the potential to bias G protein signalling. We were able to show a robust activation of $G\alpha_q$ by all polymorphic variants, whereby the maximal responses were equal to the wild-type AT_1R (Figure 3.2e). Here, the T282M-AT_1R and C289W-AT_1R presented a decreased potency in their responses, which could merit two possible explanations: (1) these receptors have a diminished affinity for Ang II, thus requiring a greater concentration of the agonist to reach the same half-maximal response (EC_{50}), or (2) the polymorphism promotes a loss in the efficiency of signal transduction, meaning the receptor is hindered in fully coupling and activating the G protein (Kenakin & Christopoulos, 2013). This loss of signal transduction could be indicative of biased signalling, where the SNP would promote a conformation of the receptor that does not allow it to actively engage $G\alpha_q$, but retain its ability to activate other G proteins (Kenakin & Christopoulos, 2013). Although, what we do see is a consistent shift in potency for other G proteins, including $G\alpha_{i2}$ and $G\alpha_{i3}$, as well as β-arrestin-2 recruitment to the plasma membrane; hence, it would be improbable that our observation is a result of a loss in the efficiency of signal transduction in all these cases, but rather these consistencies would point to a diminished affinity of these receptors for Ang II. Furthermore, when we assess the activation of the effector Protein Kinase C downstream of $G\alpha_q$, this phenomenon of the rightward shift in the EC_{50}s of T282M-AT_1R and C289W-AT_1R can be reproduced to an equivalent degree (Figure 3.3). Thus, our results suggest that the consistent change in potency was indicative of a loss of Ang II affinity.

While we can see patterns exist in the G protein signalling paradigm between polymorphic receptors, there are anomalies also present in our data. Namely, the T282M-AT_1R had a 32-fold change in potency of $G\alpha_{12}$ coupling – an effect of greater magnitude that we cannot simply

attribute to a loss in Ang II affinity. Following the logic that potency is a result of both the affinity of Ang II and the efficiency of signal transduction, indeed, the results we observed could be further attributed to the T282M variant's inability to efficiently couple to the $G\alpha_{12}$ protein. Conversely, we do not see a dramatic change in coupling to $G\alpha_{12}$ for C289W-AT_1R, where this variant produced a response representative to its other G proteins. Interestingly, all receptors were able to reach the same maximal response for $G\alpha_{12}$. So despite the fact that the T282M-AT_1R may have intrinsically lost sensitivity to this G protein, it does not completely lose its ability to interact with the protein and efficiently mediate a pharmacological response to a similar extent as the wild-type receptor at higher concentrations of Ang II. These results highlight a possible G protein bias where the SNP biochemically stabilizes a different receptor conformation, which decreases the sensitivity of the T282M variant for $G\alpha_{12}$, but not its association with other G proteins; this understanding has been previously applied to biased signalling by ligands (Kenakin & Christopoulos, 2013).

If there is a true signalling bias for $G\alpha_{12}$, it should also be evident in the control of its downstream effectors. $G\alpha_{12}$ and $G\alpha_{13}$ have been reported to activate the small GTPase Rho A for actin stress fiber formation through the regulation of a subfamily of RhoGEF proteins (Vogt et al., 2003). Our initial assessment of Rho A activation was not able to replicate the G protein signalling bias (Figures 3.5a, c, and e), but this was likely due to the integration of the Rho A response from both $G\alpha_{q/11}$- and $G\alpha_{12/13}$-activated RhoGEFs (Vogt, Grosse, Schultz, & Offermanns, 2003). In order to dissociate this composite signalling of Rho A, we used the $G\alpha_{q/11}$ inhibitor UBO-QIC (Bernard et al., 2014). UBO-QIC, also named FR900359, is a guanosine nucleotide dissociation inhibitor, which maintains the $G\alpha_{q/11}$ proteins in the GDP-bound, inactive state without having off-target effects cellular metabolic homeostasis, even at high concentrations (Bernard et al., 2014; Schrage et al., 2015). The recorded response following UBO-QIC pretreatment was representative

of the $G\alpha_{12/13}$-only component of the Ang II-mediated activation of Rho A (Figures 3.5b, d, and f). We were also able to use this inhibitor to establish the PKC biosensor was under control of only the $G\alpha_{q/11}$ pathway, since the signalling could be completely blocked with UBO-QIC (Supplemental Figure 1). Now, we were able to discern the same $G\alpha_{12}$ signalling bias for T282M-AT_1R when compared to the other polymorphic variants, thus, supporting the evidence that this variant is less efficacious to activate this $G\alpha_{12/13}$ pathway. Furthermore, the T282M-AT_1R fails to activate the Rho A effector with the same efficacy as the wild-type AT_1R, which was indicative by the reduced maximal response (Figure 3.5g). Similarly, the C289W-AT_1R also produced a sub-maximal response relative to the wild-type AT_1R. However, this requires further validation to determine if there is reduced $G\alpha_{13}$ RhoGEF activation, as both the T282M and C289W variants were able to activate $G\alpha_{12}$ to the same maximal response as the wild-type AT_1R at 1×10-5 M Ang II. There is a possibility that the differences detected are reflection of a "system bias" between the two biosensors, where indirect analysis of Rho A activation is dependent on the relative efficiency of the signalling pathway to produce a robust response (Kenakin & Christopoulos, 2013).

Although not well characterized in the literature, the AT_1R has the ability to couple to $G\alpha_i$ proteins, namely $G\alpha_{i2}$ and $G\alpha_{i3}$ (Navarro et al., 2008). We assessed the coupling of each receptor to these two final G proteins using similar BRET-based biosensors. In addition, we observed a consistent signalling profile of $G\alpha_{i2}$ to the other G proteins: a rightward shift in the potency of both T282M-AT_1R's and C289W-AT_1R's concentration-response curves, whereas there was no change in efficacy. These results further support that the rightward shift in the EC_{50}s observed are in fact an artifact of a decreased Ang II affinity for these two variants. However, the $G\alpha_{i3}$ response did vary from the $G\alpha_{i2}$ response, since both the T282M and C289W variants did not reach the maximal response of the wild-type receptor (Figure 3.7e); although, it is unclear if this observation

can be attributed to a weaker or reduced coupling of the G protein for these two variants, which would result in a decreased efficacy. Furthermore, the C289W-AT_1R had a greater rightward shift in potency than the T282M-AT_1R, which was unlike the trend we observed in the other G protein assays, where the T282M variant always had the greatest magnitude of change in its potency (Figure 3.7d).

4.4 Effect of AT_1R SNPs on β-arrestin-2's role in receptor trafficking

Following the rapid activation of G proteins, G protein receptor kinases (GRKs) translocate to the plasma membrane to phosphorylate the receptor on its cytoplasmic domains, allowing for the recruitment of β-arrestin to the plasma membrane to act as a scaffold of the endocytic machinery (Laporte et al., 1999; Oakley et al., 1999). Additionally, the association of β-arrestin with the receptor uncouples it from its G protein signalling capabilities, making the receptor refractory to external stimuli (Chuang et al., 1996; Laporte et al., 1999; Oakley et al., 1999). We assessed whether the polymorphic variants retained the ability to recruit β-arrestin to the plasma membrane following receptor activation and phosphorylation. The T282M-AT_1 and C289W-AT_1 receptors exhibited a decrease in their potency to a degree consistent throughout all the BRET-based assays. Moreover, these two variants presented a decrease in their maximal responses of their concentration-response curves, which were significantly different than the wild-type AT_1R. Although the assays were performed at a time point where the biosensors were validated to have the maximal response for the wild-type receptor (i.e., 2 min; Namkung, Le Gouill et al., 2016), it does not take into account if the GRK kinetic properties differ considerably between the polymorphic and wild-type receptors. Indeed, the synergy between GRK and β-arrestin proteins are important for receptor desensitization, but internalization largely depends on the

phosphorylation of serine and threonine residues located on the receptor's C-terminal tail by GRKs to activate the recruited β-arrestin (Oakley et al., 1999; Charest, Terrillon, & Bouvier, 2005). Thus, we may observe a decrease in efficacy at 2 min for T282M-AT_1R and C289W-AT_1R, but it would need to be validated whether these responses would reach the wild-type maximal response at longer time points. More importantly, what these results demonstrate are that agonist treatment will induce recruitment of β-arrestin-2 to the plasma membrane for all the AT_1 receptors assessed.

Following internalization mediated by the endocytic machinery, type B GPCRs engage β-arrestin-2 with high avidity, resulting in the accumulation of the receptor/β-arrestin-2 complexes in endosomes, which prevents fast receptor recycling (Oakley et al., 1999). Next, we evaluated the capacity of each receptor variant/β-arrestin-2 complex to enrich within early endosomes (Figure 3.9). Although A163T-AT_1R and C289W-AT_1R were able to reach the same maximal response as the wild-type receptor and remain associated in a complex following 30 minutes of Ang II stimulation, T282M-AT_1R failed to remain in a complex with β-arrestin-2 in the early endosomes (Figure 3.9e). We demonstrate the decrease in BRET signal was not from the inability of the T282M-AT_1 receptor to internalize from the plasma membrane into endosomes, since we observed intracellular trafficking of the receptor through confocal microscopy (Figure 3.12). Also through confocal microscopy, we could observe β-arrestin-2 recruitment to the plasma membrane after 5 minutes into puncta, which disappear at 15 min (Figure 3.14c). The loss of β-arrestin avidity for the receptor suggests that the SNP could promote a conformational change in the β-arrestin-2 protein that is distinctive from the conformations stabilized by the other polymorphic or wild-type receptors. Indeed, a similar phenomenon has been shown where biased Ang II analogues can mediate ligand-specific β-arrestin conformations of the AT_1R distinct from Ang II stimulation (Zimmerman et al., 2012; Lee et al., 2016). These Ang II analogues are also able to promote

reduced AT_1 receptor accumulation in early endosomes and biased intracellular sorting through Rab4 and Rab11 recycling endosomes (Namkung, Le Gouill et al., 2016). Recently, Lee *et al.* were able to show that GPCRs can also impose distinct β-arrestin-2 confirmations that affect the stability of the receptor-arrestin complexes in endosomes (2016). Alternatively, the SNP could stabilize a conformation of the receptor that prevents adequate and sustained binding of the β-arrestin protein to the phosphorylation sites on the receptor. Taken together, the results obtained with the T282M-AT_1R resemble the biased signalling paradigm seen with respect to the actions of Ang II analogues and the formation of a distinct β-arrestin-2 or receptor conformation that can destabilize the receptor-arrestin complex. It would be of interest to use the β-arrestin-2–FlAsH BRET sensor developed by Lee *et al.* to validate this notion of a β-arrestin-2 conformation stabilized by T282M-AT_1R, which is distinct from either the A163T-AT_1R or C289W-AT_1R.

4.5 Establishing a signalling signature of the AT_1R and the polymorphic variants

To quantify biased agonism for the data collected across the panel of BRET-based biosensors, we used a method to define a single parameter called relative activity (RA) to assess differences and apply statistical analyses. Kenakin & Christopoulos describe this parameter as a ratio of the maximal response to the EC_{50} value in a given system (log (Relative Activity) = $\log(E_{MAX}/EC_{50})$; 2013). Using the calculated RA of each receptor, we can compare the relative activities across assays with a standard reference point (i.e., the wild-type receptor). We expressed these logRA calculations as a heat map, where the visual clustering of the signalling signatures provided insight into patterns emerging from these polymorphic variants (Figure 3.15). For example, we can note that the A163T-AT_1R couples equally well to both its $G\alpha_q$ and $G\alpha_{12}$ proteins, whereas the wild-type receptor tends to couple better to $G\alpha_q$ than its other G proteins. Although

we were using the wild-type AT_1 receptor as a reference, it does not exclude this receptor from its own biases. Furthermore, due to the sensitivity of sensors in given system, certain pathways present better in this heat map, such as PKC and β-arrestin in endosomes, which have EC_{50}s near 1 nM and logRA values closer to 0 (Table 3.1). In order to correct for this observational bias, we used the transformed parameter of ΔlogRA to determine the change in relative activity with respect to the wild-type AT_1R (Figure 3.16). The differences in the mean ΔlogRAs from the wild-type AT_1R for both the T282M-AT_1R and C289W-AT_1R were found to be statistically significant, whereas the A163T-AT_1R maintained the same relative activity as the wild-type receptor in every assay. What is important to highlight is that a Tukey post-hoc multiple comparisons test found that for the T282M-AT_1R, the relative activities from its $G\alpha_{12}$ and β-arrestin-2 in endosomes assays were statistically different from every other BRET assay reported for this receptor (shown by the ϕ in Fig 3.16). Conversely, although we found significance when comparing ΔlogRAs within the C289W-AT_1R between $G\alpha_q$ vs $G\alpha_{i2}$ and $G\alpha_q$ vs Rho A, the ΔlogRAs of $G\alpha_{i2}$ and Rho A were not statistically different from the other pathways within the C289W's signalling profile. Taken together, these results imply that the T282M-AT1R bias is evident within its signalling profile, as demonstrated in its diminished efficiency in coupling to $G\alpha_{12}$ and its inability to remain complexed with β-arrestin-2 in early endosomes.

These results underscore the role some polymorphic variants can play in different signalling paradigms relative to the wild-type AT_1R. By defining a signalling profile, we have created a predictive signalling signature of each polymorphic variant. Although, there are limitations that exist, since these polymorphic receptor signatures are intrinsic to the HEK293 cell line and would only be predictive in a model when using similar cellular contexts. However, what

is more important is that these approaches could be translated into other cellular contexts to define signatures that would better predict physiological responses *in vivo*.

4.6 Future Directions

Although we did not co-express the wild-type AT_1 receptor with a polymorphic variant, it may be worthwhile given the growing evidence supporting receptor–receptor dimerization. Receptors have been shown to be allosterically modulated by other GPCRs to bias their signalling through heterodimeration or homodimerization. Goupil *et al.* showed that the angiotensin II type 1 receptors have the capacity to heterodimerize with prostaglandin F2α receptors and both receptors allosterically modulated each other's function on abdominal aortic ring contraction (2015). Perhaps if a carrier of one of these SNPs is heterozygous at their *AGTR1* gene, the variant may have the capacity to dimerize with the wild-type and act in a dominant negative fashion to modulate the response. The T282M and C289W loss-of-function variants may pose a risk to the carrier if they are homozygously expressed; however, heterozygous expression could permit viability, but could antagonize the Ang II-mediated response.

Moreover, the T282M-AT_1R may provide a new tool to further investigate receptor internalization without β-arrestins, with the possibility to bifurcate β-arrestin signalling occurring at the plasma membrane from when the receptors are in endosomes. It was previously thought that β-arrestin signalling occurs exclusively from endosomal structures, where it generates a second wave of MAPK/ERK1/2 phosphorylation (activation) (Khoury, Nikolajev et al., 2014). Recently, Eichel *et al.* have reported that β-arrestin can drive MAPK activation directly from clathrin-coated structures without forming early endosomes (2016). Resolving these two β-arrestin-mediated signalling events remains an important challenge that could be addressed using the T282M-AT_1R,

which recruits β-arrestin to the plasma membrane, but may not produce a second wave of signalling from endosomes due to its inability to remain in a complex with the receptor. Further investigation of the temporal MAPK profile could uncover a novel receptor model to study the influence of β-arrestin-mediated intracellular signalling.

4.7 Conclusion

In our study, we found that a SNP can not only bias G protein and effector signalling, but also the avidity of the receptor/β-arrestin-2 complex in early endosomes. By affecting the receptor's ability to engage certain G proteins or β-arrestins, this can direct the signalling of the receptor through a specific therapeutic pathway, while mitigating the role of undesired responses – much like how biased ligands are being developed for this purpose. For example, the ligand TRV120027 is a competitive agonist of the AT_1R in clinical trials that selectively engages the β-arrestin pathway without activating any G protein signalling. As previously mentioned in the literature review, the benefit of β-arrestin signalling has been shown to reduce apoptosis, stimulate chemotaxis, promote protein synthesis, proliferation, and cardiac contractility (DeWire & Violin, 2011). If β-arrestin signalling can be selectively activated to increase cardiomyocyte contractility and anti-apoptotic signals, while blocking Ang II-induced hypertension, this would be of great benefit in acute heart failure. We show this interplay between G proteins and β-arrestins can now be modulated by naturally-occurring mutations of the receptor and this mosaicism of behaviours can potentially impact responses through biased signalling. Understanding the links between the signalling signatures and the physiological or pathophysiological responses may help identify and developing new biased ligands – and perhaps better targeted therapeutics.

Supplemental Figures

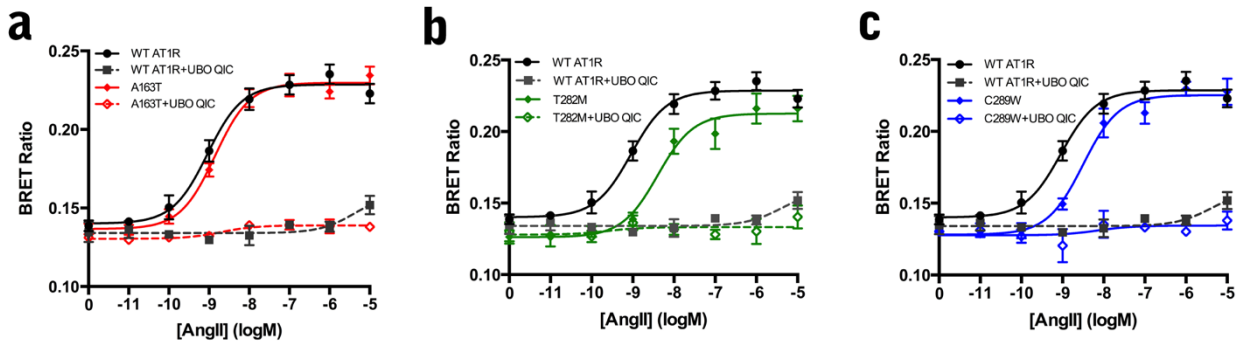

Supplemental Figure 1: PKC activation is blocked by UBO-QIC (FR. Angiotensin II concentration-response curves of the PKC biosensor following in the presence or absence of UBO-QIC (**a**) Wild-type AT_1R and A163T-AT_1R. (**b**) Wild-type AT_1R and T282M-AT_1R. (**c**) Wild-type AT_1R and C289W-AT_1R. Responses are reported with the raw BRET Ratios (515 nm/410 nm). Cells were incubated with various concentrations of Ang II for 2 min. Data are mean ± s.e.m of triplicates from two to three independent experiments.

References

Arsenault, J., Lehoux, J., Lanthier, L., Cabana, J., Guillemette, G., Lavigne, P., Leduc, R., & Escher, E. (2010). A single-nucleotide polymorphism of alanine to threonine at position 163 of the human angiotensin II type 1 receptor impairs Losartan affinity. *Pharmacogenetics and Genomics*. 20(6), 377-388.

Bannert, N., Craig, S., Farzan, M., Sogah, D., Santo, NV., Choe, H., & Sodroski, J. (2001). Sialylated O-glycans and sulfated tyrosines in the NH2-terminal domain of CC chemokine receptor 5 contribute to high affinity binding of chemokines. *The Journal of Experimental Medicine*. 194(11), 1661-1674.

Beaulieu, JM., Sotnikova, TD., Marion, S., Lefkowitz, RJ., Gainetdinov, RR., & Caron, MG. (2005). An Akt/β-arrestin-2/PP2A signaling complex mediates dopaminergic neurotransmission and behavior. *Cell*. 122(2), 261-273.

Bernard, R., Thach, L., Kamato, D., Osman, N., & Little, PJ. (2014). Assessing the role of Gαq/11 in cellular responses: an analysis of investigative tools. *Clinical & Experimental Pharmacology*, 2014.

Bonnardeaux, A., Davies, E., Jeunemaitre, X., Fery, I., Charru, A., Clauser, E., Tiret, L., Cambien, F., Corvol, P., & Soubrier, F. (1994). Angiotensin II type 1 receptor gene polymorphisms in human essential hypertension. *Hypertension*. 24(1), 63-69.

Boucard, AA., Wilkes, BC., Laporte, SA., Escher, E., Guillemette, G., & Leduc, R. (2000). Photolabeling identifies position 172 of the human AT1 receptor as a ligand contact point: receptor-bound angiotensin II adopts an extended structure. *Biochemistry*. 39(32), 9662-9670.

Braun-Menendez, E., Fasciolo, JC., Leloir, LF., & Munoz, JM. (1940). The substance causing renal hypertension. *The Journal of Physiology*. 98(3), 283.

Bridges, TM., & Lindsley, CW. (2008). G-protein-coupled receptors: from classical modes of modulation to allosteric mechanisms. *ACS Chemical Biology*. 3(9), 530-541.

Chai, BX., Neubig, RR., Millhauser, GL., Thompson, DA., Jackson, PJ., Barsh, GS., Dickinson, CJ., Li, JY., Lai, YM., & Gantz, I. (2003). Inverse agonist activity of agouti and agouti-related protein. *Peptides*. 24(4), 603-609.

Charest, PG., Terrillon, S., & Bouvier, M. (2005). Monitoring agonist-promoted conformational changes of β-arrestin in living cells by intramolecular BRET. *EMBO reports*. 6(4), 334-340.

Chuang, TT., Iacovelli, L., Sallese, M., & De Blasi, A. (1996). G protein-coupled receptors: heterologous regulation of homologous desensitization and its implications, *Trends in Pharmacological Sciences*. 17(11), 416-421.

Conn, PJ., Christopoulos, A., & Lindsley, CW. (2009). Allosteric modulators of GPCRs: a novel approach for the treatment of CNS disorders. *Nature reviews Drug discovery.* 8, 41-54.

Crick, FH. (1966). Codon–anticodon pairing: the wobble hypothesis. *Journal of Molecular Biology*. 19(2), 548-555.

de Gasparo, M., Catt, KJ., Inagami, T., Wright, JW., & Unger, TH. (2000). International union of pharmacology. XXIII. The angiotensin II receptors. *Pharmacological reviews*. 52(3), 415-472.

DeWire, SM., & Violin, JD. (2011). Biased ligands for better cardiovascular drugs dissecting G-protein-coupled receptor pharmacology. *Circulation Research*. 109(2), 205-216.

Drake, MT., Shenoy, SK., & Lefkowitz, RJ. (2006). Trafficking of G protein–coupled receptors. *Circulation research*. 99(6), 570-582.

Dunham, TD., & Farrens, DL. (1999). Conformational changes in rhodopsin. Movement of helix f detected by site-specific chemical labeling and fluorescence spectroscopy. *J Biol Chem*. 274(3), 1683–1690.

Dutt, P., Nguyen, N., & Toksoz, D. (2004). Role of Lbc RhoGEF in Gα12/13-induced signals to Rho GTPase. *Cellular signalling*. 16(2), 201-209.

Ebrahimi, FA., & Chess, A. (1998). Olfactory G proteins: simple and complex signal transduction. *Current Biology*. 8(12), R431-433.

Eichel, K., Jullié, D., & von Zastrow, M. (2016). β-Arrestin drives MAP kinase signalling from clathrin-coated structures after GPCR dissociation. *Nature Cell Biology*.

Fessart, D., Simaan, M., & Laporte, SA. (2005). c-Src regulates clathrin adapter protein 2 interaction with β-arrestin and the angiotensin II type 1 receptor during clathrin-mediated internalization. *Molecular endocrinology*, 19(2), 491-503.

Foord, SM., Bonner, TI., Neubig, RR., Rosser, EM., Pin, JP., Davenport, AP., Spedding, M., & Harmar, AJ. (2005). International Union of Pharmacology. XLVI. G protein-coupled receptor list. *Pharmacol Rev*. 57(2). 279-288.

Fredriksson, R., Lagerström, MC., Lundin, L., & Schiöth, HB. (2003). The G-protein coupled receptors in the human genome form five main families. Phylogenetic analysis, paralogon groups, and fingerprints. *Molecular pharmacology*. 63(6), 1256-1272.

Goh, LK., & Sorkin, A. (2013). Endocytosis of receptor tyrosine kinases. *Cold Spring Harbor perspectives in biology*. 5(5), a017459.

Goupil, E., Fillion, D., Clément, S., Luo, X., Devost, D., Sleno, R., Pétrin, D., Saragovi, HU., Thorin, É., Laporte, SA., & Hébert, TE. (2015). Angiotensin II type I and prostaglandin F2α receptors cooperatively modulate signaling in vascular smooth muscle cells. *Journal of Biological Chemistry*. 290(5), 3137-3148.

Gribouval, O., Gonzales, M., Neuhaus, T., Aziza, J., Bieth, E., Laurent, N., Bouton, JM., Feuillet, F., Makni, S., Amar, HB., & Laube, G. (2005). Mutations in genes in the renin-angiotensin system are associated with autosomal recessive renal tubular dysgenesis. *Nature Genetics*. 37(9), 964-968.

Griffin, MT., Figueroa, KW., Liller, S., & Ehlert, FJ. (2007). Estimation of agonist activity at G protein-coupled receptors: analysis of M2 muscarinic receptor signaling through Gi/o, Gs, and G15. *Journal of Pharmacology and Experimental Therapeutics*. 321(3), 1193-1207.

Gutkind, JS. (2000). Regulation of mitogen-activated protein kinase signaling networks by G protein-coupled receptors. *Sci. Stke*. 2000(40), re1-re1.

Hamm, HE., Deretic, D., Hofmann, KP., Schleicher, A., & Kohl, B. (1987). Mechanism of action of monoclonal antibodies that block the light activation of the guanyl nucleotide-binding protein, transducin. *Journal of Biological Chemistry*. 262(22), 10831-10838.

Hansen, JL., Haunsø, S., Brann, MR., Sheikh, SP., & Weiner, DM. (2004). Loss-of-function polymorphic variants of the human angiotensin II type 1 receptor. *Molecular Pharmacology*. 65(3), 770-777.

Hulme, EC., & Trevethick, MA. (2010). Ligand binding assays at equilibrium: validation and interpretation. *British journal of pharmacology*, 161(6), 1219-1237.

Hunyady, L., Vauquelin, G., & Vanderheyden, P. (2003). Agonist induction and conformational selection during activation of a G-protein-coupled receptor. *TRENDS in Pharmacological Sciences*. 24(2), 81-86.

Karnik, SS., Unal, H., Kemp, JR., Tirupula, KC., Eguchi, S., Vanderheyden, PM., & Thomas, W. G. (2015). International Union of basic and clinical pharmacology. XCIX. Angiotensin receptors: interpreters of pathophysiological angiotensinergic stimuli. *Pharmacological Reviews*. 67(4), 754-819.

Kenakin, T., & Christopoulos, A. (2013). Signalling bias in new drug discovery: detection, quantification and therapeutic impact. *Nature Reviews Drug Discovery*. 12(3), 205-216.

Khan, SM., Sleno, R., Gora, S., Zylbergold, P., Laverdure, JP., Labbé, JC., Miller, GJ., & Hébert, TE. (2013). The expanding roles of Gβγ subunits in G protein–coupled receptor signaling and drug action. *Pharmacological reviews.* 65(2), 545-577.

Khoury, E., Clément, S., & Laporte, SA. (2014). Allosteric and biased G protein-coupled receptor signaling regulation: potentials for new therapeutics. *Frontiers in endocrinology*. 5, 68-68.

Khoury, E., Nikolajev, L., Simaan, M., Namkung, Y., & Laporte, SA. (2014). Differential regulation of endosomal GPCR/β-arrestin complexes and trafficking by MAPK. *Journal of Biological Chemistry*. 289(34), 23302-23317.

Kirchhausen, T. (2000). Clathrin. *Annual Review of Biochemistry*. 69(1), 699-727.

Klco, JM., Nikiforovich, GV., & Baranski, TJ. (2006). Genetic analysis of the first and third extracellular loops of the C5a receptor reveals an essential WXFG motif in the first loop. *Journal of Biological Chemistry*. 281(17), 12010-12019.

Kobilka, BK. (2007). G protein coupled receptor structure and activation. *Biochem Biophys Acta.* 1768(4), 794–807.

Koenig, JA., & Edwardson, JM. (1997). Endocytosis and recycling of G protein-coupled receptors. *TRENDS in Pharmacological Sciences*. 18(8), 276-287.

Kristiansen, K. (2004). Molecular mechanisms of ligand binding, signaling, and regulation within the superfamily of G-protein-coupled receptors: molecular modeling and mutagenesis approaches to receptor structure and function. *Pharmacol Ther*. 103, 21-80.

Lagerström, MC., & Schiöth, HB. (2008). Structural diversity of G protein-coupled receptors and significance for drug discovery. *Nature reviews Drug discovery*. 7(4), 339-357.

Laporte, SA., Oakley, RH., Zhang, J., Holt, JA., Ferguson, SS., Caron, MG., & Barak, LS. (1999). The β2-adrenergic receptor/βarrestin complex recruits the clathrin adaptor AP-2 during endocytosis. *Proceedings of the National Academy of Sciences*. 96(7), 3712-3717.

Latek D., Modzelewska, A., Trzaskowski, B., Palczewski, K., & Filipek, S. (2012). G protein-coupled receptors–recent advances. *Acta Biochim Pol*. 59, 515-529.

Le, MT., Vanderheyden, PM., Szaszák, M., Hunyady, L., Kersemans, V., & Vauquelin, G. (2003). Peptide and nonpeptide antagonist interaction with constitutively active human AT 1 receptors. *Biochemical pharmacology*, 65(8), 1329-1338.

Lee, T., Schwandner, R., Swaminath, G., Weiszmann, J., Cardozo, M., Greenberg, J., Jaeckel, P., Ge, H., Wang, Y., Jiao, X., Liu, J., Kayser, F., Tian, H., & Li, Y. (2008). Identification and functional characterization of allosteric agonists for the G protein-coupled receptor FFA2. *Molecular pharmacology*. 74(6), 1599-1609.

Lin, SY., & Goodfriend, TL. (1970). Angiotensin receptors. *American Journal of Physiology–Legacy Content*. 218(5), 1319-1328.

Luciani, DS., Gwiazda, KS., Yang, TLB., Kalynyak, TB., Bychkivska, Y., Frey, MH., Jeffrey, KD., Sampaio, AV., Underhill, TM., & Johnson, JD. (2009). Roles of IP3R and RyR Ca2+ channels in endoplasmic reticulum stress and β-cell death. *Diabetes*. 58(2), 422-432.

Marinissen, MJ., & Gutkind, JS. (2001). G-protein-coupled receptors and signaling networks: emerging paradigms. *Trends in Pharmacological Sciences*. 22(7), 368-376.

Maurice, P., Guillaume, J., Benleulmi-Chaachoua, A., Daulat, AM., Kamal, M., & Jockers, R. (2011). GPCR-interacting proteins, major players of GPCR function. *Advances in Pharmacology*. 62, 349-369.

Morrell, NW., Upton, PD., Kotecha, S., Huntley, A., Yacoub, MH., Polak, JM., & Wharton, J. (1999). Angiotensin II activates MAPK and stimulates growth of human pulmonary artery smooth muscle via AT1 receptors. *Am J Physiol*. 277, L440–L448.

Nabi, IR., & Le, PU. (2003). Caveolae/raft-dependent endocytosis. *J of Cell Bio*. 161(4), 673-677.

Namkung, Y., Le Gouill, C., Lukashova, V., Kobayashi, H., Hogue, M., Khoury, E., Song, M., Bouvier, M., & Laporte, SA. (2016). Monitoring G protein-coupled receptor and [beta]-arrestin trafficking in live cells using enhanced bystander BRET. *Nature Communications*, 7.

Namkung, Y., Radresa, O., Armando, S., Devost, D., Beautrait, A., Le Gouill, C., & Laporte, S. A. (2016). Quantifying biased signaling in GPCRs using BRET-based biosensors. *Methods*, 92, 5-10.

Navarro, G., Carriba, P., Gandí, J., Ciruela, F., Casadó, V., Cortés, A., Mallol, J., Canela, EI., Lluis, C., & Franco, R. (2008). Detection of heteromers formed by cannabinoid CB1, dopamine D_2, and adenosine A_{2A} G-protein-coupled receptors by combining bimolecular fluorescence complementation and bioluminescence energy transfer. *The Scientific World Journal*. 8, 1088-1097.

Oakley, RH., Laporte, SA., Holt, JA., Barak, LS., & Caron, MG. (1999). Association of β-arrestin with G protein-coupled receptors during clathrin-mediated endocytosis dictates the profile of receptor resensitization. *Journal of Biological Chemistry*. 274(45), 32248-32257.

Oro, C., Qian, H., & Thomas, WG. (2007). Type 1 angiotensin receptor pharmacology: signaling beyond G proteins. *Pharmacology & Therapeutics*. 113(1), 210-226.

Overington, JP., Al-Lazikani, B., & Hopkins, AL. (2006). How many drug targets are there? *Nat Reviews Drug Discovery*. 5(12), 993-996.

Page, IH., & Helmer, OM. (1940). A crystalline pressor substance (angiotonin) resulting from the reaction between renin and renin-activator. *The Journal of Experimental Medicine.* 71(1), 29-42.

Palmer, BF. (2004). Managing hyperkalemia caused by inhibitors of the renin–angiotensin–aldosterone system. *New England Journal of Medicine*. 351(6), 585-592.

Pierce, KL., Premont, RT., & Lefkowitz, RJ. (2002). Seven-transmembrane receptors. *Nature Reviews Molecular Cell Biology*. 3(9), 639-650.

Pobiner, BF., Northup, JK., Bauer, PH., Fraser, ED., & Garrison, JC. (1991). Inhibitory GTP-binding regulatory protein Gi_3 can couple angiotensin II receptors to inhibition of adenylyl cyclase in hepatocytes. *Mol Pharmacol*. 40, 156-167.

Remuzzi, G., Perico, N., Macia, M., & Ruggenenti, P. (2005). The role of renin-angiotensin-aldosterone system in the progression of chronic kidney disease. *Kidney International*. 68, S57-S65.

Roettger, BF., Rentsch, RU., Pinon, D., Holicky, E., Hadac, E., Larkin, JM., & Miller, LJ. (1995). Dual pathways of internalization of the cholecystokinin receptor. *The Journal of Cell Biology*. 128(6), 1029-1041.

Rosenbaum, DM., Rasmussen, SGF., & Kobilka, BK. (2009) The structure and function of G-protein-coupled receptors. *Nature.* 459(7245), 356-363.

Schrage, R., Schmitz, A.L., Gaffal, E., Annala, S., Kehraus, S., Wenzel, D., Büllesbach, KM., Bald, T., Inoue, A., Shinjo, Y. & Galandrin, S. (2015). The experimental power of FR900359 to study Gq-regulated biological processes. *Nature Communications*, 6.

Siehler, S. (2009). Regulation of RhoGEF proteins by G12/13-coupled receptors. *British journal of Pharmacology*. 158(1), 41-49.

Simon, MI., Strathmann, MP., & Gautam, N. (1991). Diversity of G proteins in signal transduction. *Science*. 252(5007), 802-808.

Stoop, R., Hegoburu, C., & van den Burg, E. (2015). New opportunities in vasopressin and oxytocin research: a perspective from the amygdala. *Annual review of Neuroscience*. 38, 369-388.

Szakadáti, G., Tóth, AD., Oláh, I., Erdélyi, LS., Balla, T., Várnai, P., Hunyady, P., & Balla, A. (2015). Investigation of the fate of type I angiotensin receptor after biased activation. *Molecular Pharmacology*. 87(6), 972-981.

Tateyama, M., Abe, H., Nakata, H., Saito, O., & Kubo, Y. (2004). Ligand-induced rearrangement of the dimeric metabotropic glutamate receptor 1α. *Nat Struct Mol Biol*. 11(7), 637-642.

Tran, D., Carpentier, JL., Sawano, F., Gorden, P., & Orci, L. (1987). Ligands internalized through coated or noncoated invaginations follow a common intracellular pathway. *Proceedings of the National Academy of Sciences*. 84(22), 7957-7961.

Vogt, S., Grosse, R., Schultz, G., & Offermanns, S. (2003). Receptor-dependent RhoA Activation in G12/G13-deficient Cells GENETIC EVIDENCE FOR AN INVOLVEMENT OF Gq/G11. *Journal of Biological Chemistry.* 278(31), 28743-28749.

von Zastrow, M., & Kobilka, BK. (1994). Antagonist-dependent and-independent steps in the mechanism of adrenergic receptor internalization. *Journal of Biological Chemistry*. 269(28), 18448-18452.

Zhang, H., Unal, H., Desnoyer, R., Han, GW., Patel, N., Katritch, V., Karnik, SS., Cherezov, V., & Stevens, RC. (2015). Structural Basis for Ligand Recognition and Functional Selectivity at Angiotensin Receptor. *Journal of Biological Chemistry*. 290(49), 29127-29139.

Zheng, H., Loh, HH., & Law, PY. (2010). Agonist-selective signaling of G protein-coupled receptor: mechanisms and implications. *IUBMB Life*. 62(2), 112-119.

Zimmerman, B., Simaan, M., Lee, MH., Luttrell, LM., & Laporte, SA. (2009). c-Src-mediated phosphorylation of AP-2 reveals a general mechanism for receptors internalizing through the clathrin pathway. *Cellular Signalling*, 21(1), 103-110.

Zimmerman, B., Beautrait, A., Aguila, B., Charles, R., Escher, E., Claing, A., Bouvier, M., & Laporte, SA. (2012). Differential β-arrestin-dependent conformational signaling and cellular responses revealed by angiotensin analogs. *Science Signaling*. 5(221), ra33-ra33.

This page intentionally left blank.